2013.11.27
Carl-Zeiss Lecture 5
IPHT Jena

Raman Spectroscopy and Imaging of Living Cells

Hiro-o HAMAGUCHI

Department of Applied Chemistry and Institute of Molecular Science, College of Science, National Chiao Tung University, Taiwan

“How can the events in space and time which take place within the spatial boundary of a living organism be accounted for by physics and chemistry ?”

In “What is Life”

Erwin Schrödinger

E. Schrödinger
(1887-1961)

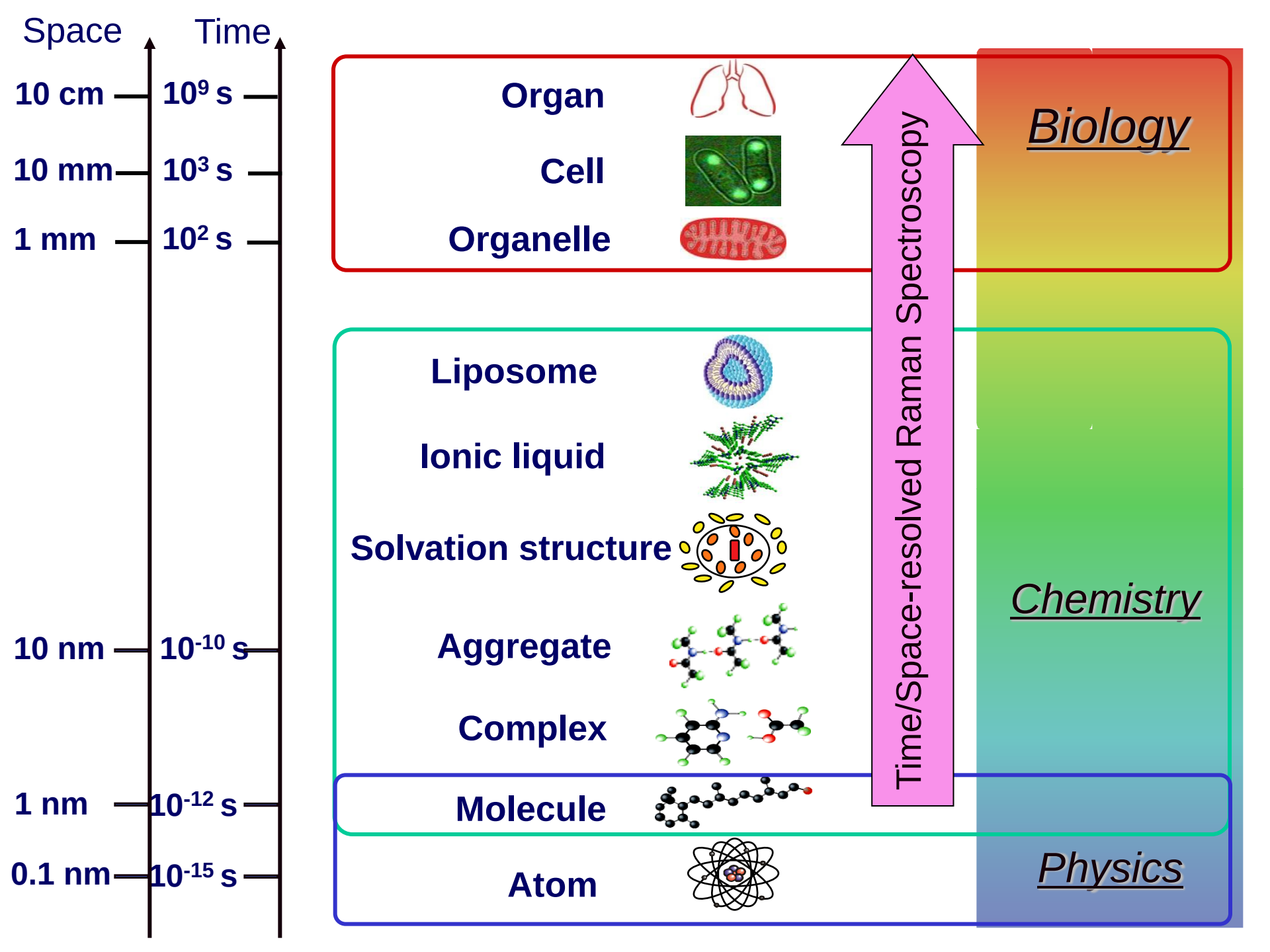
Space
Time
10 cm
10 mm
1 mm
10 nm
1 nm
0.1 nm
10^9 s
10^3 s
10^2 s
10^-10 s
10^-12 s
10^-15 s
Organ
Cell
Organelle
Liposome
Ionic liquid
Solvation structure
Aggregate
Complex
Molecule
Atom
Time/Space-resolved Raman Spectroscopy
Biology
Chemistry
Physics

Fission Yeast (Schizosaccharomyces pombe)

Simplest eukaryote that is familiar to our life

Safe and easy to handle (even for a physical chemist)

Model for higher organisms

Cell division by septum formation

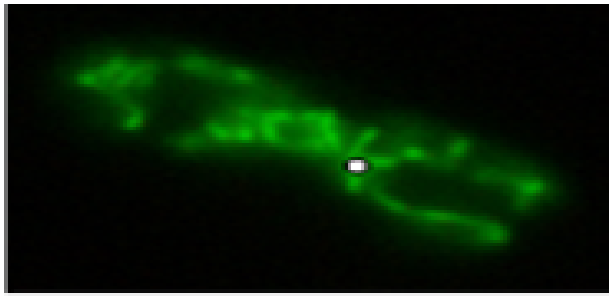

GFP image of mitochondria in a fission yeast cell

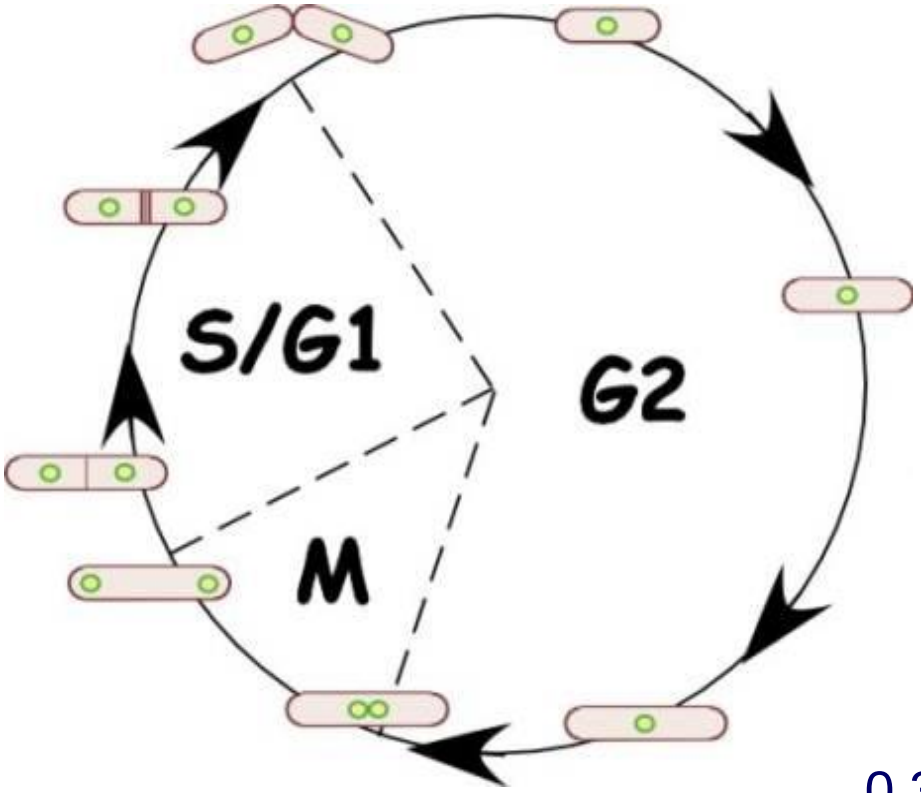

Cycle duration: typically 3 hours

1 s time-resolution is sufficient

Cell size: 6-20 μm x 2 μm

0.3 μm spatial resolution is sufficient

Raman Spectroscopy of a Really Living Cell

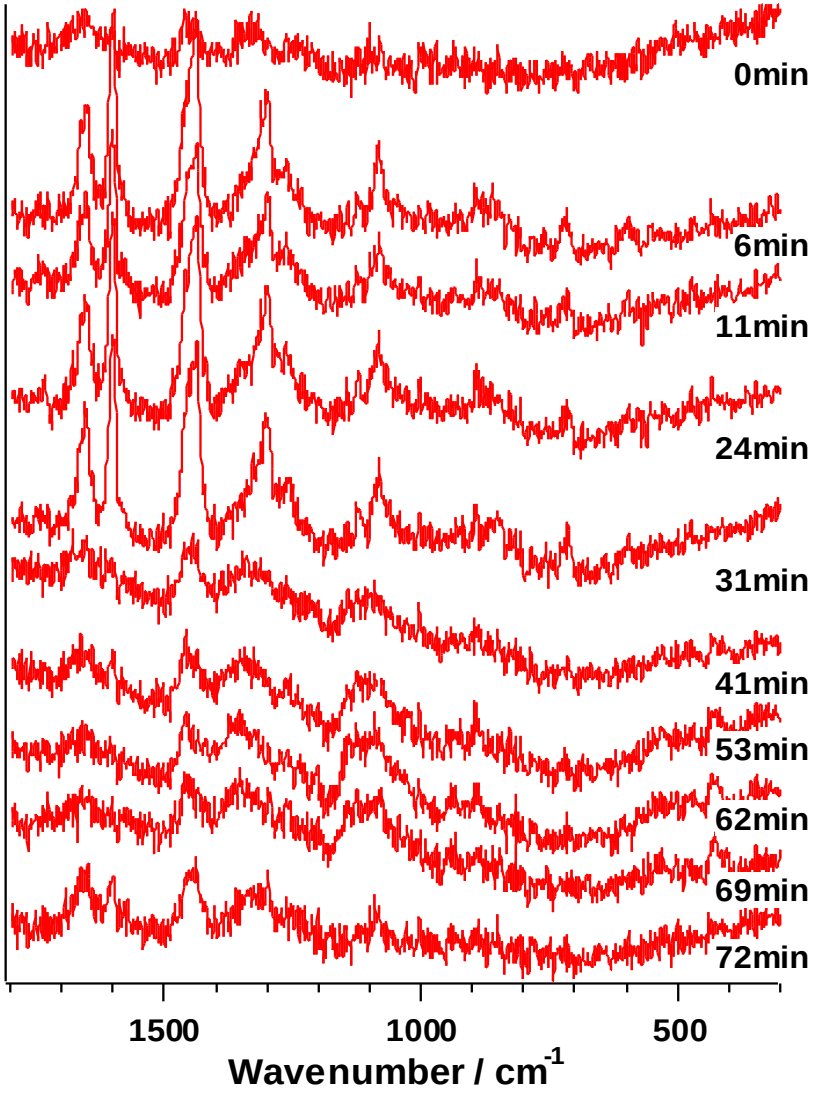

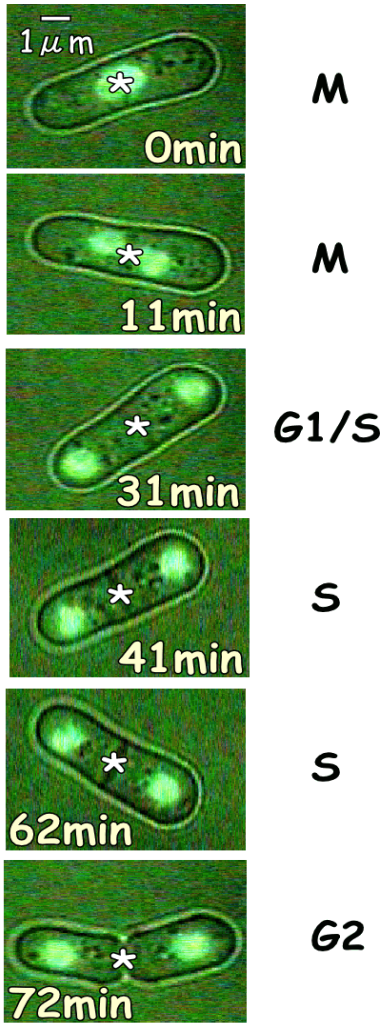

Y-S Huang, T. Karashima, M. Yamamoto, H. Hamaguchi, J. Raman Spectrosc., **34,** 1-3 (2003).

Raman Spectra of Mitochondria (?) and Phosphatidylcholine

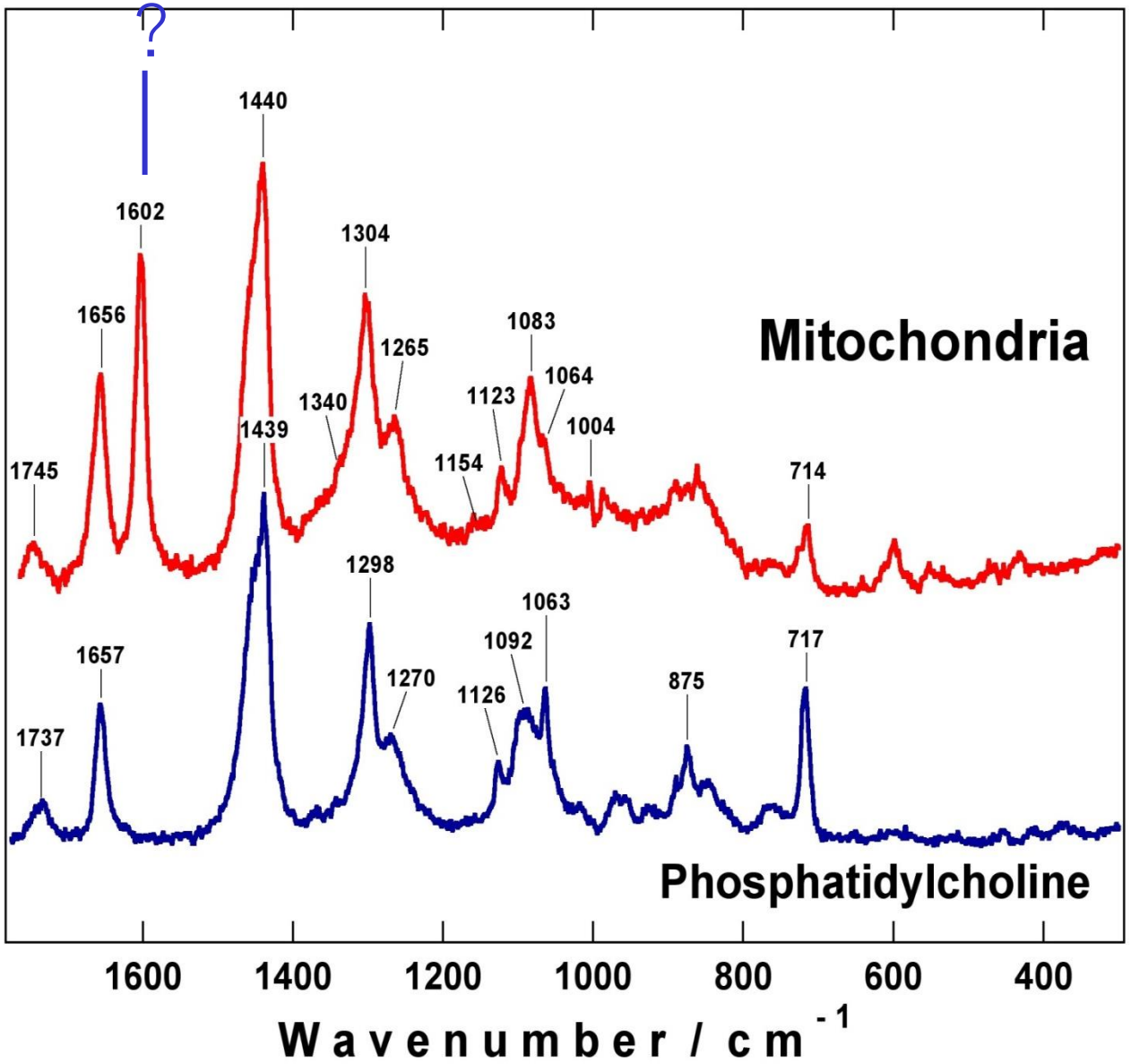

Unknown

1602

Lipids

1745	C=O str
1656	C=C str, cis -CH=CH-
1440	CH bending
1304	CH_2 twisting
1265	C=C-H bending

1000-1150 region:

1064, 1123	} all-trans chain
1083	gauche

714 phospholipids headgroup

Proteins

1656	amide I
1440	CH bending
1340	CH_2 deformation
1265	amide III
1154	C-C, C-N str
1004	phe

The 1602 cm^{-1} band seems to reflect cell metabolic activity (Raman Spectroscopic Signature of Life ?)

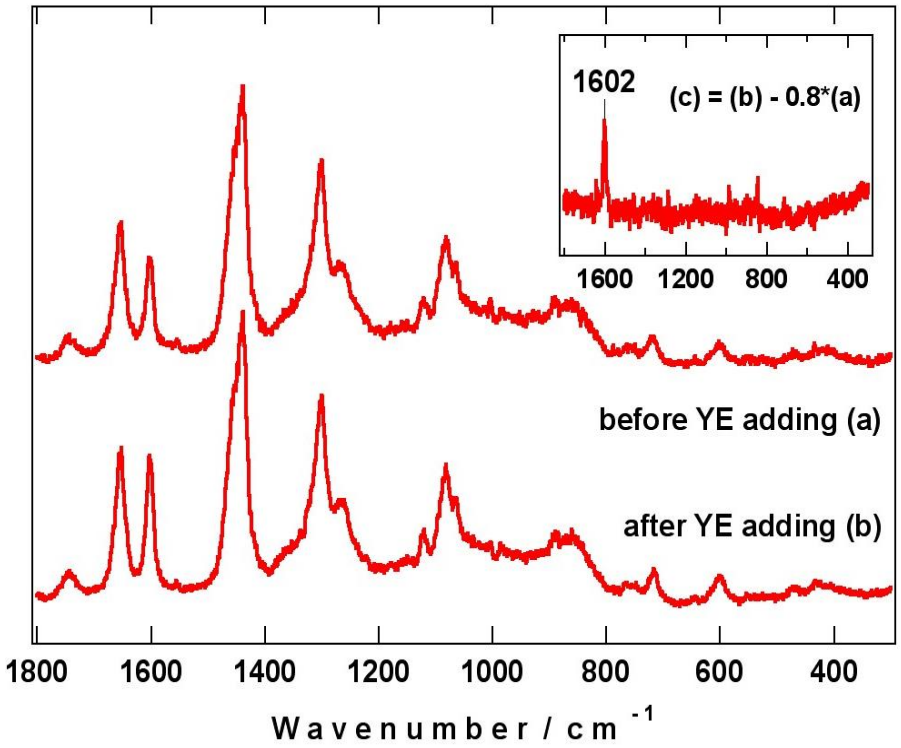

Addition of nutrients increases its intensity.

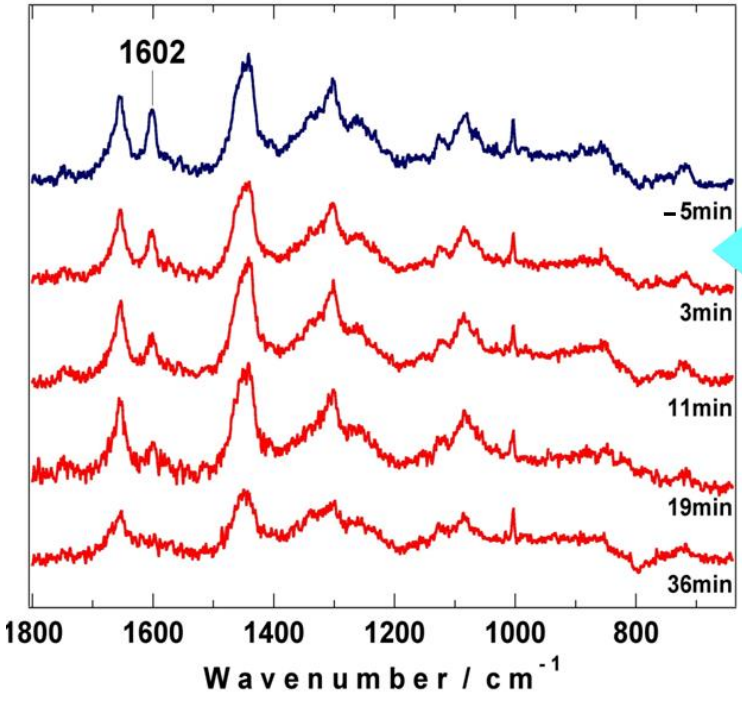

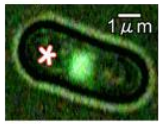

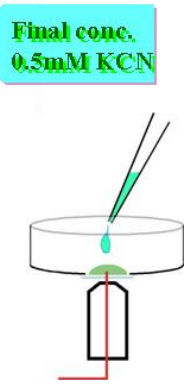

Addition of KCN decreases its intensity.

The 1602 cm^{-1} band seems to reflect cell metabolic activity (Raman Spectroscopic Signature of Life = Ergosterol)

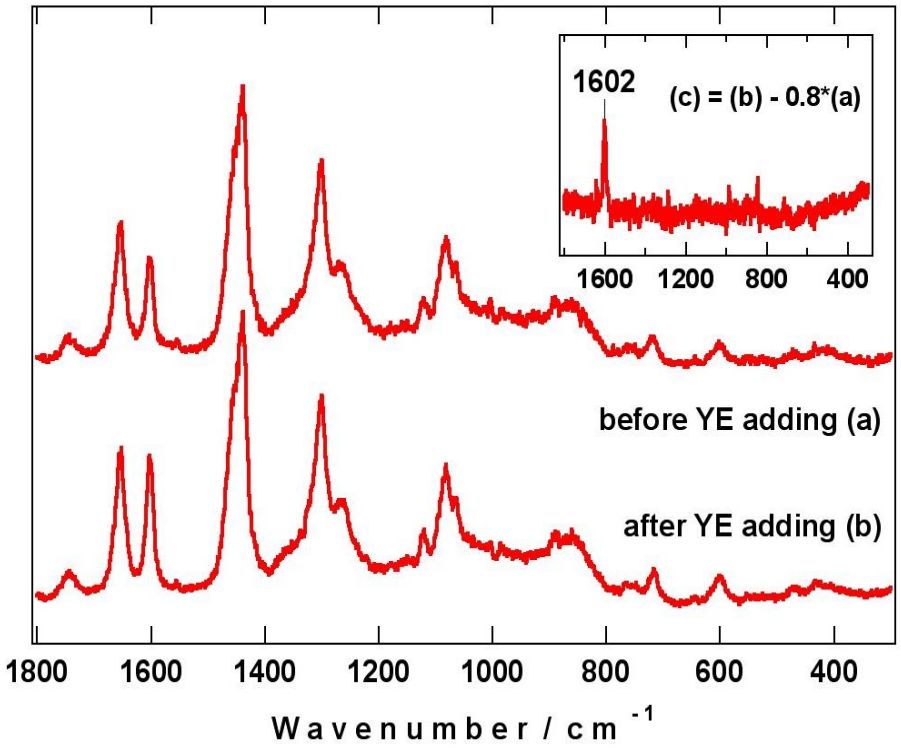

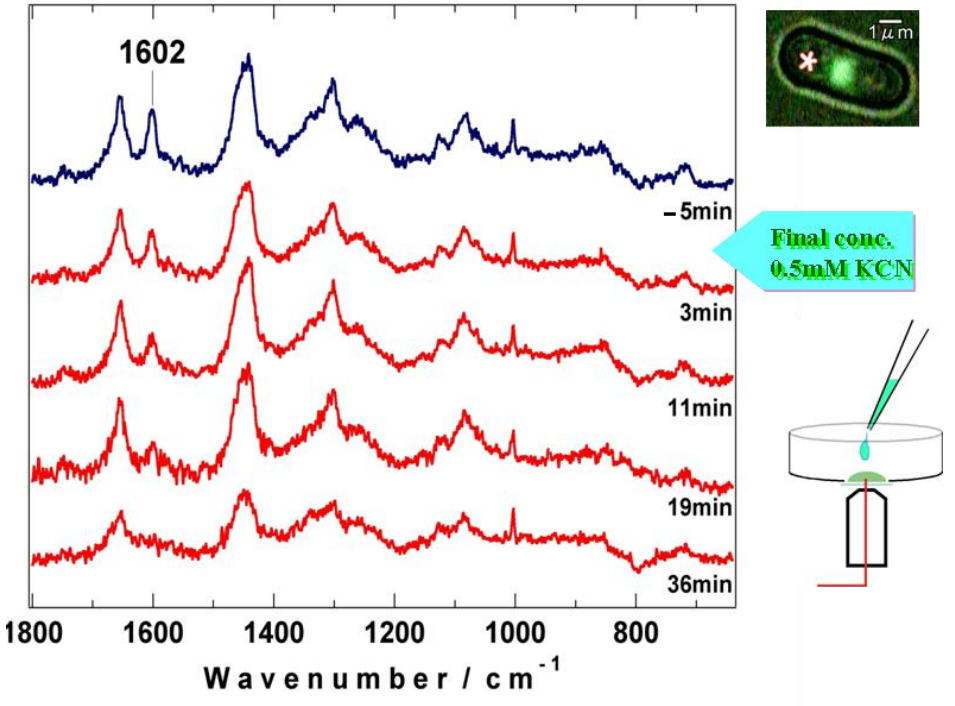

Addition of nutrients increases its intensity.

Addition of KCN decreases its intensity.

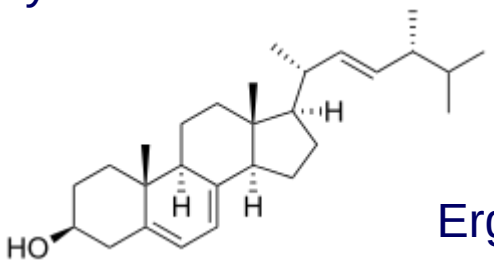

Ergosterol

Dancing Body in a Vacuole of *S. cerevisiae*

A black particle that appears in a vacuole

An active dancing body moves around vigorously in a vacuole.

The main component is thought to be polyphosphate.

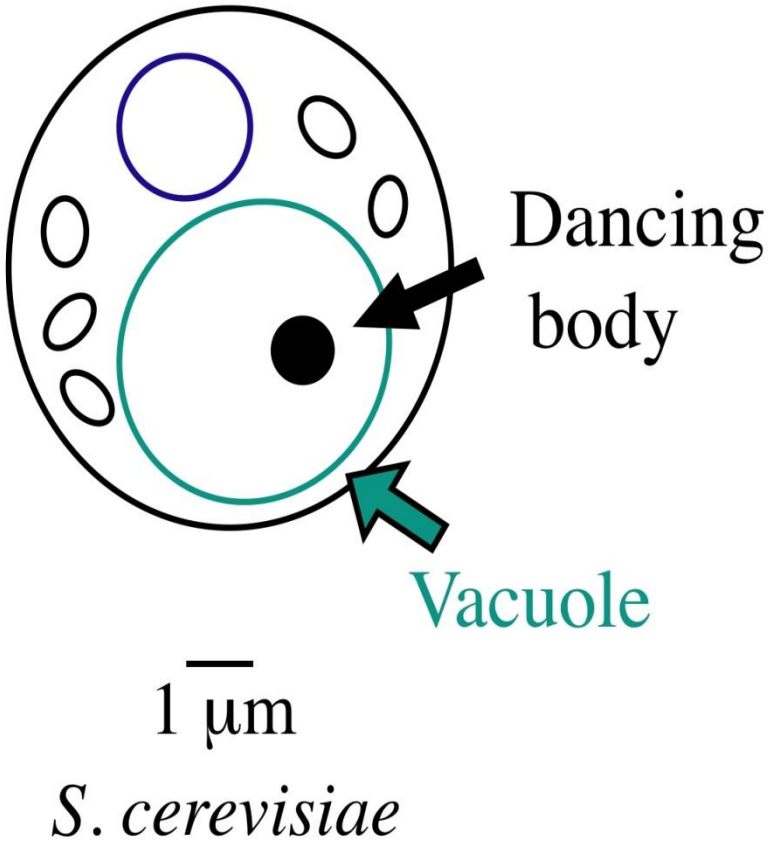

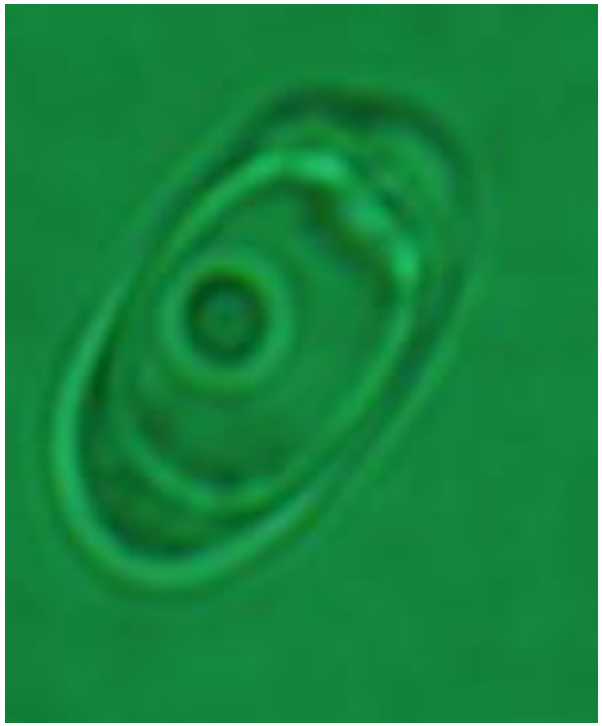

Sudden Apperance of a Dancing Body and Subsequent Cell Death in a Sttarving Budding Yeast Cell

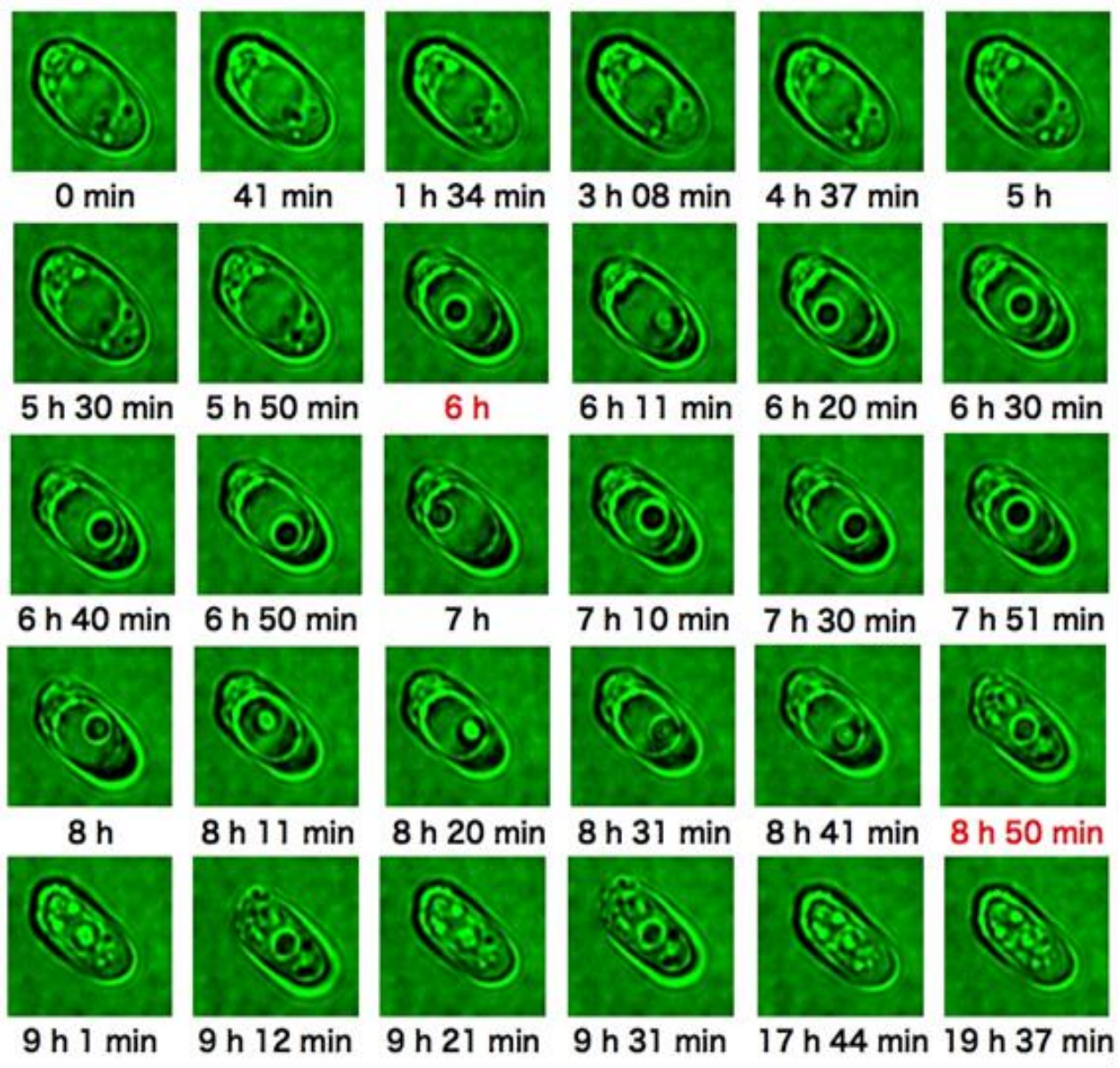

Time-resolved Raman Imaging of a Death Process in a Single Living Budding Yeast Cell

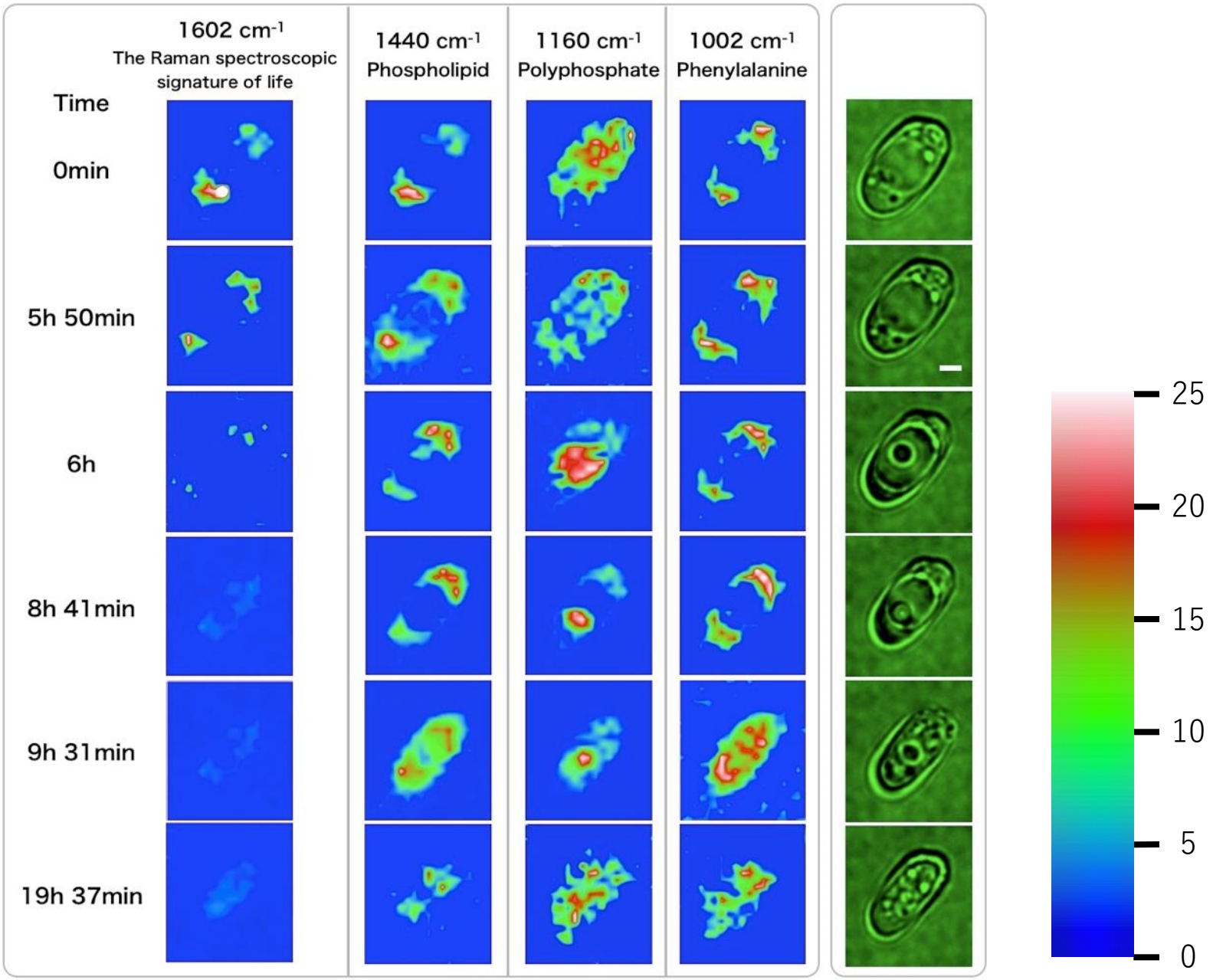

Time-resolved Raman Imaging of a Death Process in a Single Living Budding Yeast Cell

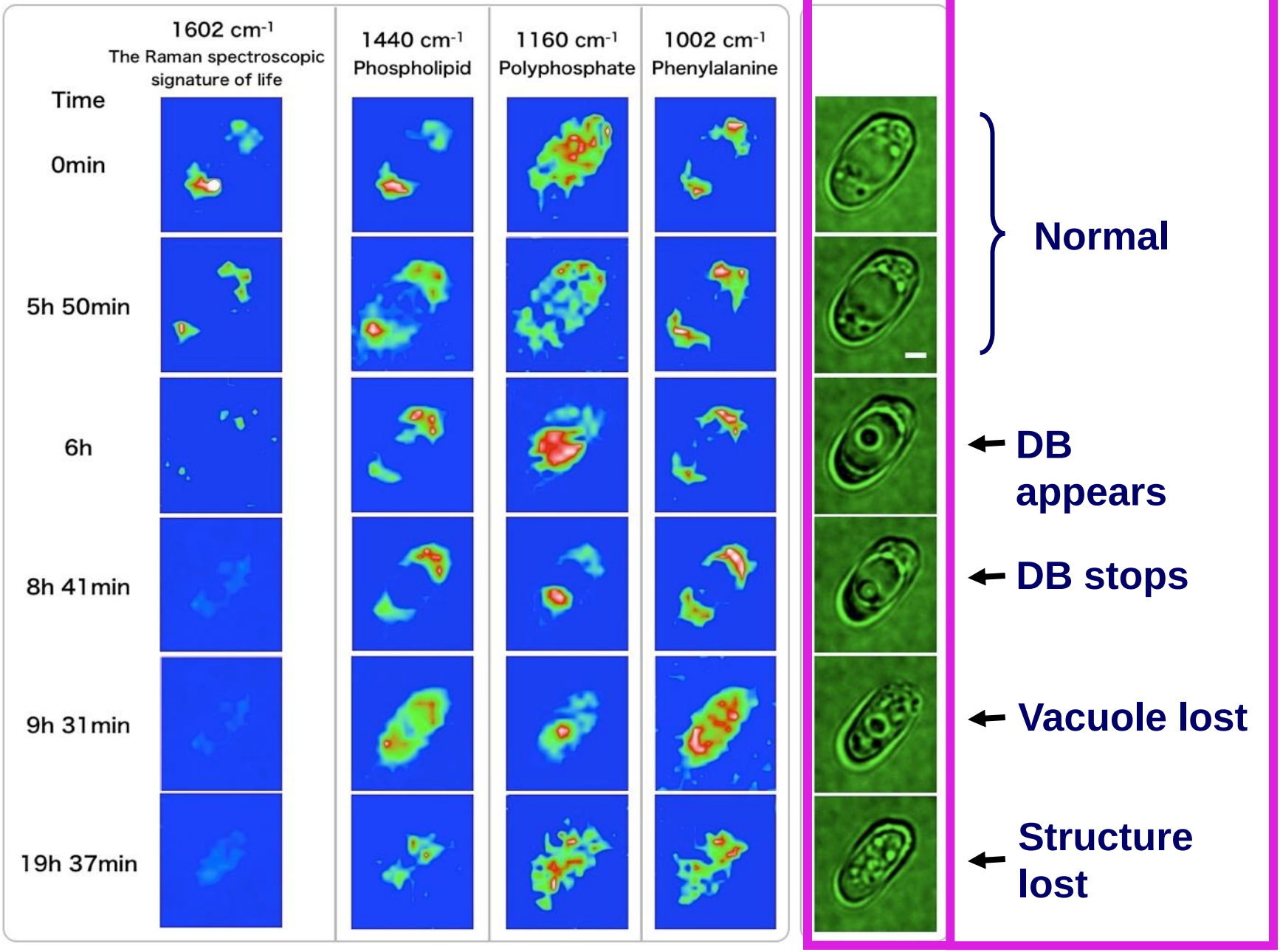

Time-resolved Raman Imaging of a Death Process in a Single Living Budding Yeast Cell

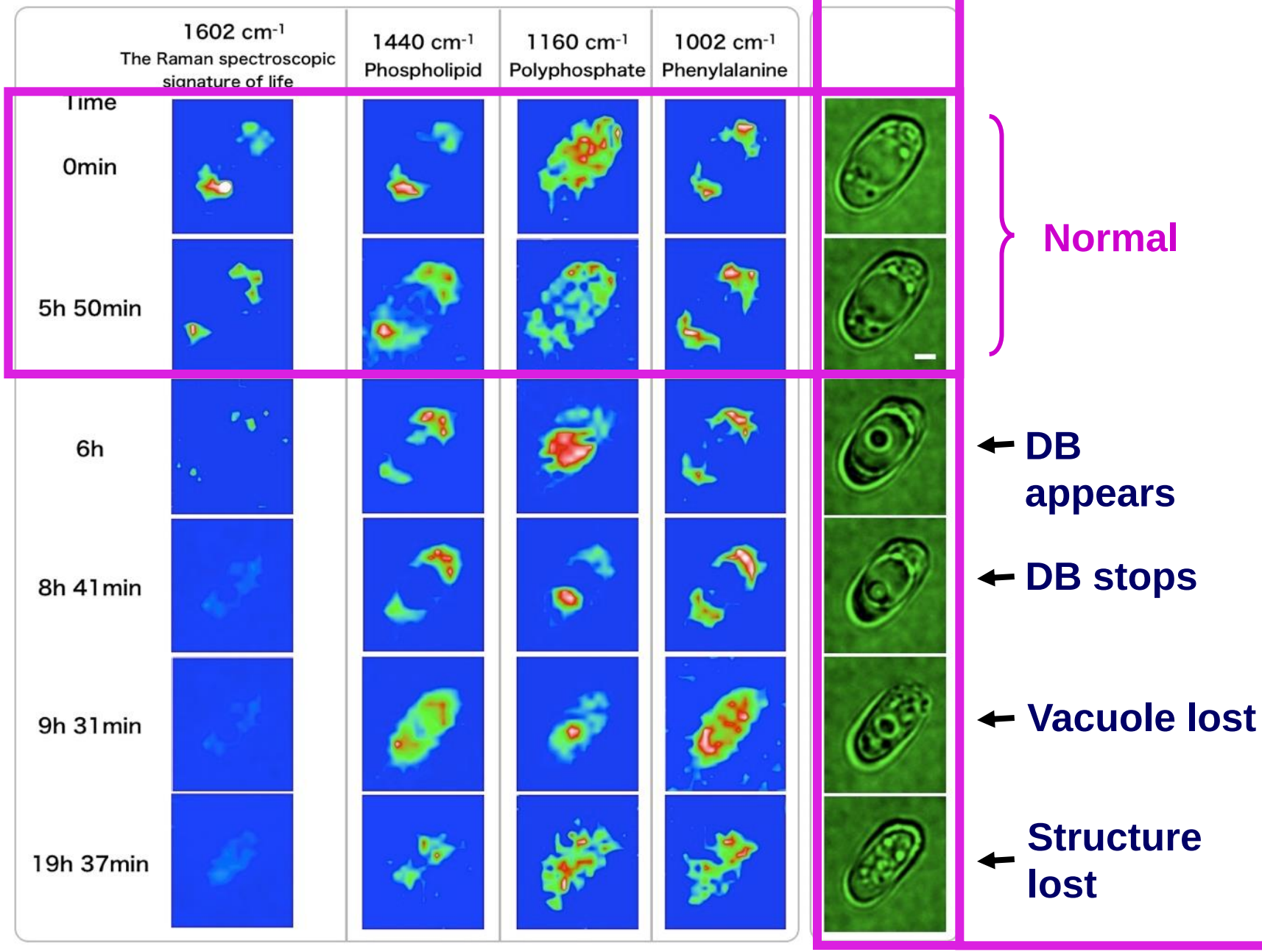

Time-resolved Raman Imaging of a Death Process in a Single Living Budding Yeast Cell

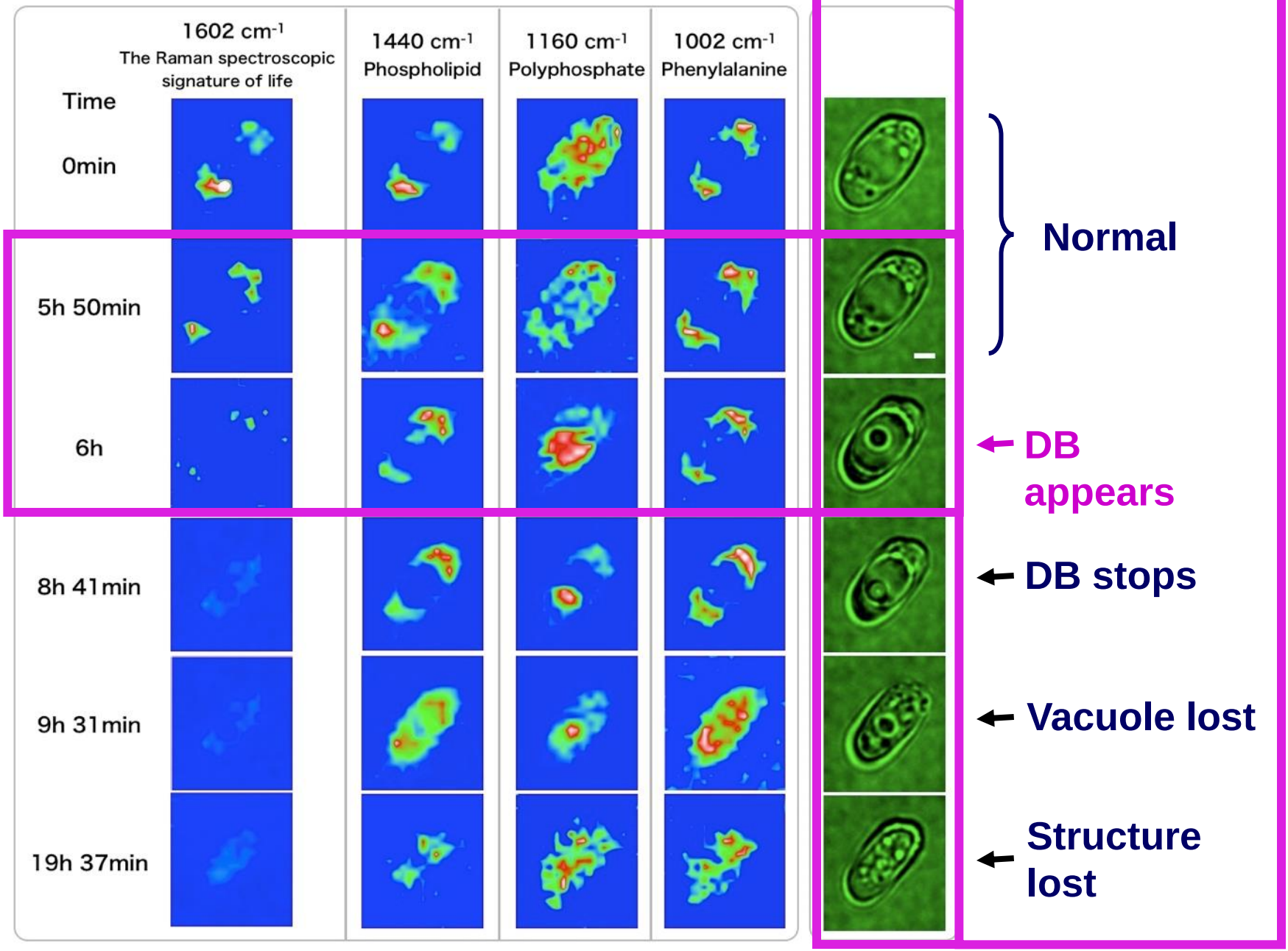

Time-resolved Raman Imaging of a Death Process in a Single Living Budding Yeast Cell

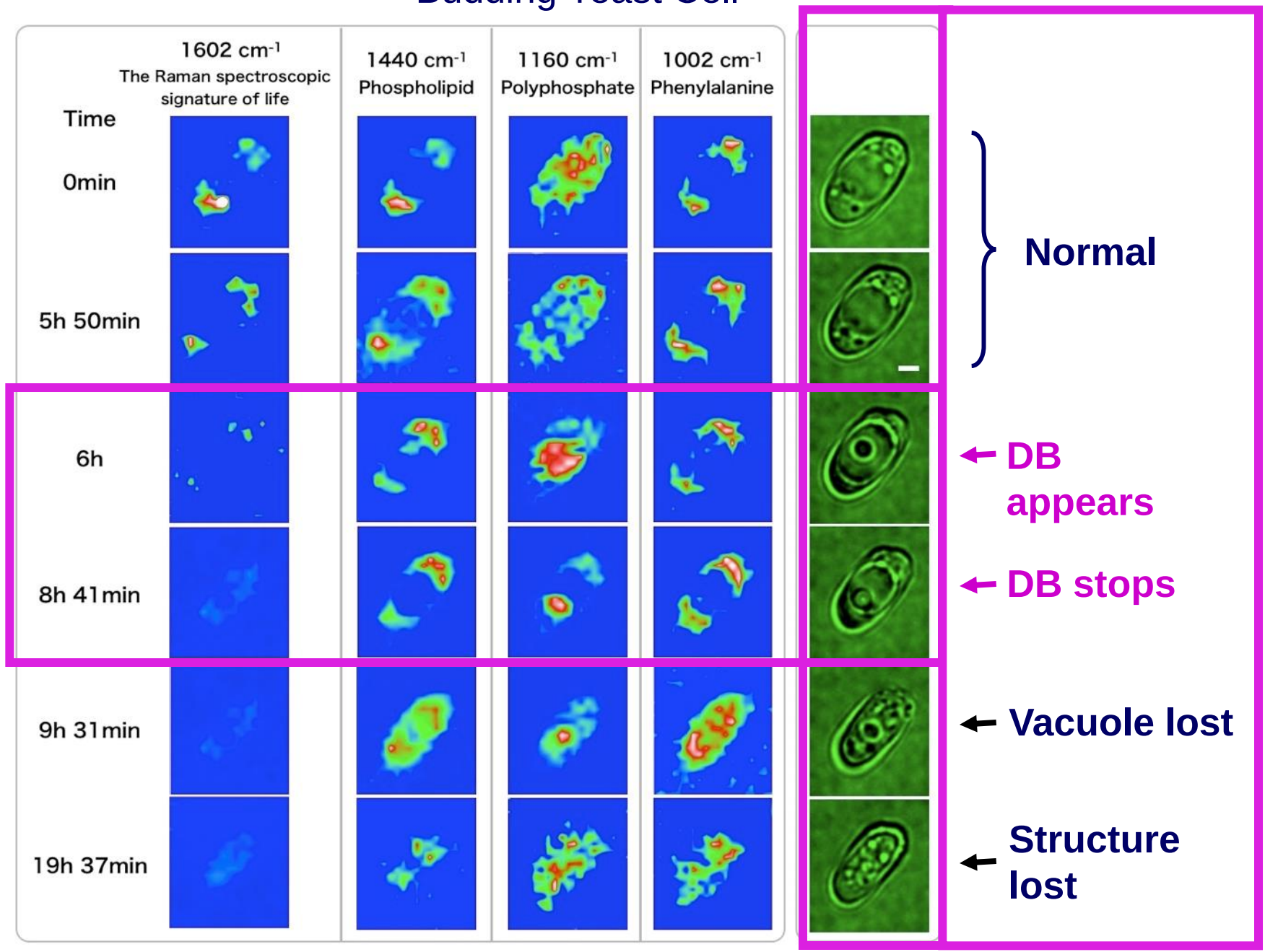

Time-resolved Raman Imaging of a Death Process in a Single Living Budding Yeast Cell

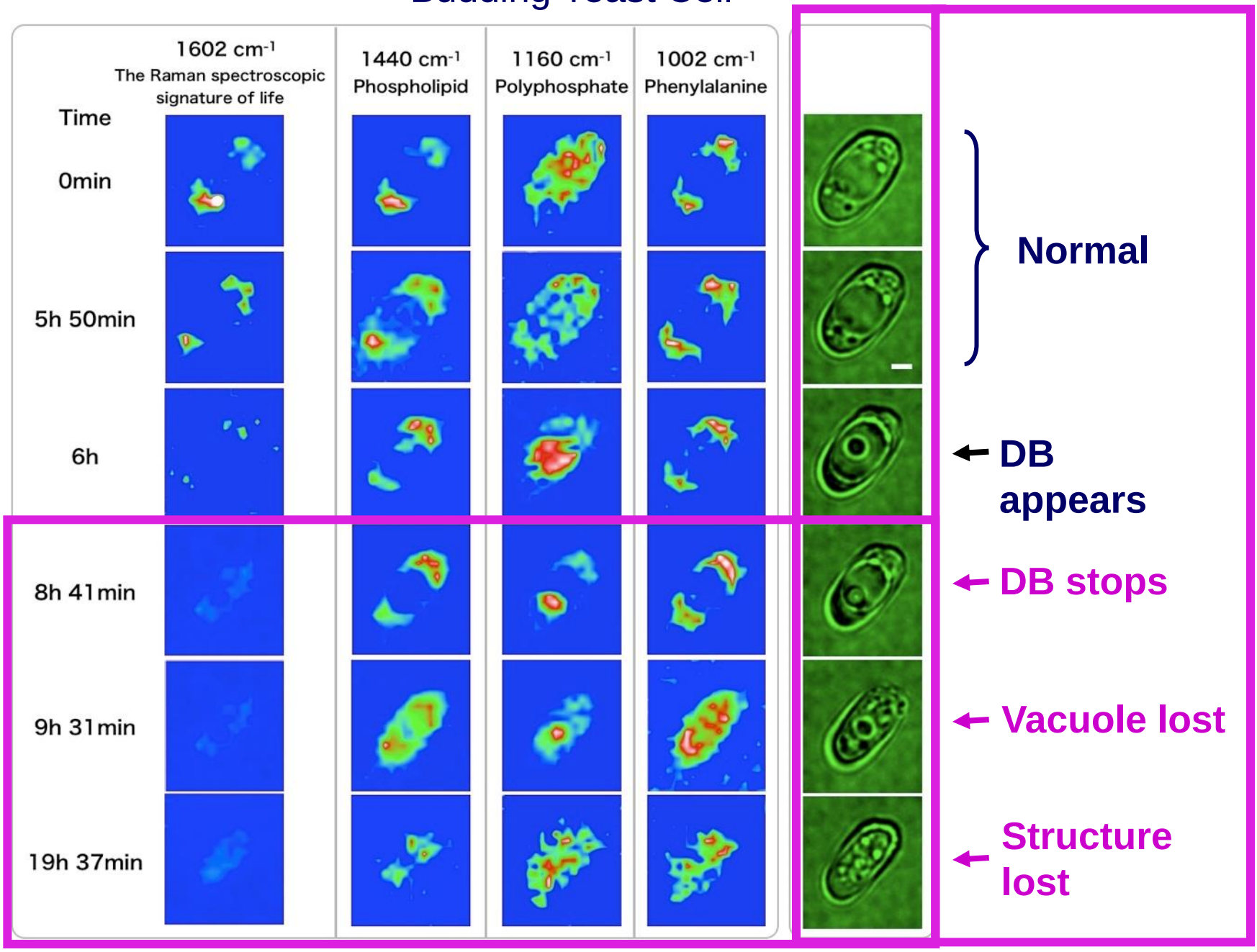

Two Different Types of Mitochondria ?

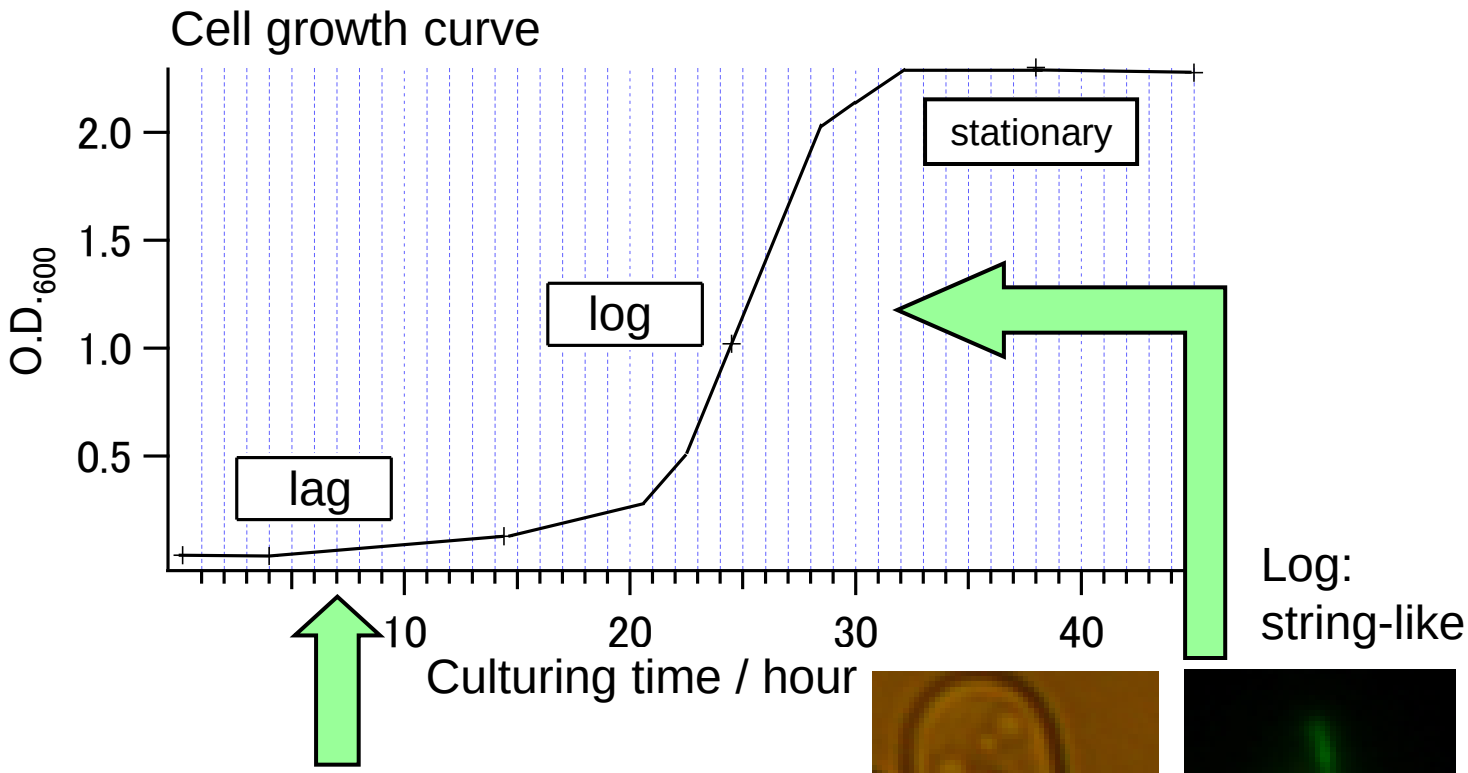

Log:
string-like

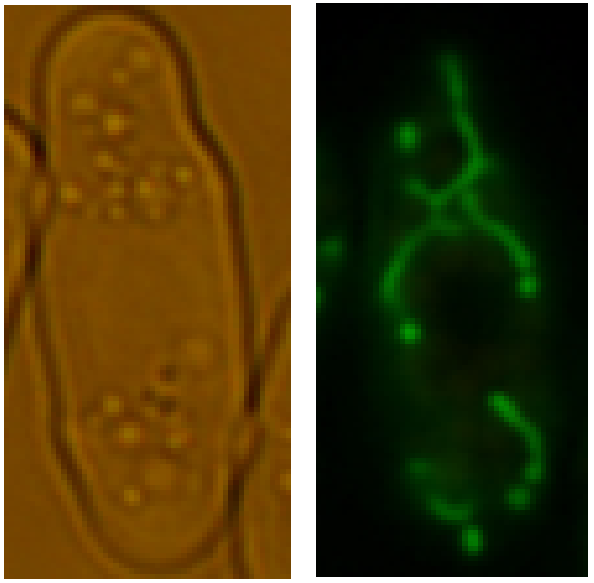

Lag:
dot-like

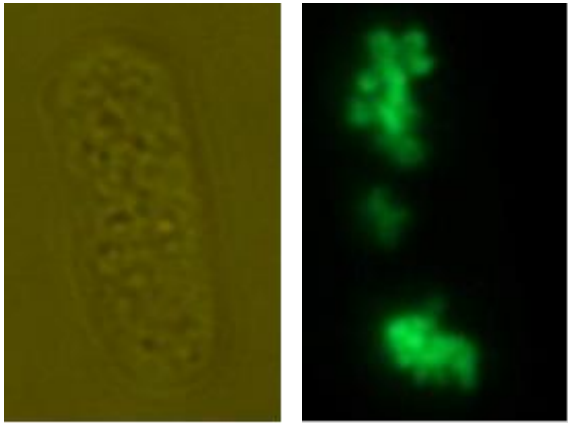

Raman Spectra of Mitochondria at the Lag Phase

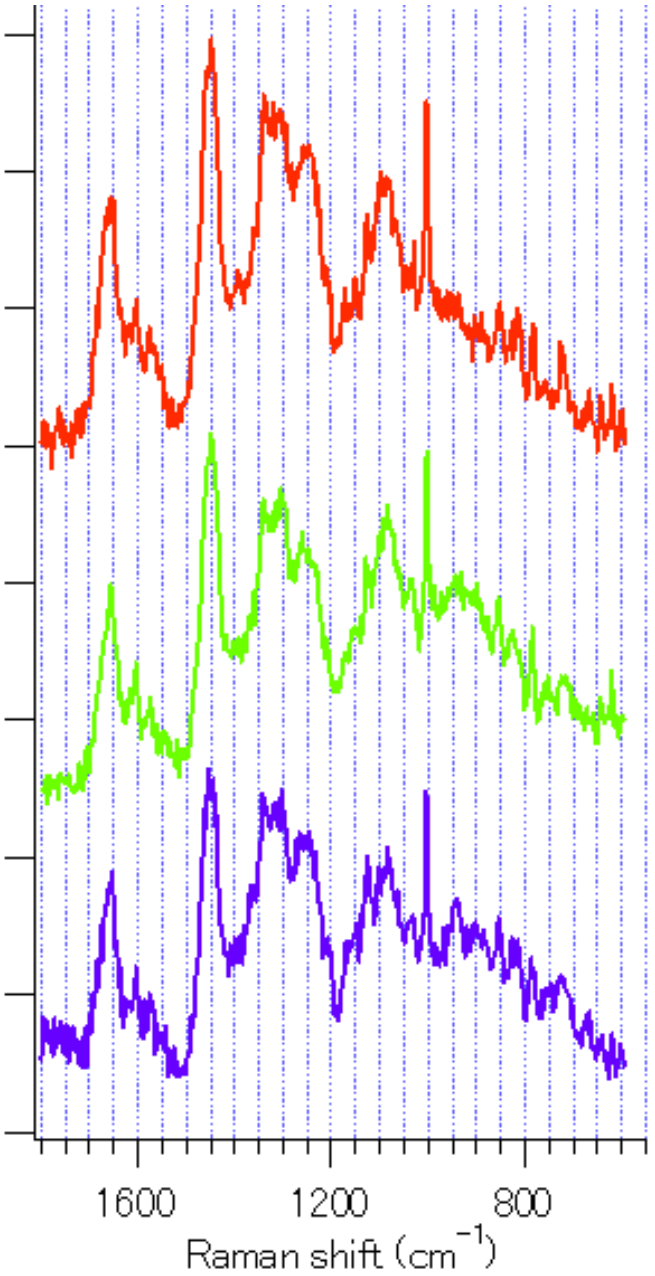

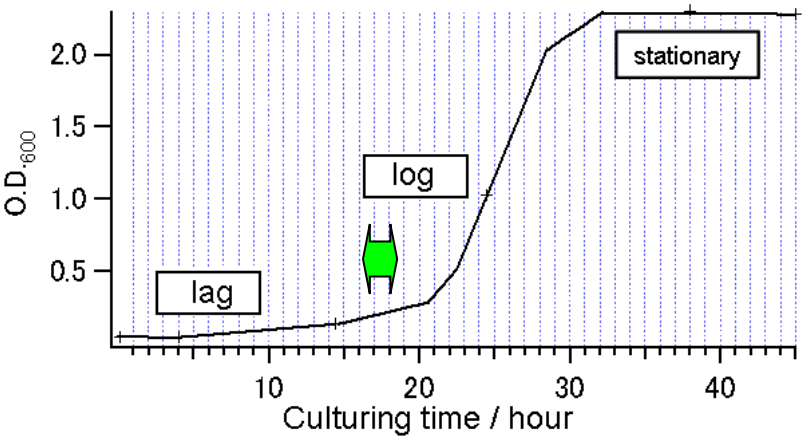

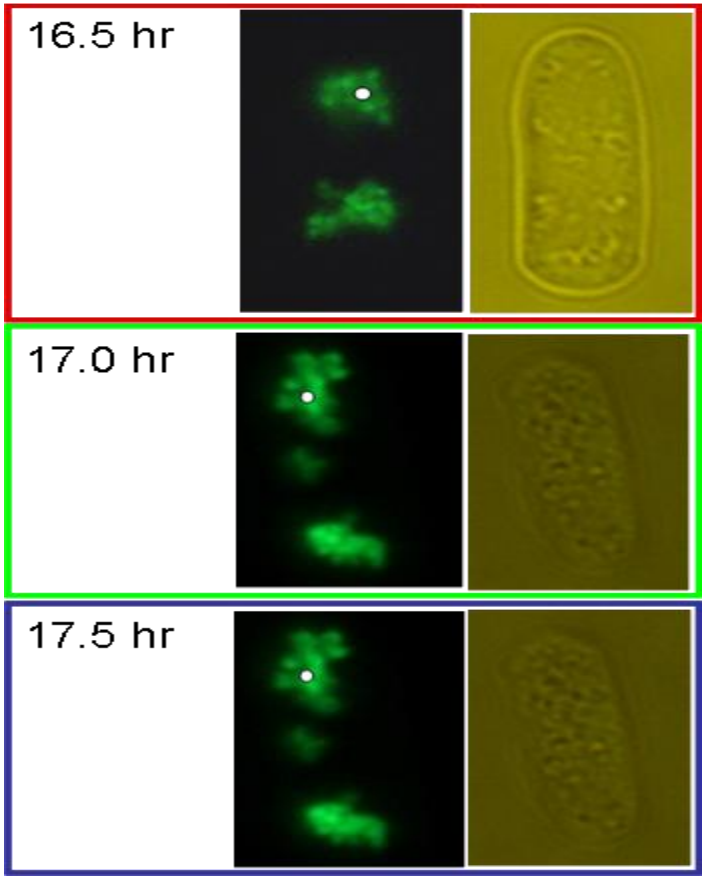

Raman Spectra of Mitochondria at the Log Phase

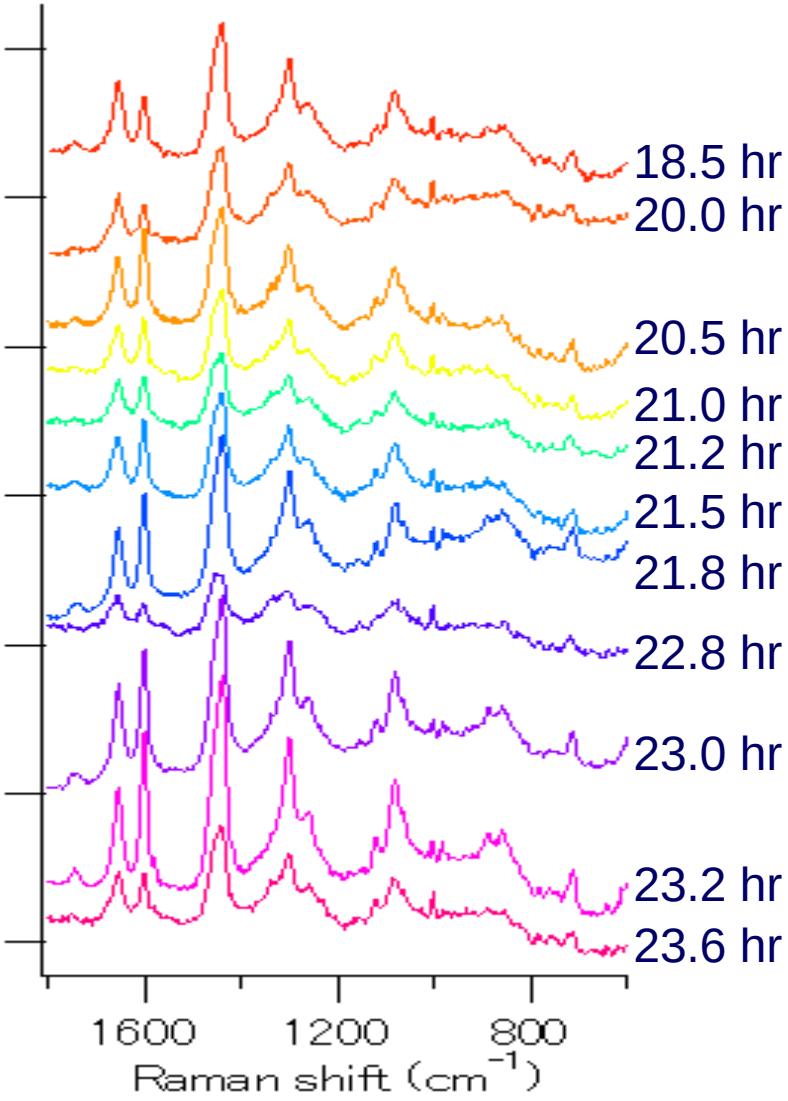

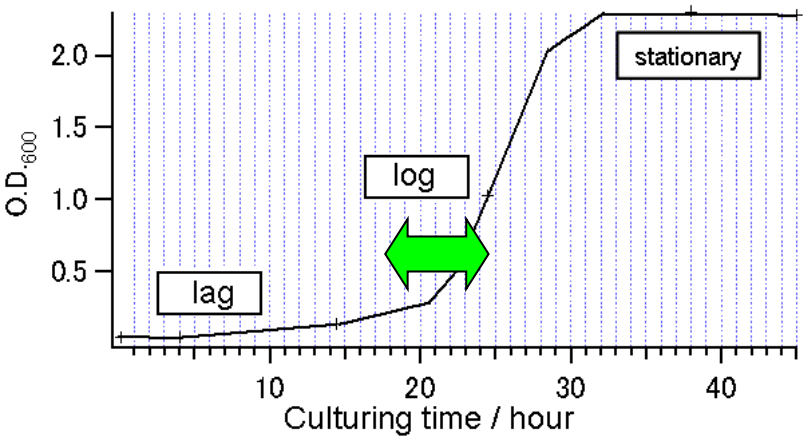

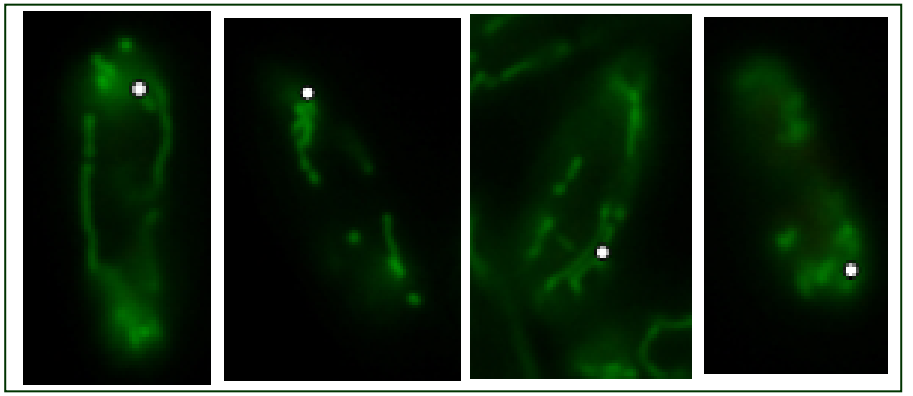

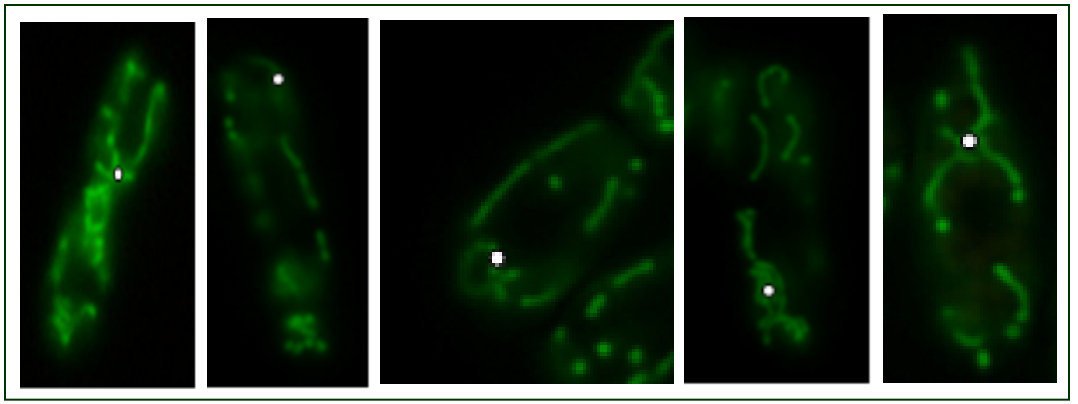

Raman Spectra of Mitochondria at the Lag →Log Phase

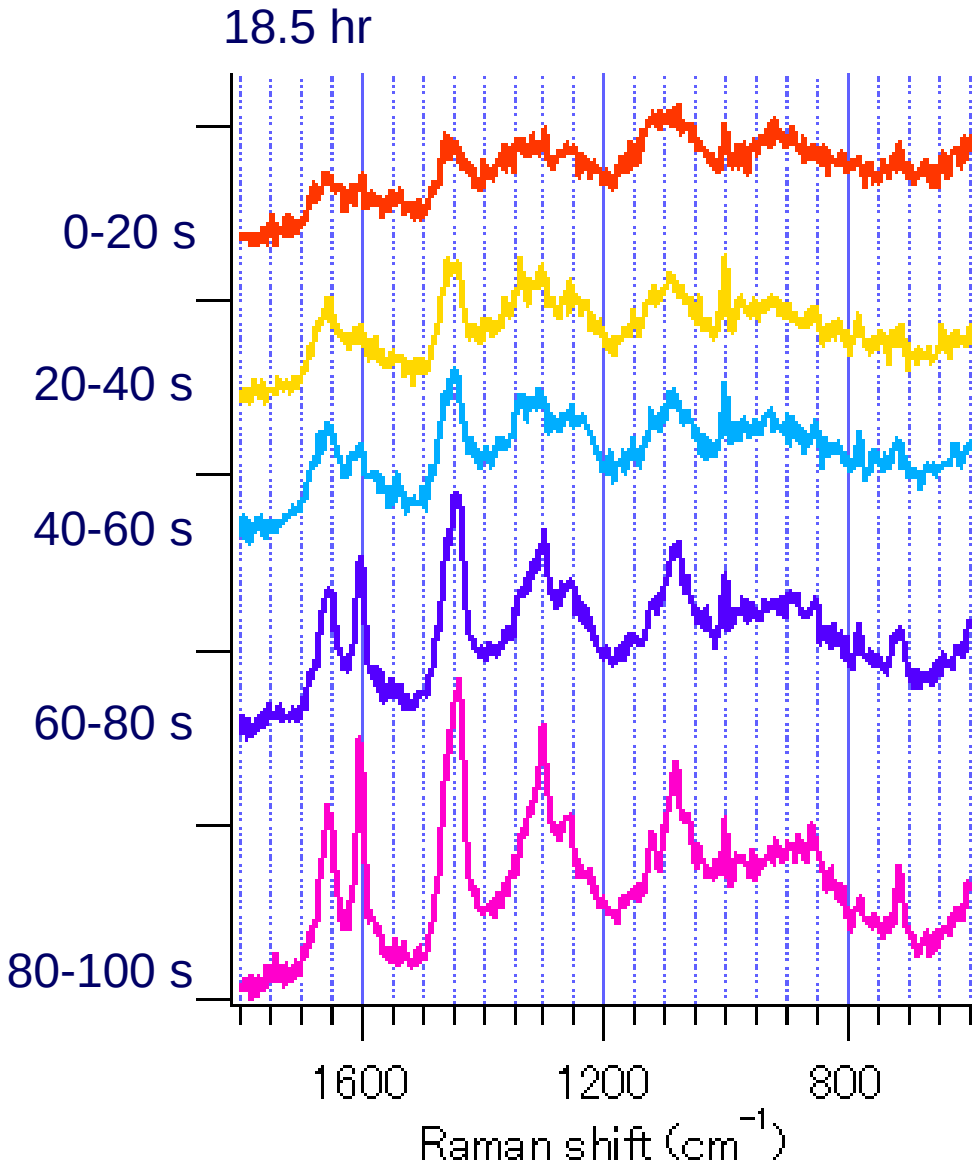

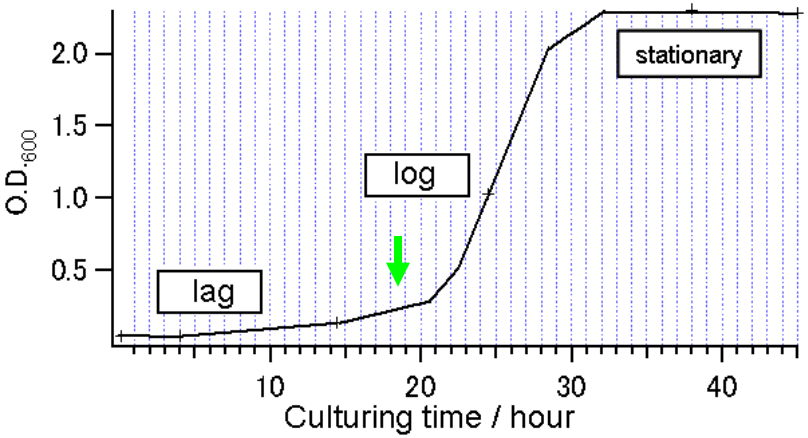

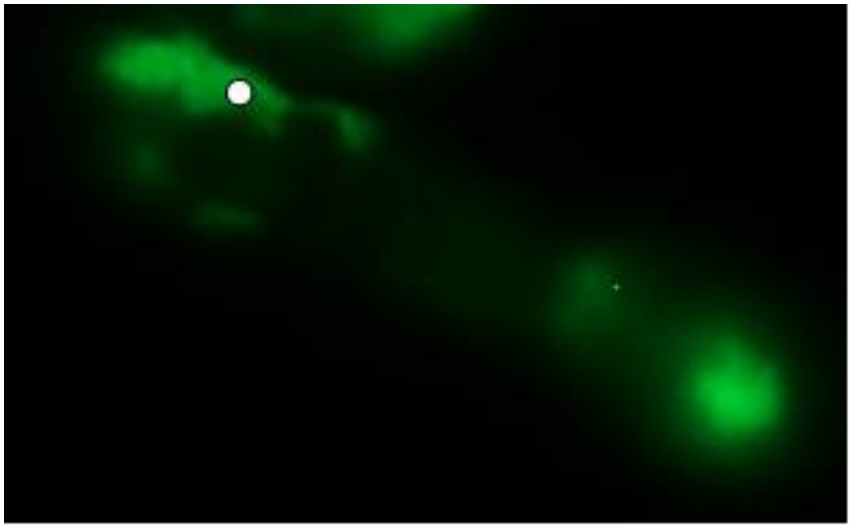

The Latest Version of Raman Microspectrometer at Tokyo: Measures a living cell Raman spectrum in 1s !!

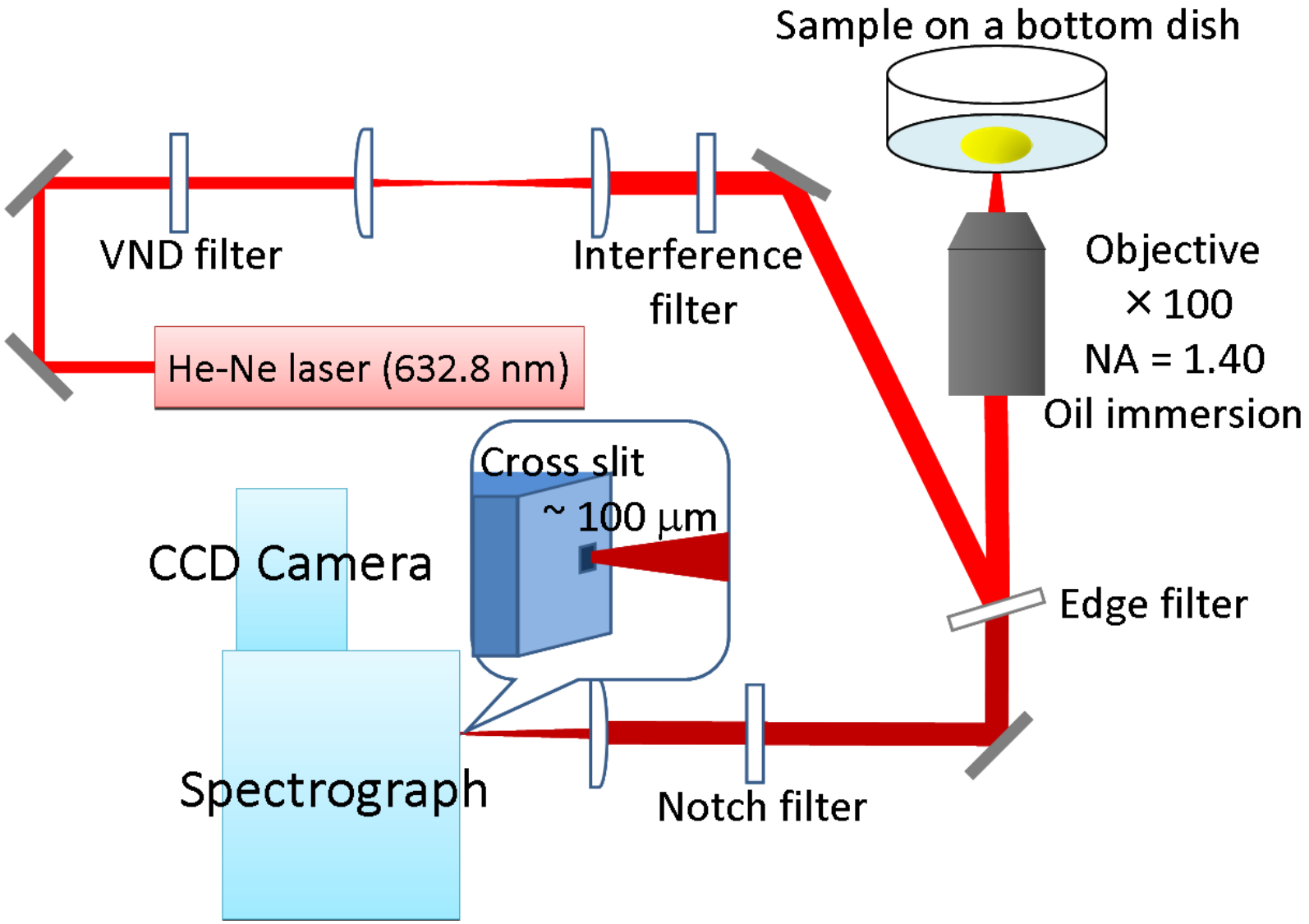

Time- and Space-resolved Raman Spectra with 1 s Exposure

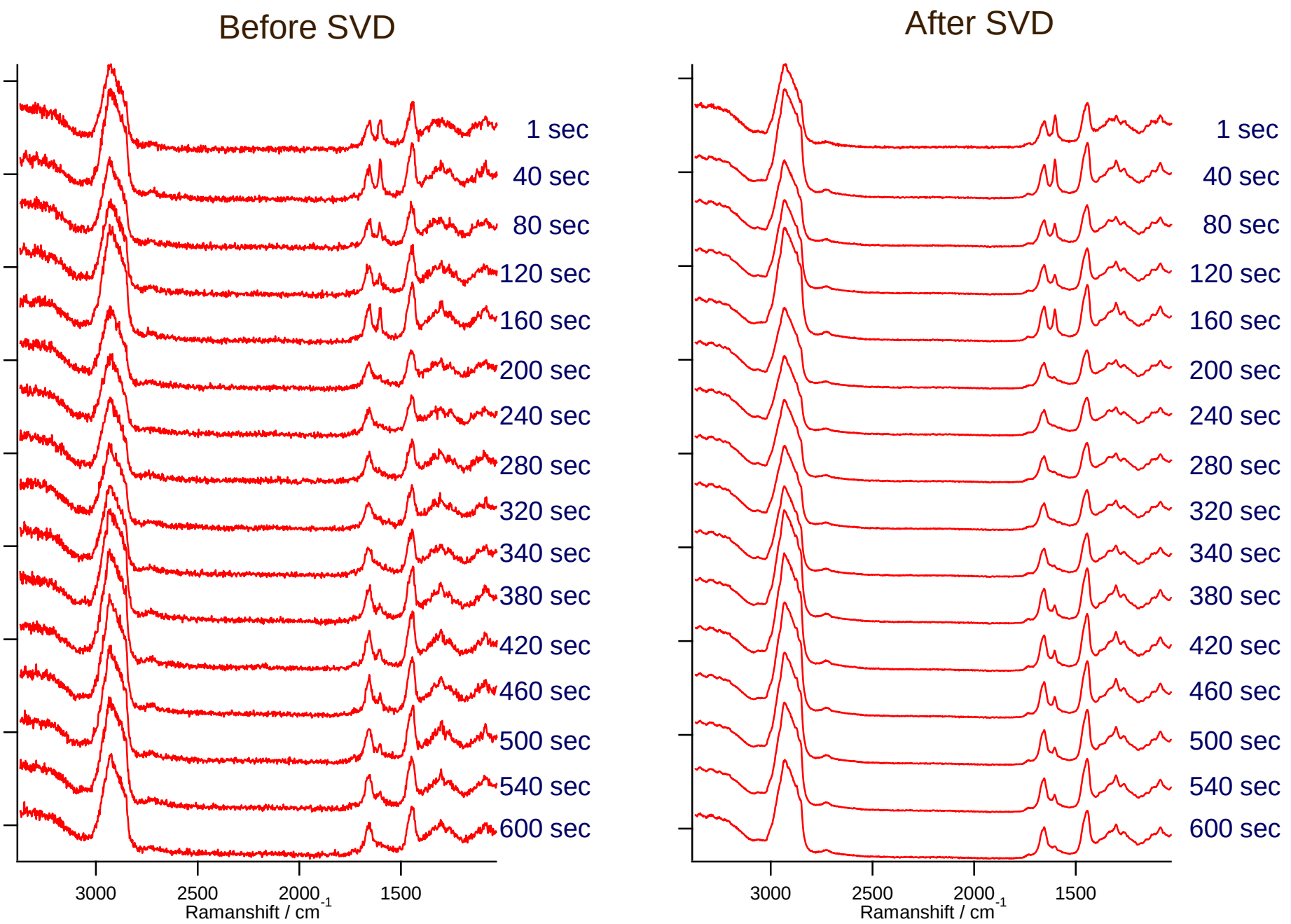

Time-dependent Change of the 1602 cm^{-1} Band

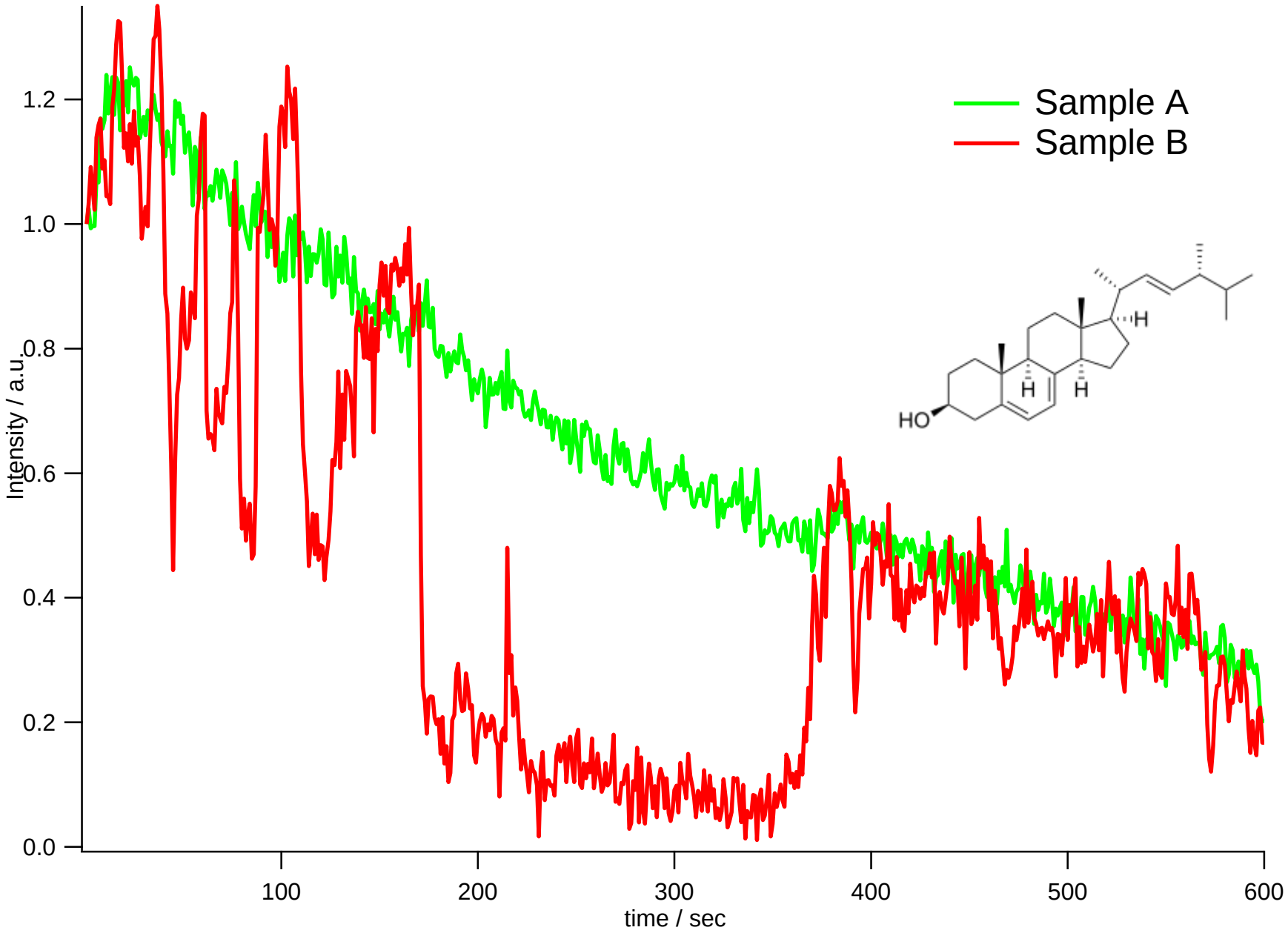

Multiplex CARS Spectroscopy

Multiplex CARS to obtain the whole Raman spectrum simultaneously

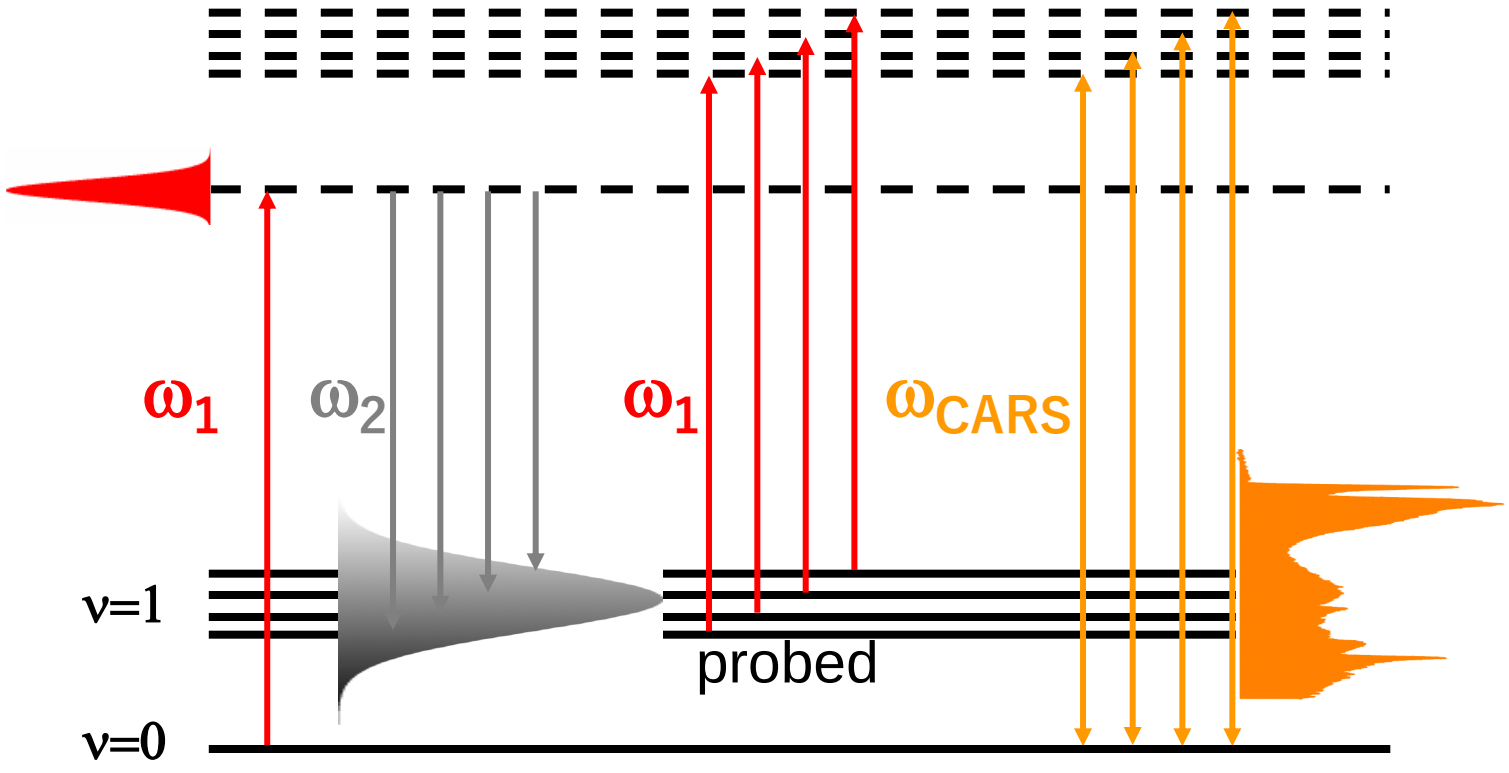

B. N. Toleutaev, T. Tahara and H. Hamaguchi, Appl. Phys. B., **59**, 369-375 (1994).

Broadband Multiplex CARS Microspectroscopy

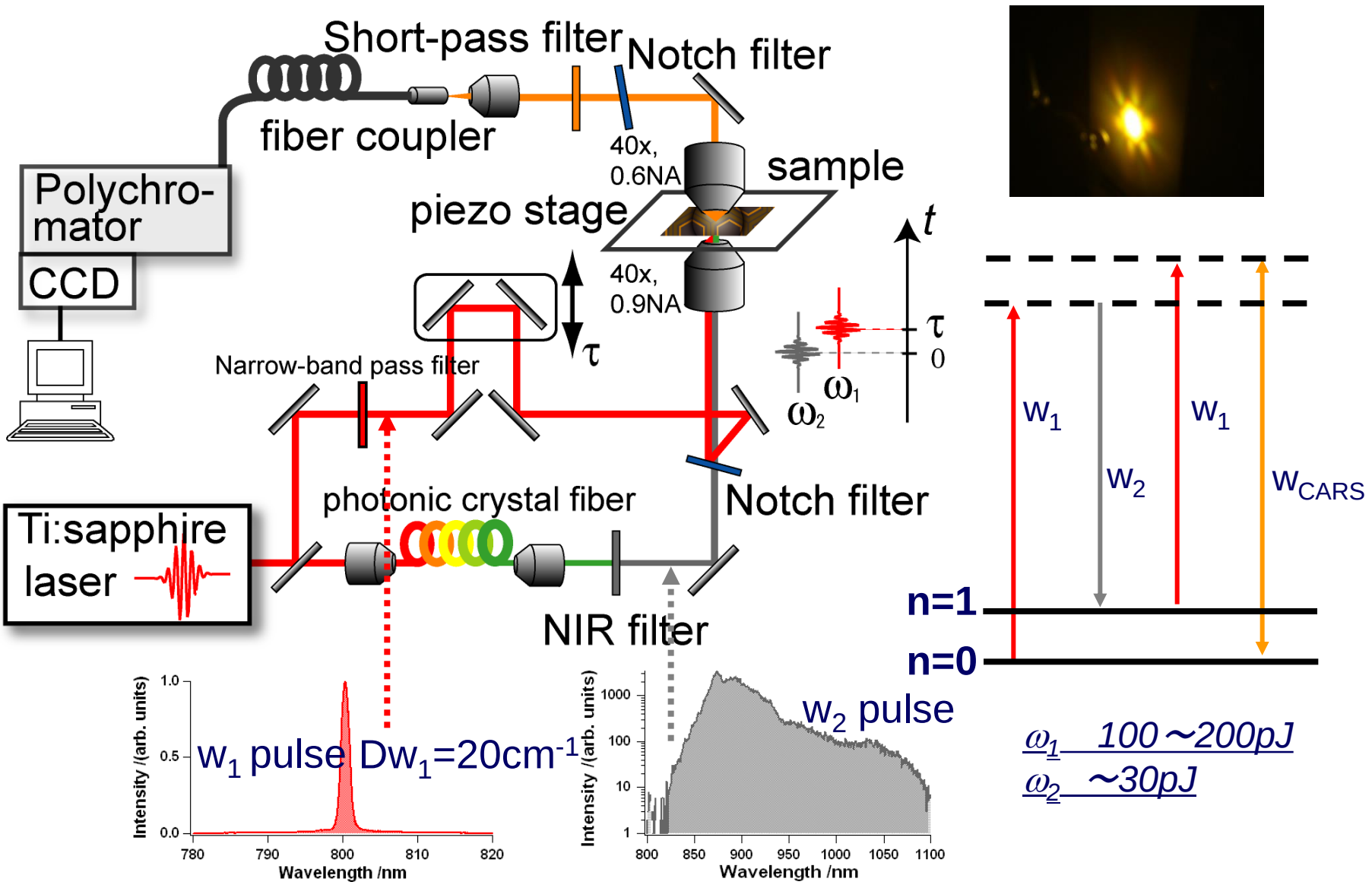

H. Kano and H. Hamaguchi, Anal. Chem., **79**, 8967-8973 (2007).

Vibrational CARS Movies of a Single Budding Yeast Cell

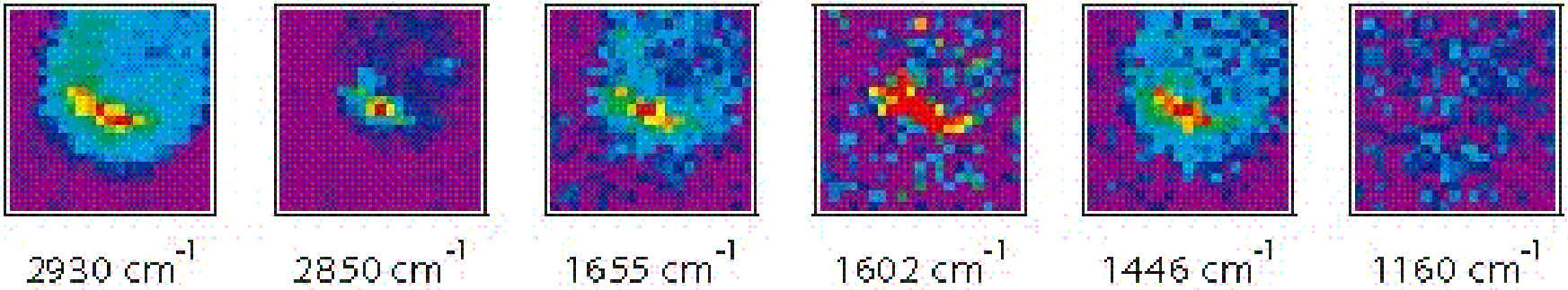

w_1: 10 mW, w_2: 10 mW

Expo. time/pixel: 30 msec

Image acquisition time: ~ 12 sec

Quantifying CARS by MEM and Noise Reduction by SVD

CARS spectra

Imc_3 spectra by MEM

Imc_3 spectra after SVD

Raman spectra

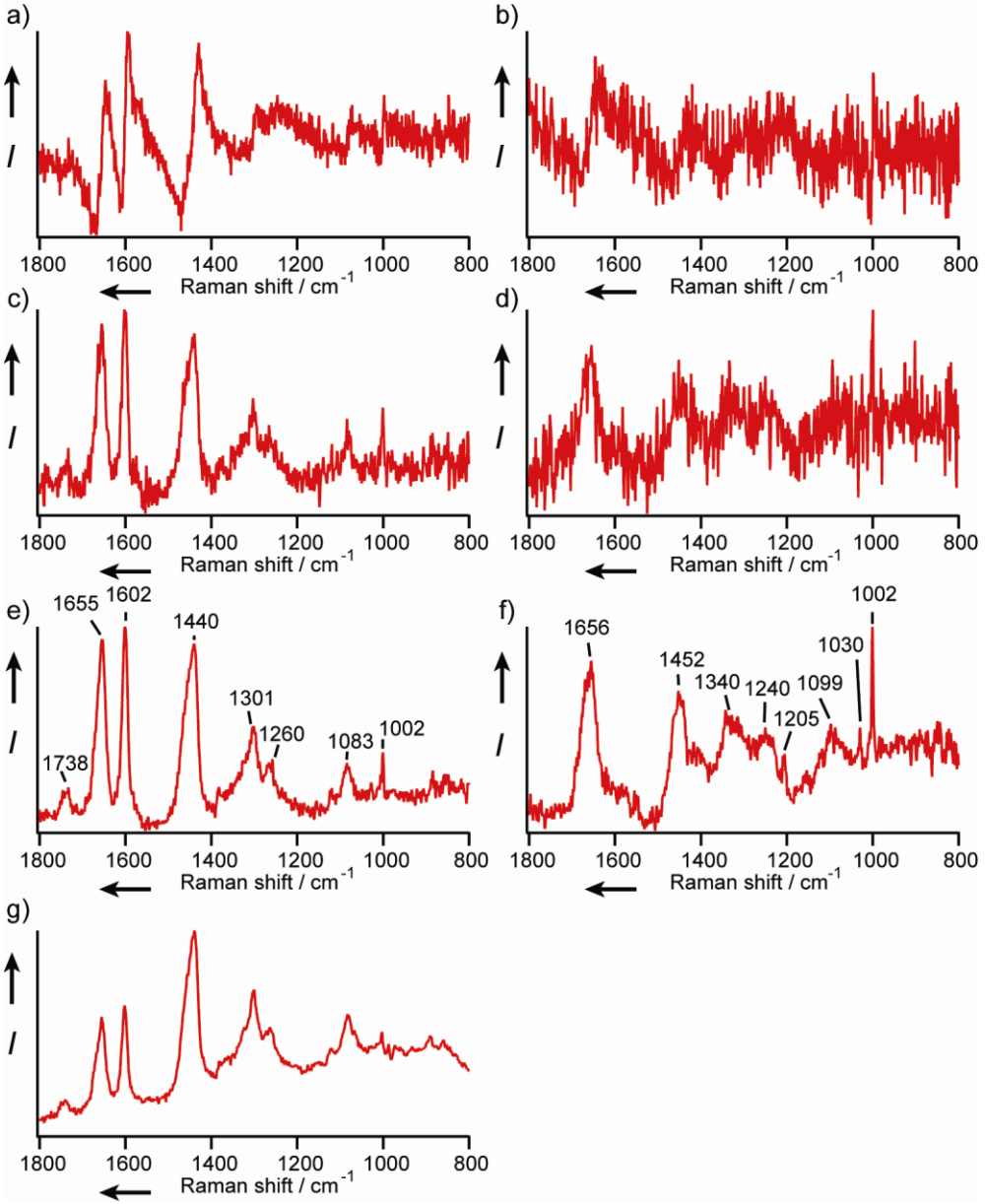

Multi-focus Confocal Raman Microspectrometer

Laser source:
Nd: YVO_4
Wavelength: 532 nm
Power: ~ 2 W

Microlens array

500 nm blaze
1200 grooves / mm

X 100
NA 1.3
oil immersion

Objective

Spectrograph

Bundle fiber

CCD camera

Edge filter

Pinhole array

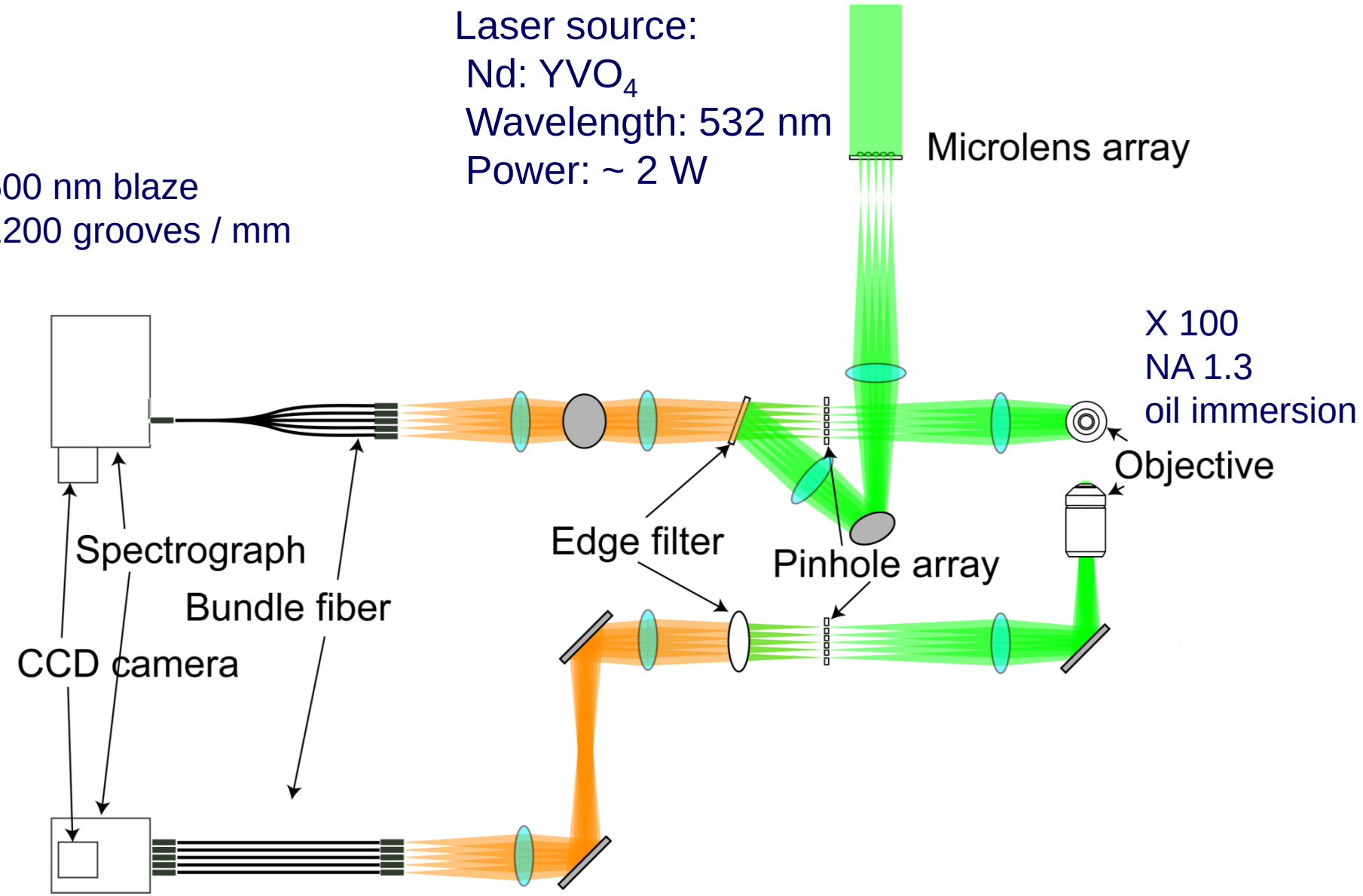

Microlens and Pinhole Arrays

Microlens array

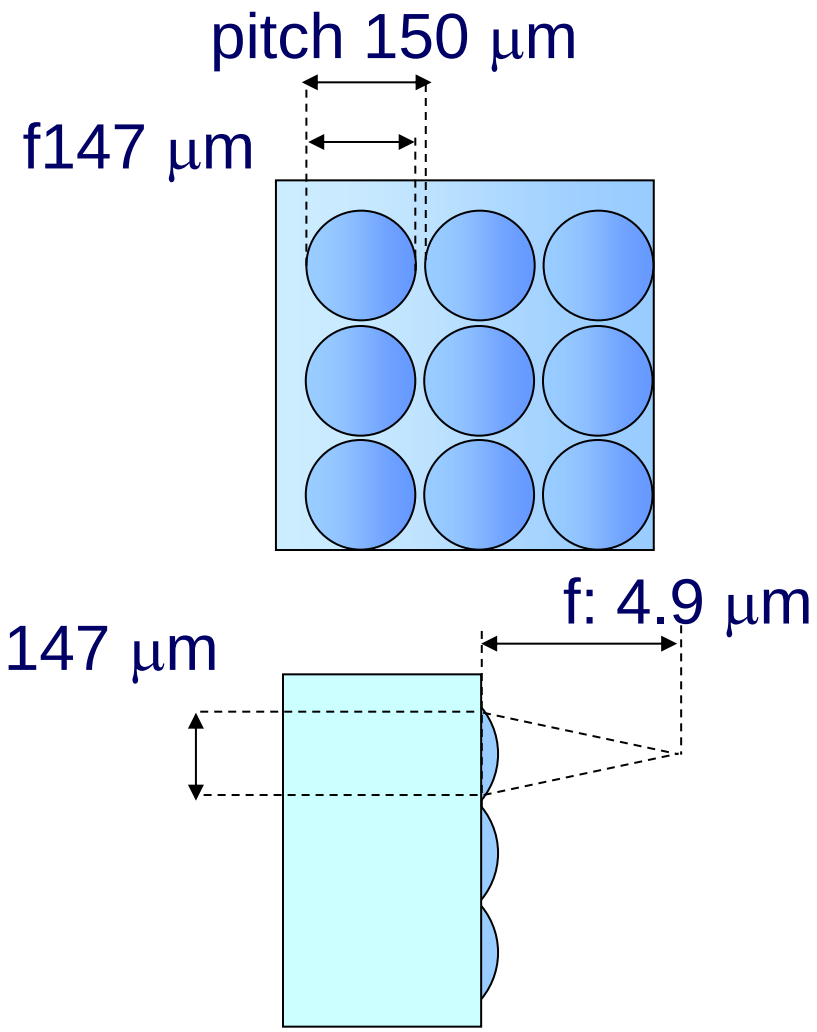

Pinhole array

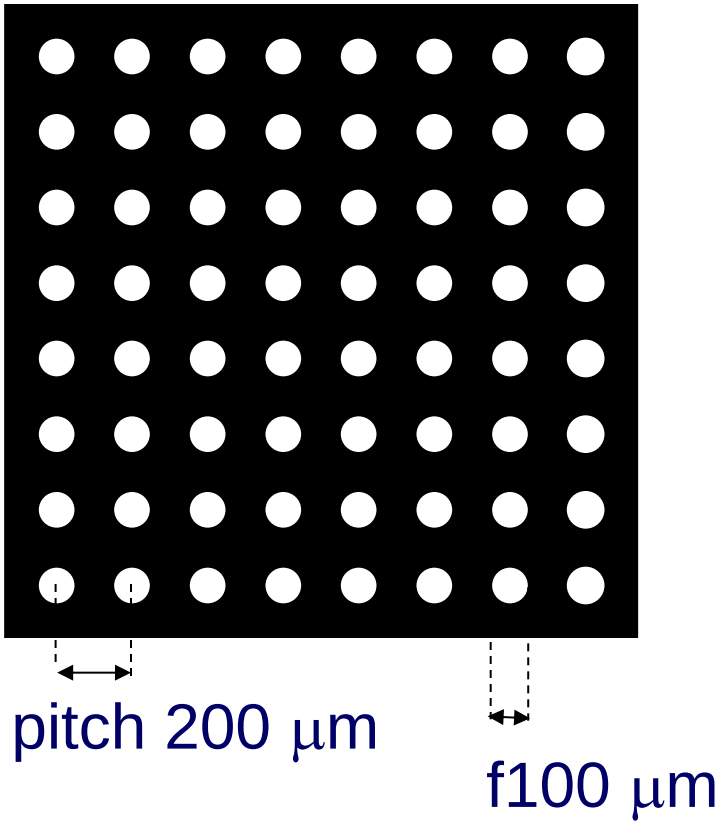

Multi-focus Scanning

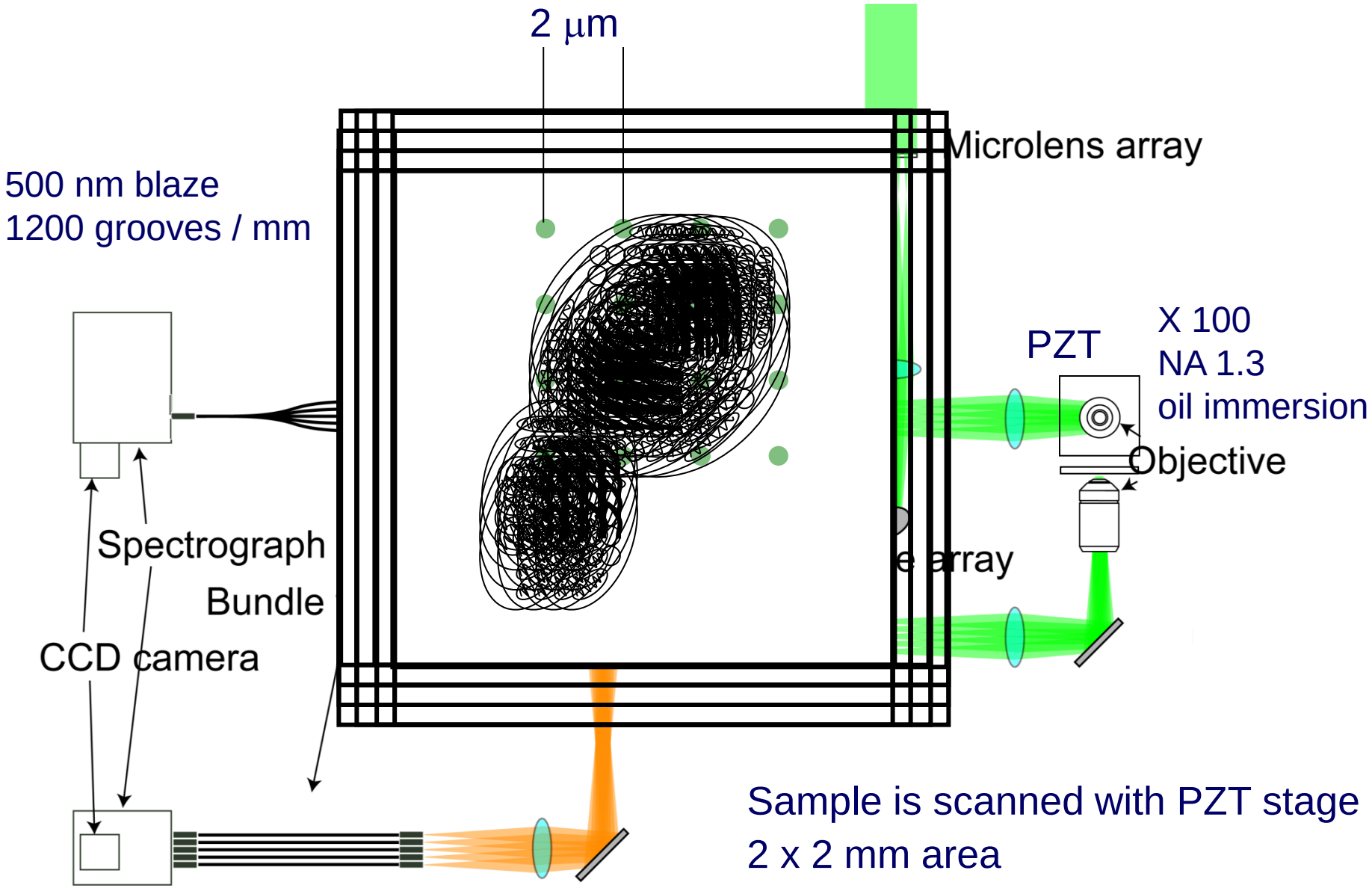

Lateral and Axial Spatial Resolution

Intensity profile of Raman band @ 1602cm^{-1} of single f 500 nm polystyrene bead

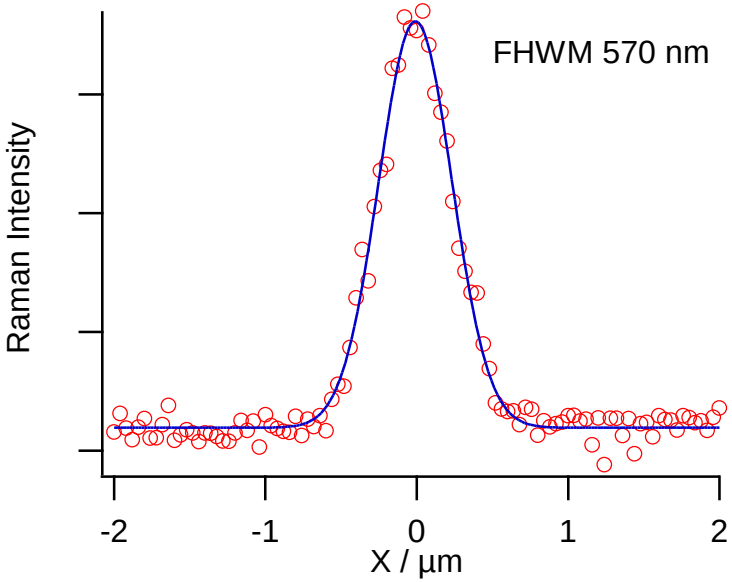

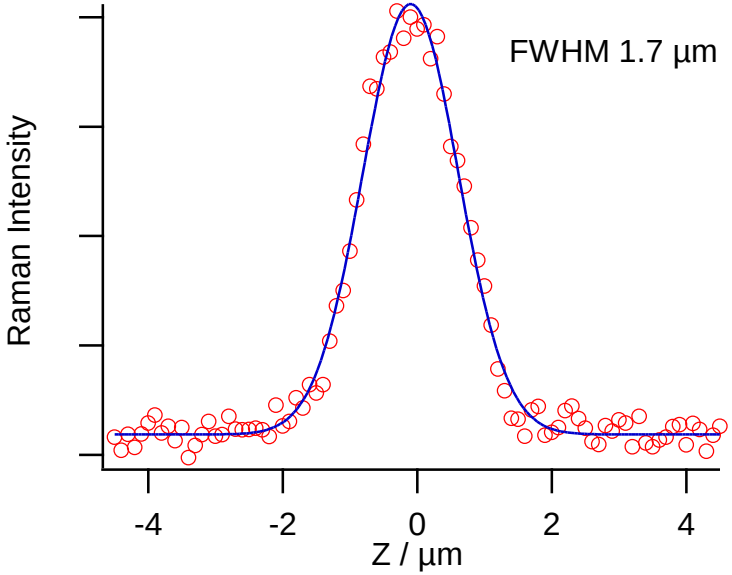

lateral

~ 500 nm

axial

~ 1.5 mm

Budding yeast cells

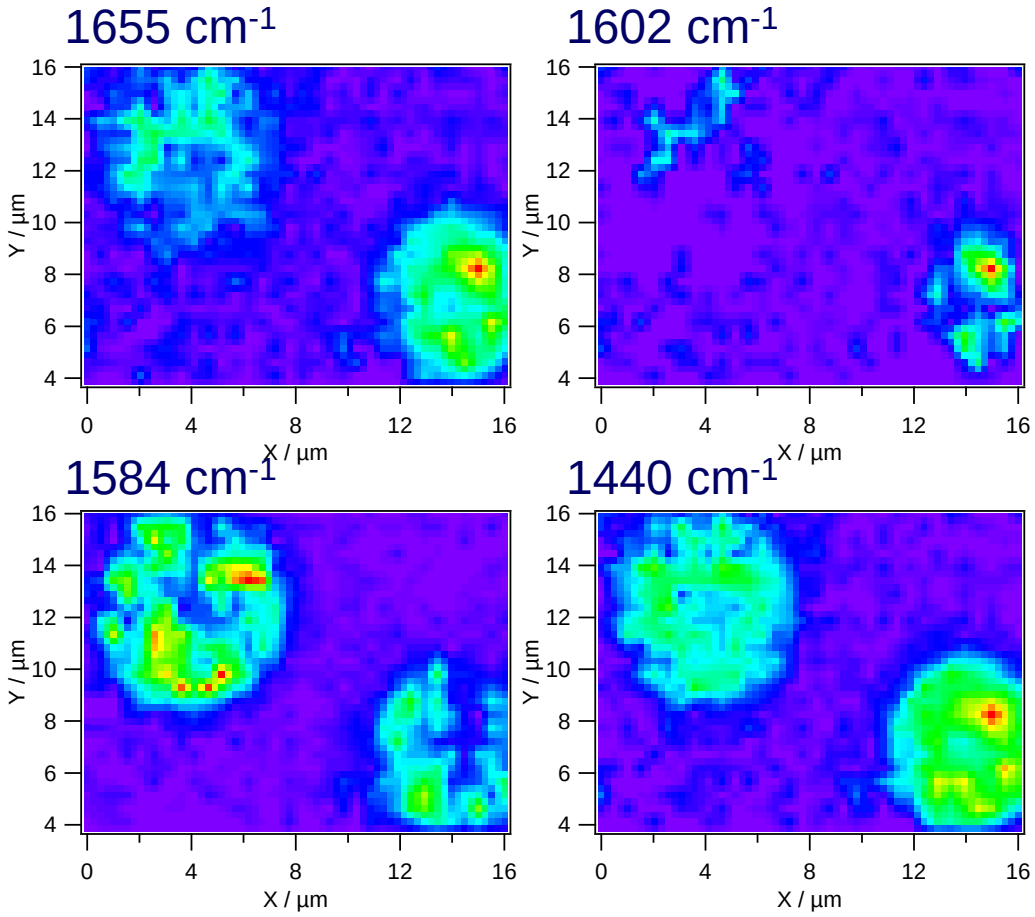

- Laser power : 1 mW
- Exposure time: 1 sec
- Readout time: ~150 msec
- PZT scan 4 x 4 points

  2 x 2 mm

  Total area: 16 x 12 mm
- Total image acquisition time

  (1 sec+ 0.2 sec) x 4 x 4

~20 sec / image !!

Raman and CARS Microspectroscopy at Tokyo

Multifocus Confocal Raman

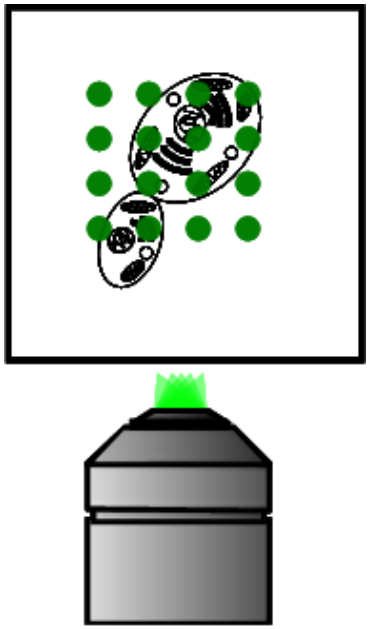

Multiplex CARS

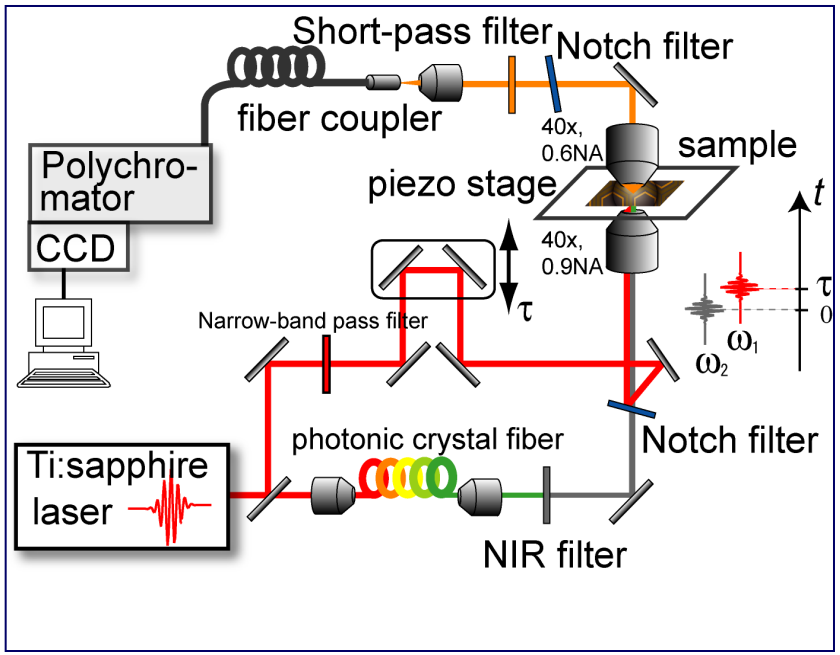

They say Raman is weak and CARS is strong. Is this true?

Spontaneous Raman vs CARS

Raman cross section $d^2s/dWdk$ vs CARS susceptibility χ_{CARS}

$$\mathrm{Im}\,\chi = \frac{\pi c^4}{24\hbar\omega_1\omega_2{}^3}\frac{Nd^2\sigma}{d\Omega d(\omega_1-\omega_2)}(1-e^{-\hbar(\omega_1-\omega_2)/kT})$$

N: number density

w_1, w_2: angular frequency of lasers

*M. D. Levenson, Introduction to Nonlinear Laser Spectroscopy

Raman signal is proportional to $d^2s/dWdk$, N

CARS signal is proportional to χ^2, N^2

Petrov et al. PANS, 104, 7776-７７７９ （２００７）.
Peslov et al. Opt. Lett. 32, 1725-1727 (2007).
Cui et al. Opt. Lett. 34, 773-775 (2009).

How Weak Is Raman?

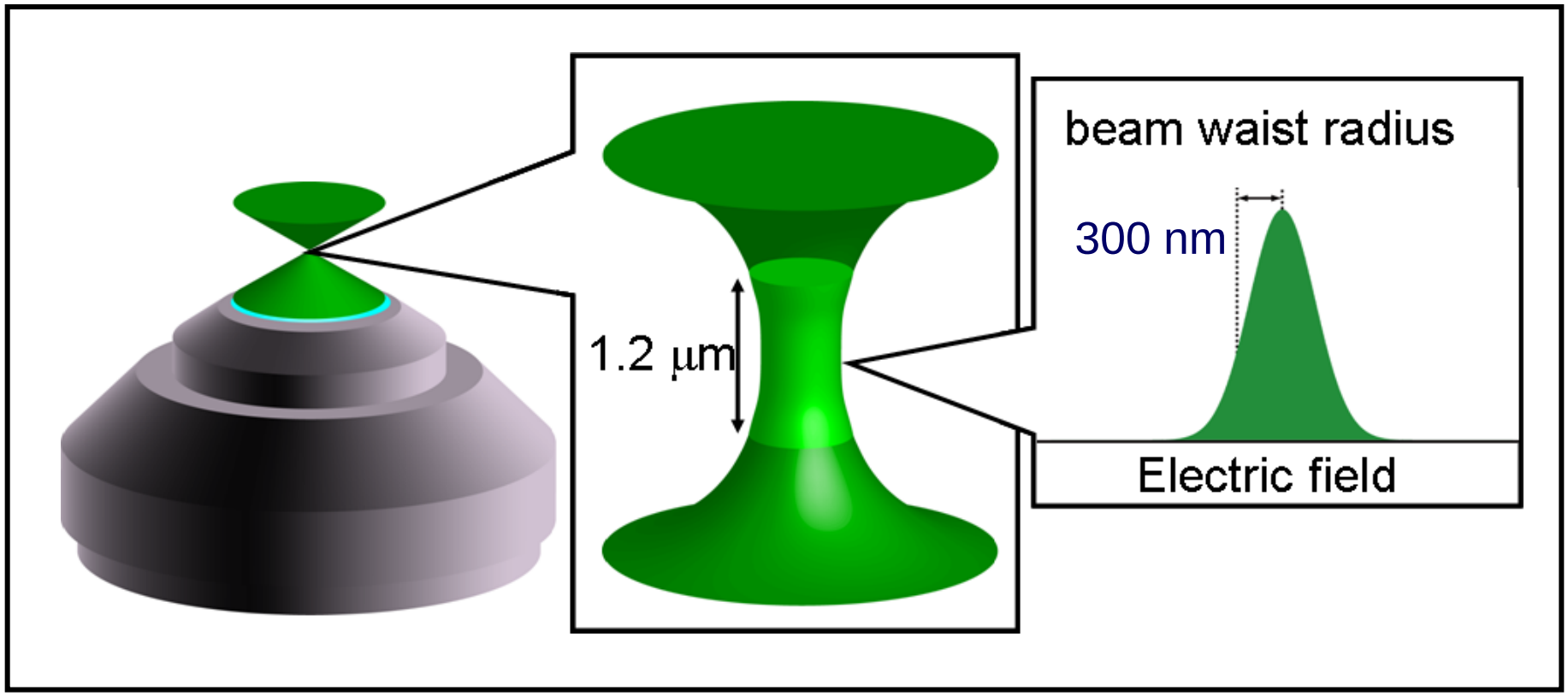

Objective: x100 NA1.3 oil immersion

Beam waist radius: 300 nm

Sample height: ~1.2 mm (confocal effect)

Laser:

Wavelength 532 nm

Average power 1 mW @ sample

Photon flux at the focal volume:

$3.5 \times 10^{5}\ _{[J]} / 3.7 \times 10^{-19}\ _{[w/cm^2]} = 0.97 \times 10^{24}\ _{[/s\ cm^2]}$

Liquid benzene:

Raman cross-section of 992 cm^{-1} band at 532 nm

2.2×10^{-29} cm^2/molecule sr *

*Y. Kato and H. Takuma, J. Chem. Phys. **54**(12) 5398 (1971).

Number of Raman photons per cm^3 per sec:

$1.4 \times 10^{17}\ _{[/cm^3\ s\ sr]}$

Number of Raman photons per sec:

Focal volume: f 600 nm x 1.2 mm

$(300 \times 10^{-7}\ _{[cm]})^2 \times p \times 1.2 \times 10^{-4}\ _{[cm]} = 3.4 \times 10^{-13}\ _{[cm^3]}$

$1.4 \times 10^{17}\ _{[/cm^3\ s\ sr]} \times 3.4 \times 10^{-13}\ _{[cm^3]} = \sim 4.8 \times 10^{5}\ _{[/s\ sr]}$

Compensation for the Collection Solid Angle

Dipole radiation

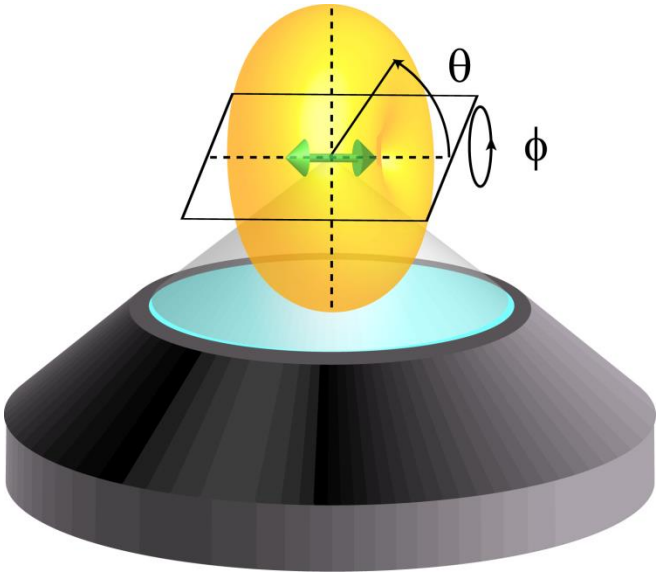

Radiation in the direction of q

Radiation intensity $\propto \sin^2 q\, dq$

NA 1.3
oil (refractive index=1.5) immersion

⇒ q: 1/6 p ~ 5/6 p

f: 1/6 p ~ 5/6 p

Integration over the volume collected by the objective

$$\int_{\frac{\pi}{6}}^{\frac{5\pi}{6}} d\phi \int_{\frac{\pi}{6}}^{\frac{5\pi}{6}} \sin\theta d\theta \sin^2\theta = \frac{2\pi}{3} \times \frac{3\sqrt{3}}{4} = 2.7 \text{[sr]}$$

4.8×10^5 [/s sr] x 2.7 [sr] = 1.4×10^5 [/s]

CCD detection

1 count / 0.71 e

Miceoscope/Spectrometer throughput

Objective lens	~80 %
Silver mirror x4	95 % for each
Lens x3	99 % for each
Spectrograph	55 %
Edge filter x2	95 & 90 %

Total ~0.3

Final counts: 5.7×10^4 [/s mW]

Comparison with Experiment: Integrated intensity of 992 cm^{-1} band

Experiment

4.0×10^4 [/s mW]

$\Longleftrightarrow$

Theory

5.7×10^4 [/s mW]

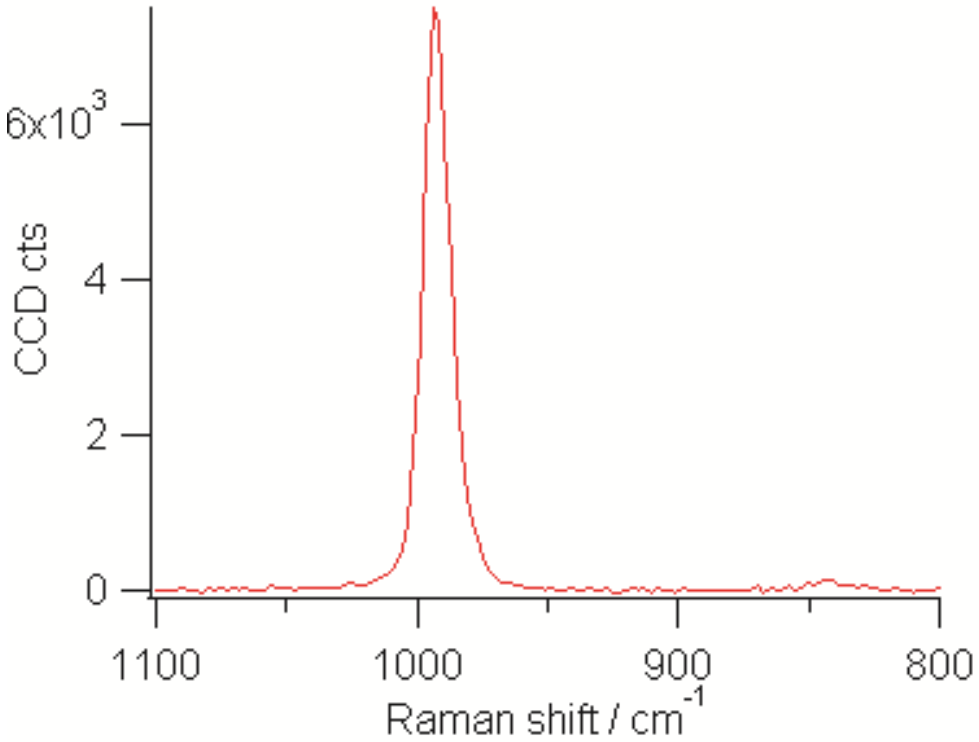

How Strong Is CARS?

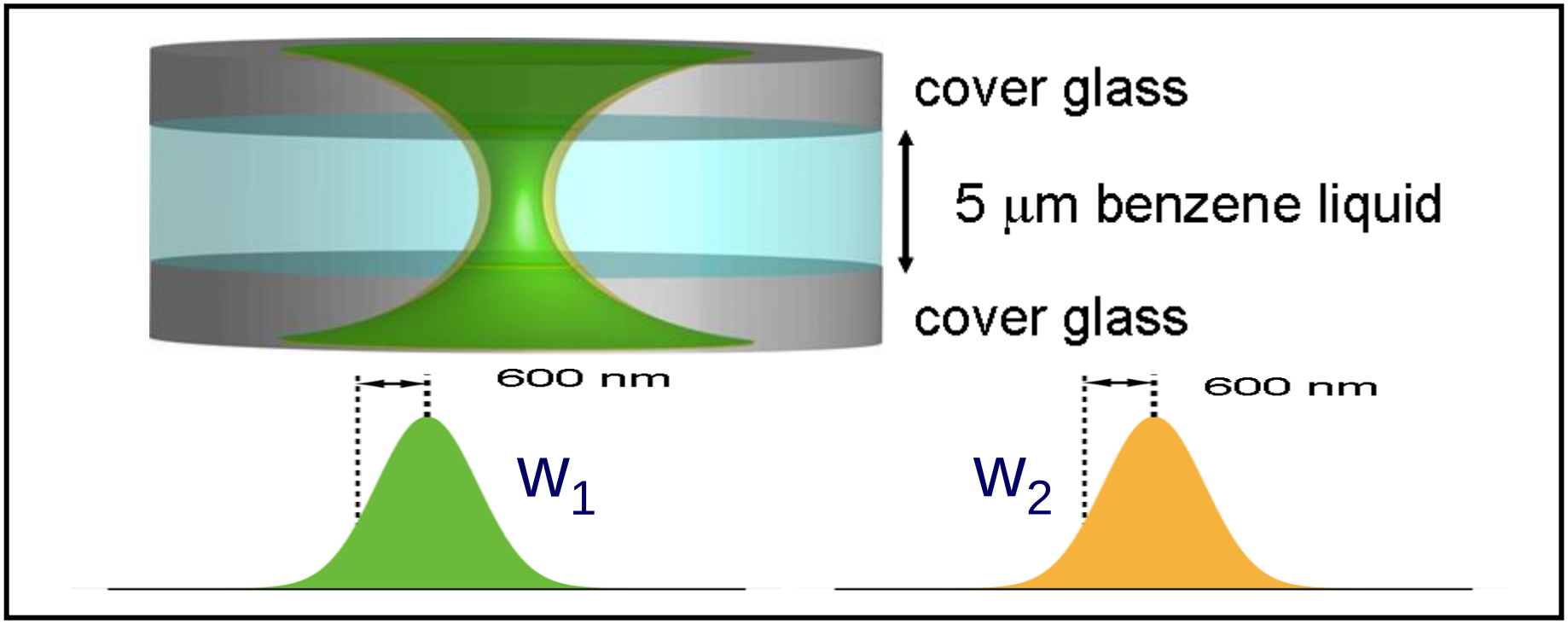

Objective: x100 NA1.3 oil immersion

Beam waist radius: 600 nm

Sample height: 5 μm

Laser: Pulse width 1 ns; Repetition rate: 33 kHz

w_1: 1064 nm, 1 mW @ sample

w_2: 1.1 -1.7 mm, 1 mW @ sample

Formulation of CARS Intensity

G. C. Bjorklund, IEEE J. Quant. Electron. **QE-11** (6) 297 (1975).

Electric field of CARS signal at **r**

$$E(\vec{r}) = i\frac{3N}{k_{CARS}}\pi k_0{}^2 b\chi E_1{}^2 E_2{}^* \times \exp(ik'z)$$

$$\times\int_{-\varsigma}^{\varepsilon} d\varepsilon' \frac{\exp[-(ib/2)\Delta k(\varepsilon'-\varepsilon)]}{(1+i\varepsilon')(k''-ik'\varepsilon')H}\exp\left[\frac{-(x^2+y^2)}{bH}\right]$$

$$H = \frac{(1+\varepsilon'^2)}{(k''-ik'\varepsilon')} - i\frac{\varepsilon'-\varepsilon}{k'}$$

confocal parameter:

$$b = \frac{2\pi\omega_0{}^2 n}{\lambda} \qquad \varepsilon' = \frac{2(z-f)}{b}$$

w_0: beam waist radius

n: refractive index of the sample

f: position of focus

wave vectors relations:

$$k' = 2k_1 - k_2$$
$$k'' = 2k_1 + k_2$$
$$\Delta k = k_{CARS} - k'$$

$k_{1,2}$: wave vectors of w_1 and w_2

k_{CARS}: wave vectors of signal in medium

k_0: wave vector of signal in vacuum

nomarized z position: e = 2(z-f)/b, z = 2f/b

How Strong is CARS?

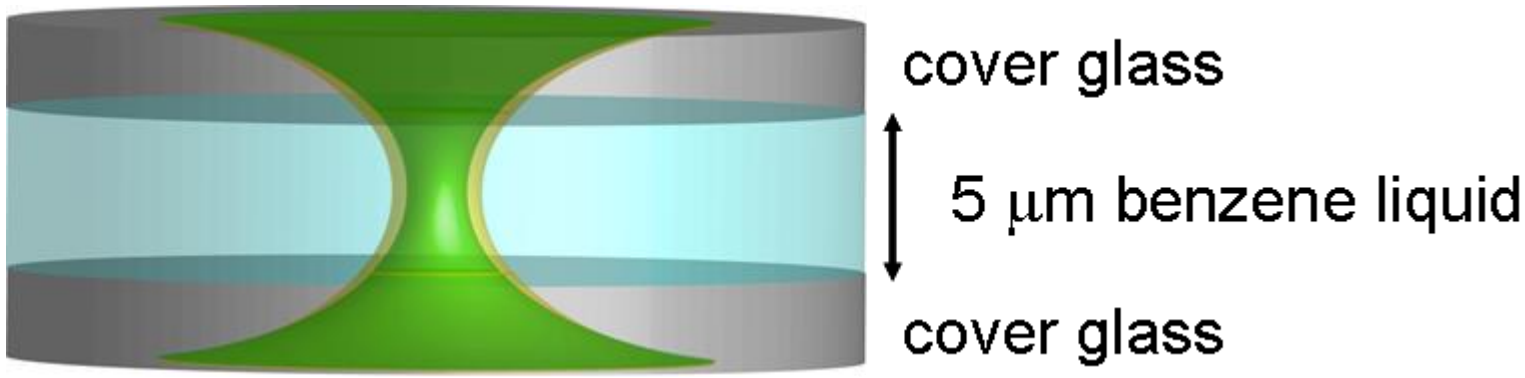

Liquid benzene:

Im $\chi^3_{1111} = 1.6 \times 10^{-13}$

*M. D. Levenson, Introduction to Nonlinear Laser spectroscopy

CARS photon: 1.1×10^8 [/s]

Experiment:

w_1: 1064 nm, 0.3 mW @ sample

w_2: 0.001 mW/ cm^{-1}@ 1190 nm

Experiment		Theory
6×10^5 [/s mW]	⟺	5.5×10^5 [/s mW]

Liquid Benzene

$N = 6.78 \times 10^{21}$ [/cm^3]

$d^2s/dWdk = 5.9 \times 10^{-30}$ [cm^2/molecule sr *]

	Spontaneous Raman	CARS
Average power	1 mW, 532 nm 1.4×10^5 [photons/s]	1 mW w_1 and w_2 1064 nm 1.1×10^8 [photons/s]
Average power	10 mW, 532 nm 1.4×10^6 [photons/s]	10 mW w_1 and w_2 1064 nm 1.1×10^{11} [photons/s]

A Model Biological Molecule (Lipids)

$N = 1 \times 10^{21}$ [/cm^3]

$d^2s/dWdk = 1 \times 10^{-32}$ [cm^2/molecule sr *]

	Spontaneous Raman	CARS
Average power	1 mW, 532 nm 35 [photons/s]	1 mW w_1 and w_2 1064 nm 7 [photons/s]
Average power	10 mW, 532 nm 350 [photons/s]	10 mW w_1 and w_2 1064 nm 7000 [photons/s]

Living Cell Microspectroscopy

CARS is much stronger than Raman
for > 10 mW

but

Raman is less weak than CARS
for < 1 mW.

Imaging under a Microscope

Wide-field

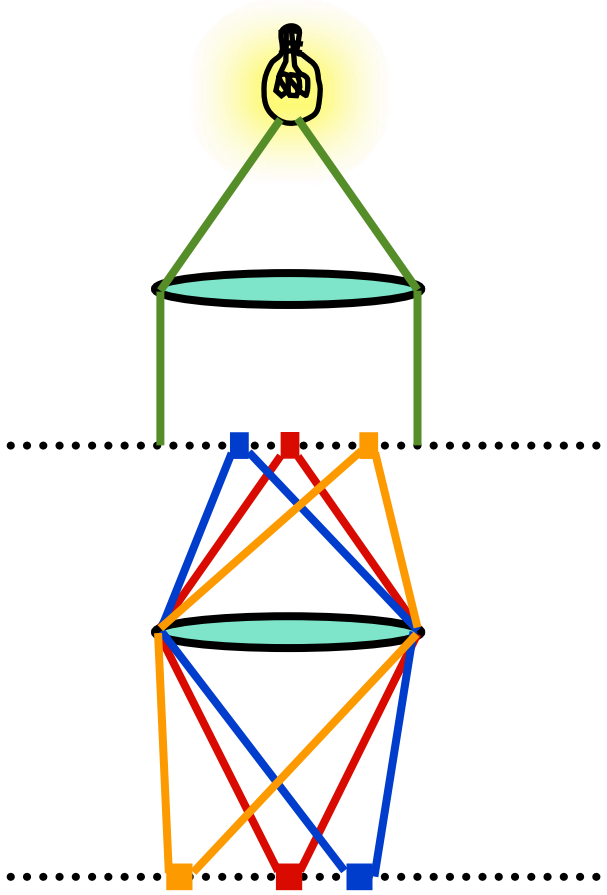

Confocal Scanning

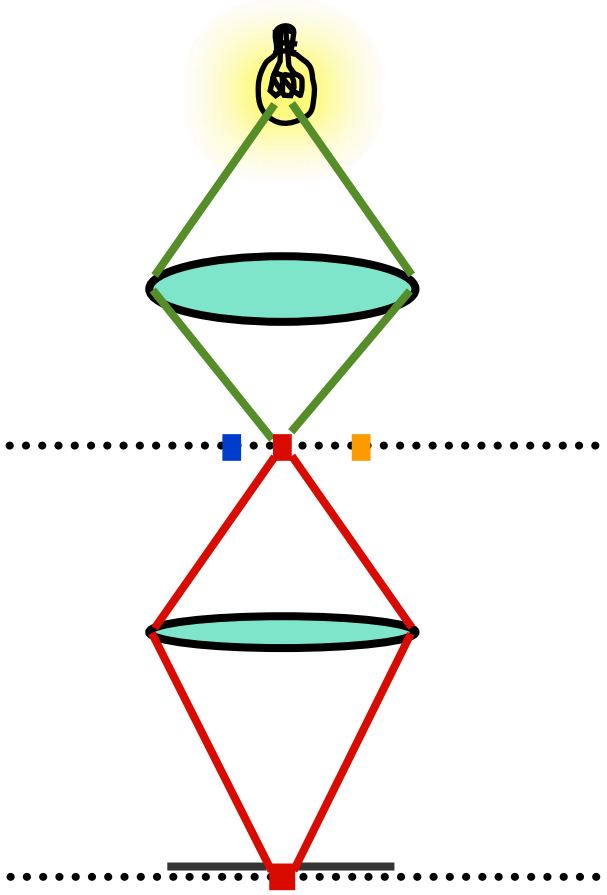

Conventional Wide-field Microscopy

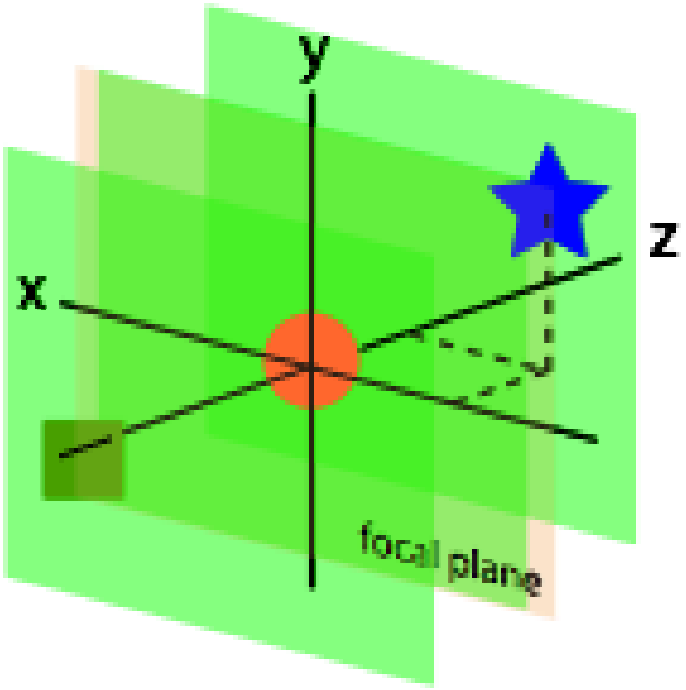

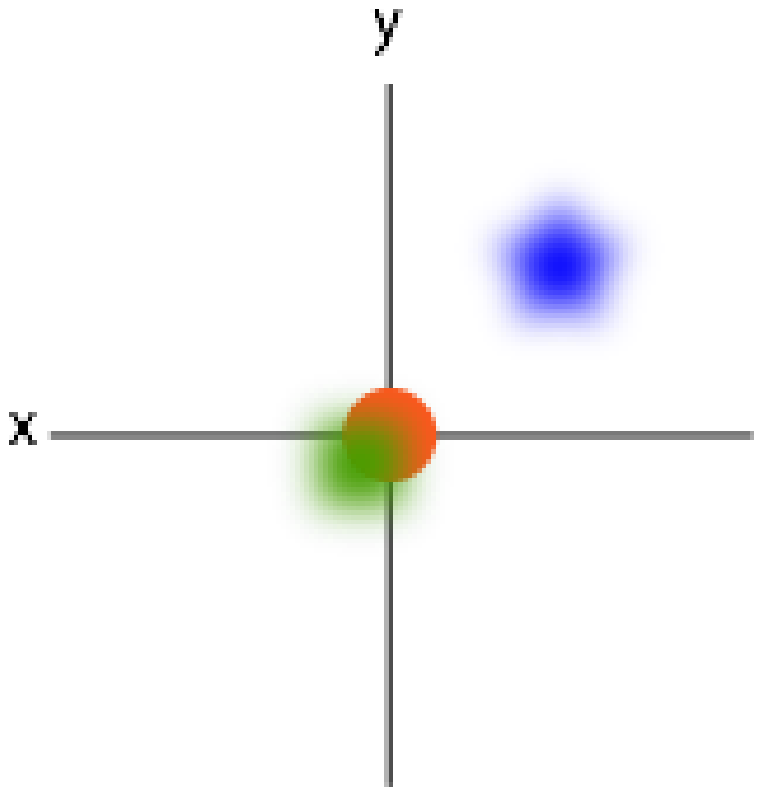

Poor axial resolution

Structured Illumination Wide-field Microscopy

December 15, 1997 / Vol. 22, No. 24 / OPTICS LETTERS 1905

Method of obtaining optical sectioning by using structured light in a conventional microscope

M. A. A. Neil, R. Juškaitis, and T. Wilson

Department of Engineering Science, University of Oxford, Parks Road, Oxford OX1 3PJ, UK

Received August 26, 1997

We describe a simple method of obtaining optical sectioning in a conventional wide-field microscope by projecting a single-spatial-frequency grid pattern onto the object. Images taken at three spatial positions of the grid are processed in real time to produce optically sectioned images that are substantially similar to those obtained with confocal microscopes.

Sectioned wide-field image

$$I_p = \left[(I_1 - I_2)^2 + (I_1 - I_3)^2 + (I_2 - I_3)^2 \right]^{1/2}, \qquad (4)$$

Conventional wide-field image

I_0, can be recovered from $I_1 + I_2 + I_3$.

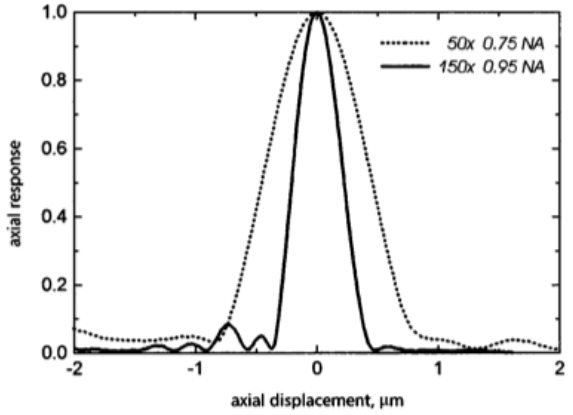

Fig. 2. Measured axial responses of the system.

Structured Illumination Microscopy

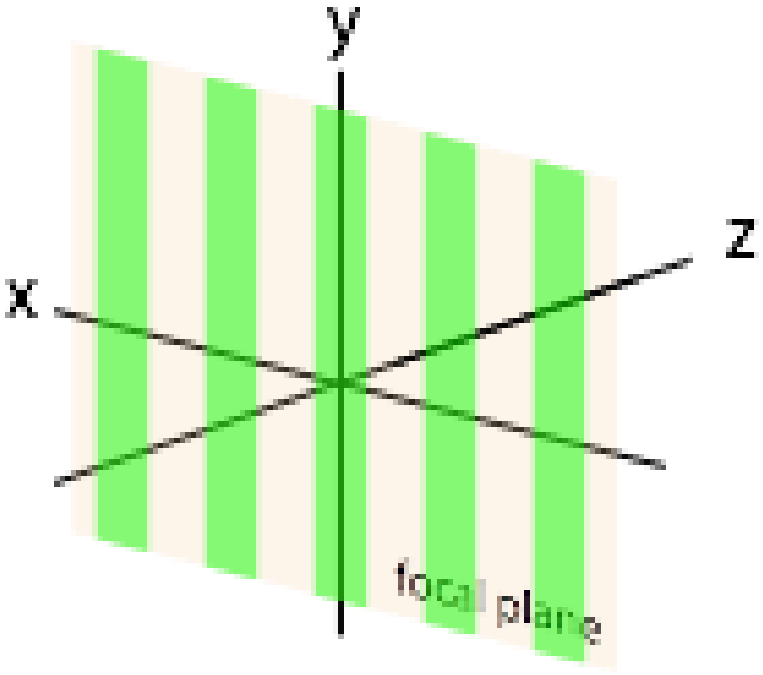

Clear structure
at the focal plane

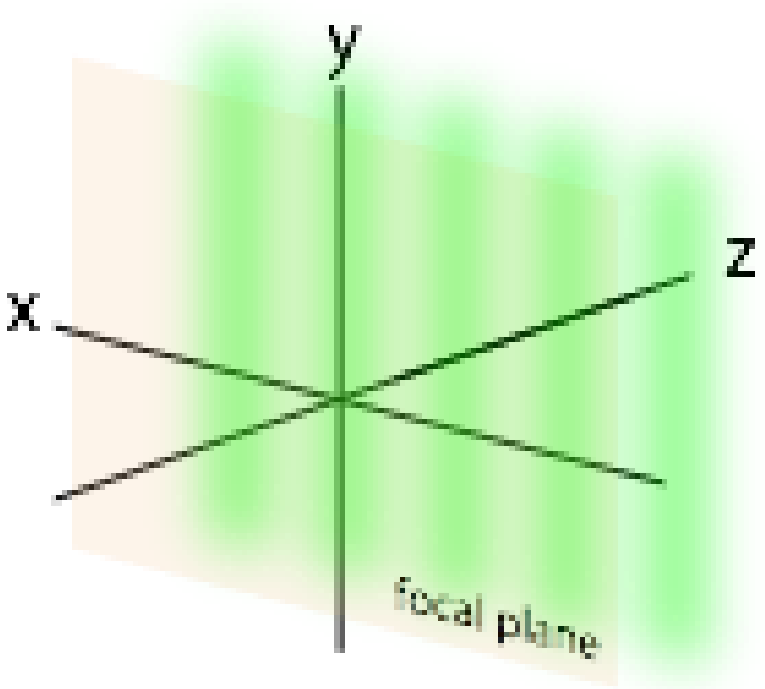

Blurred structure
off the focal plane

Structured Illumination Microscopy

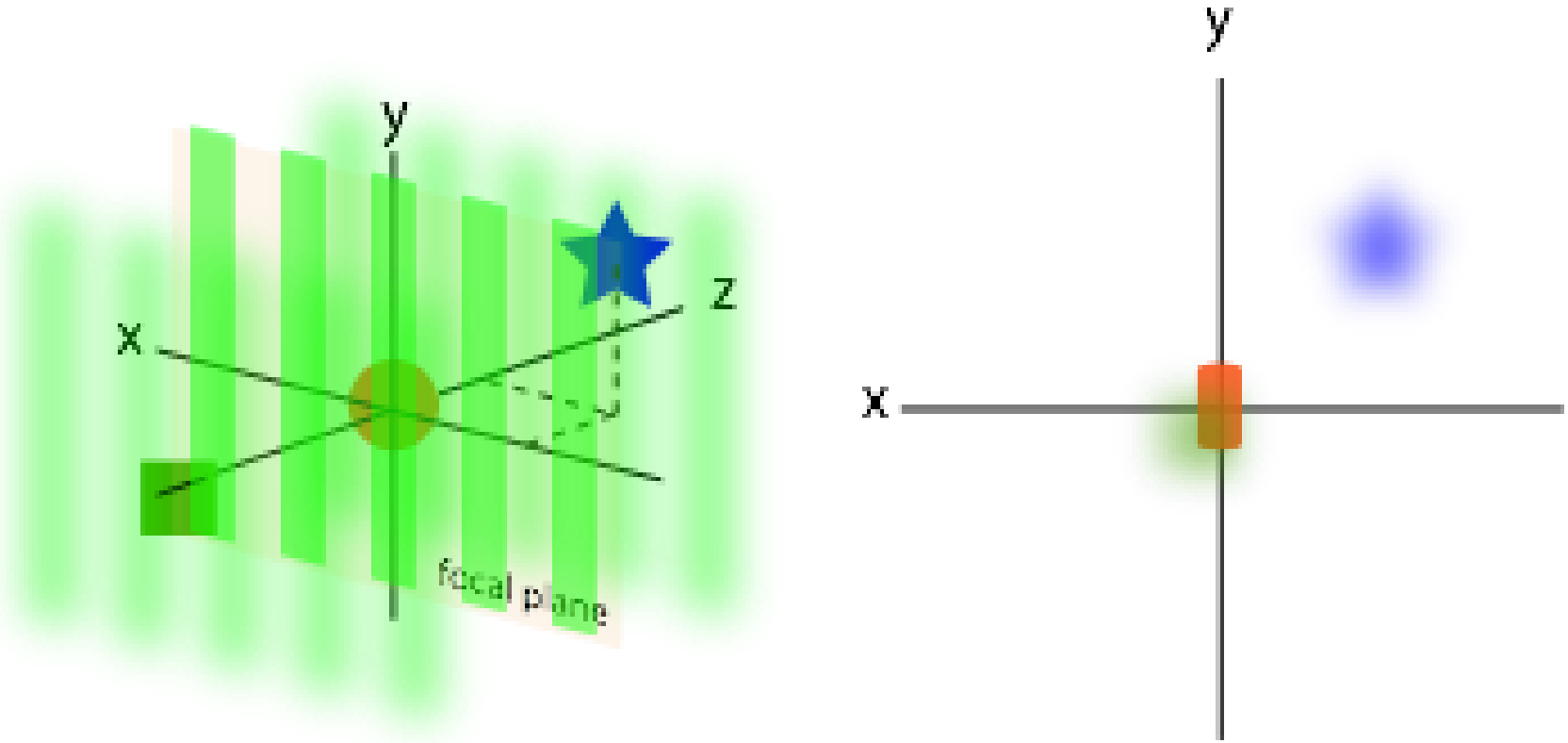

Images of the objects on the focal plane clearly reflect the structure of the illumination.

Structured illumination microscopy

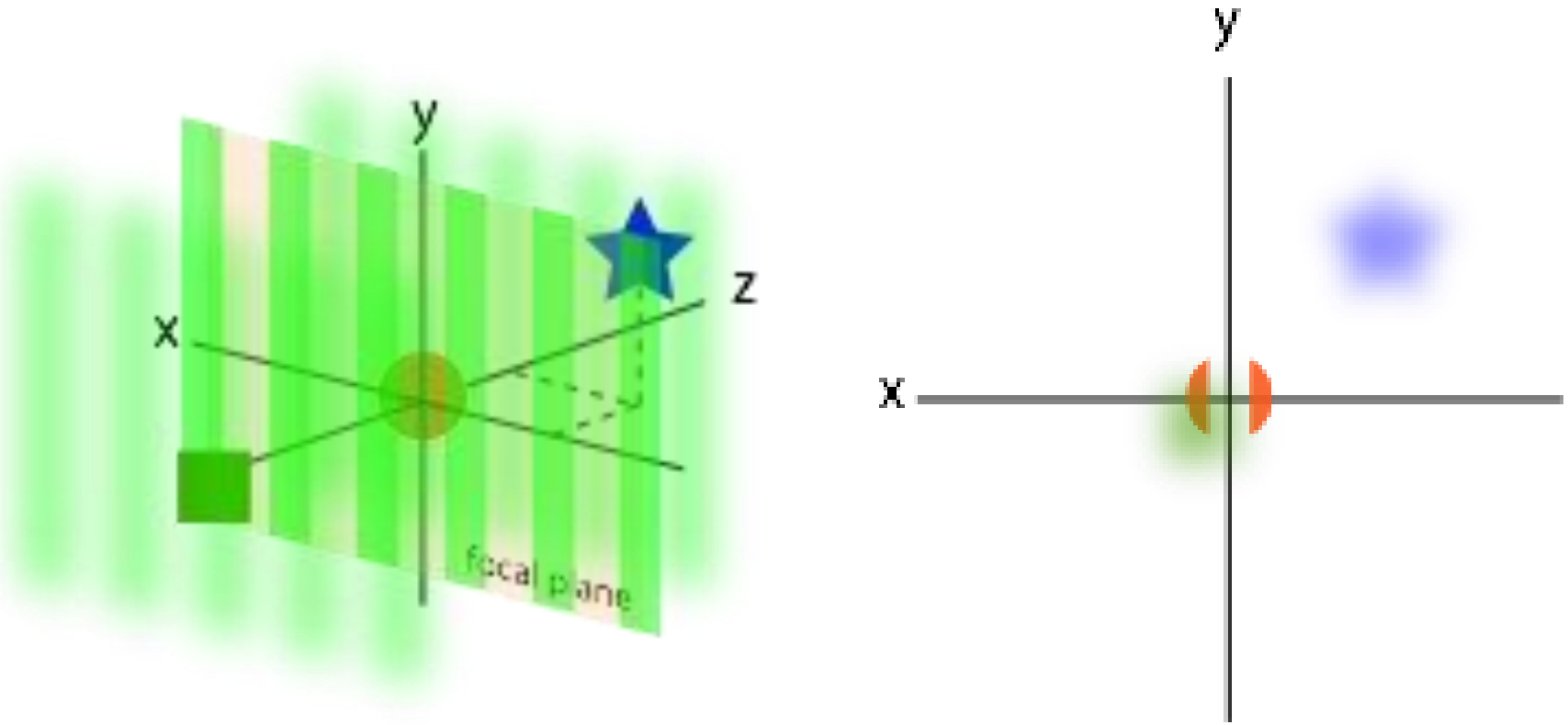

Images of the objects on the focal plane clearly reflect the structure of the illumination.

Structured illumination: Reconstruction

Series of images with different grid positions...

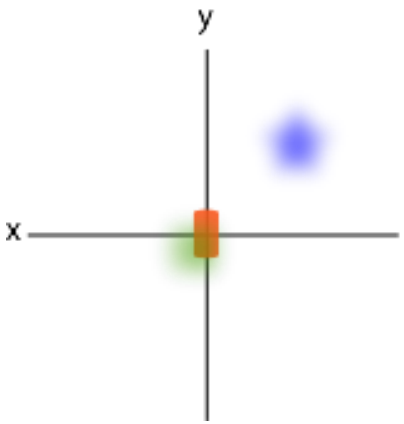

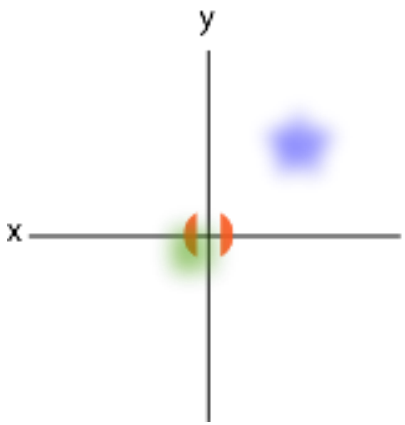

Post processing of those images to extract AC component

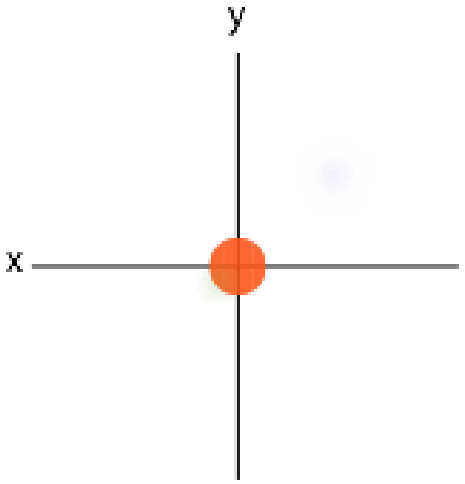

High axial resolution!

SIRM setup

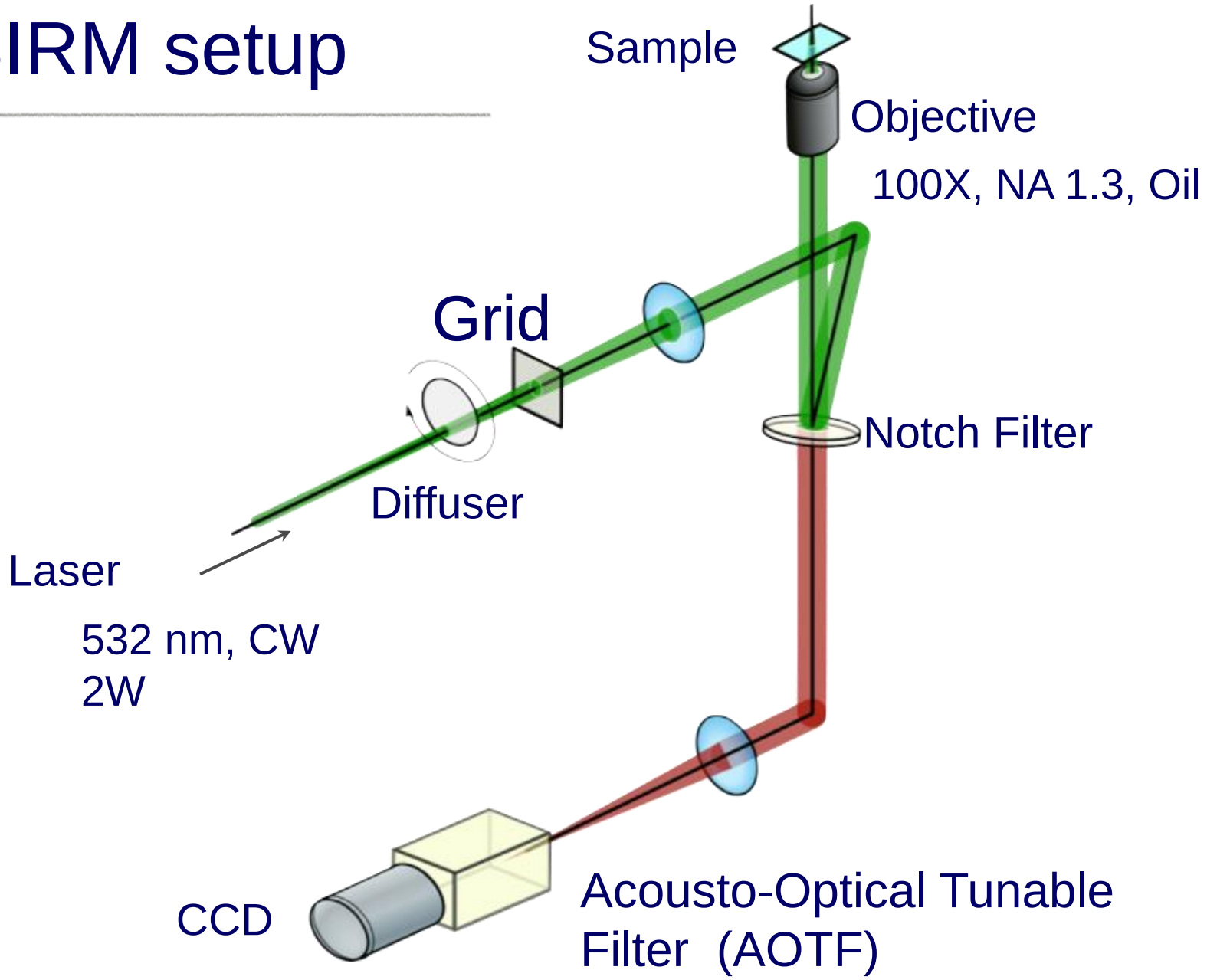
Sample
Objective
100X, NA 1.3, Oil
Grid
Notch Filter
Diffuser
Laser
532 nm, CW
2W
CCD
Acousto-Optical Tunable
Filter (AOTF)

Wide-field Raman images of polystyrene beads

Optical Image

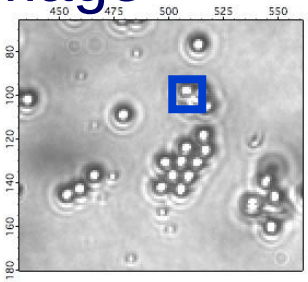

950 cm^{-1}

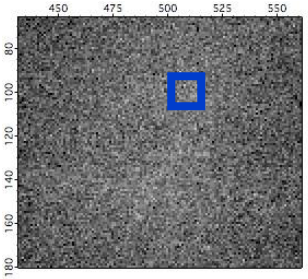

980

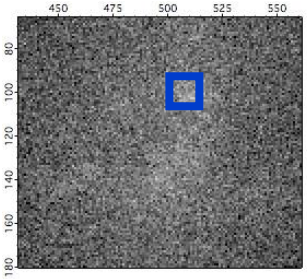

990

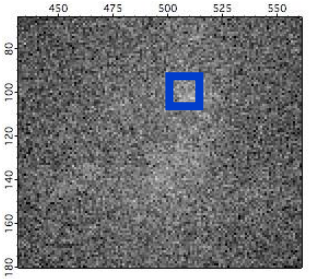

1000

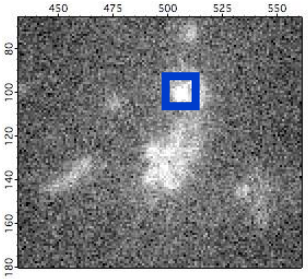

1010

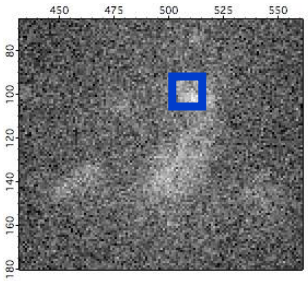

1020

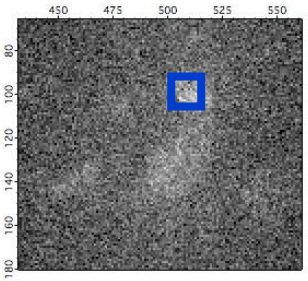

1050

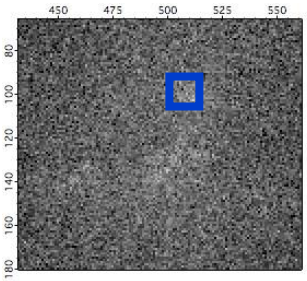

1100

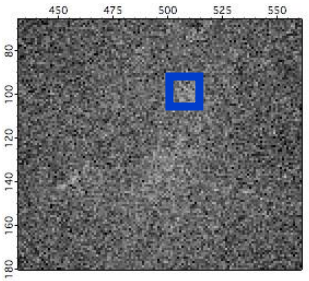

1200

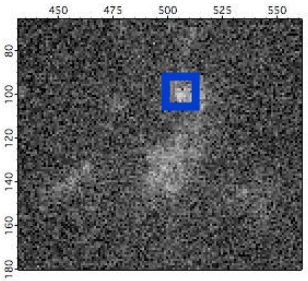

1300

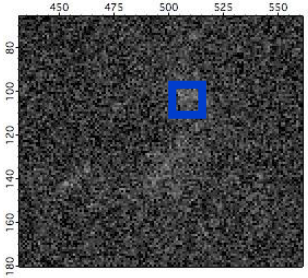

1400

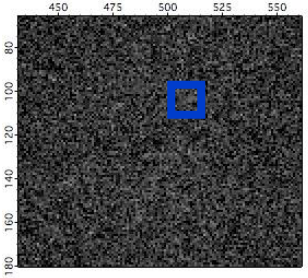

1500

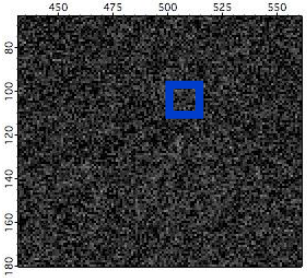

1600

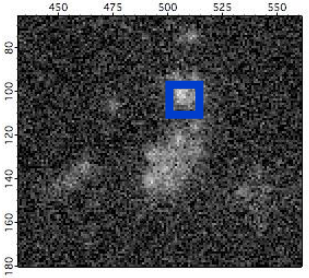

1700

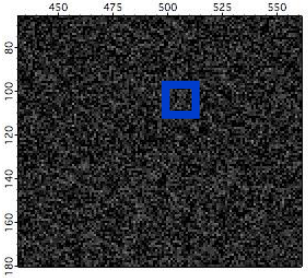

Illumination pattern

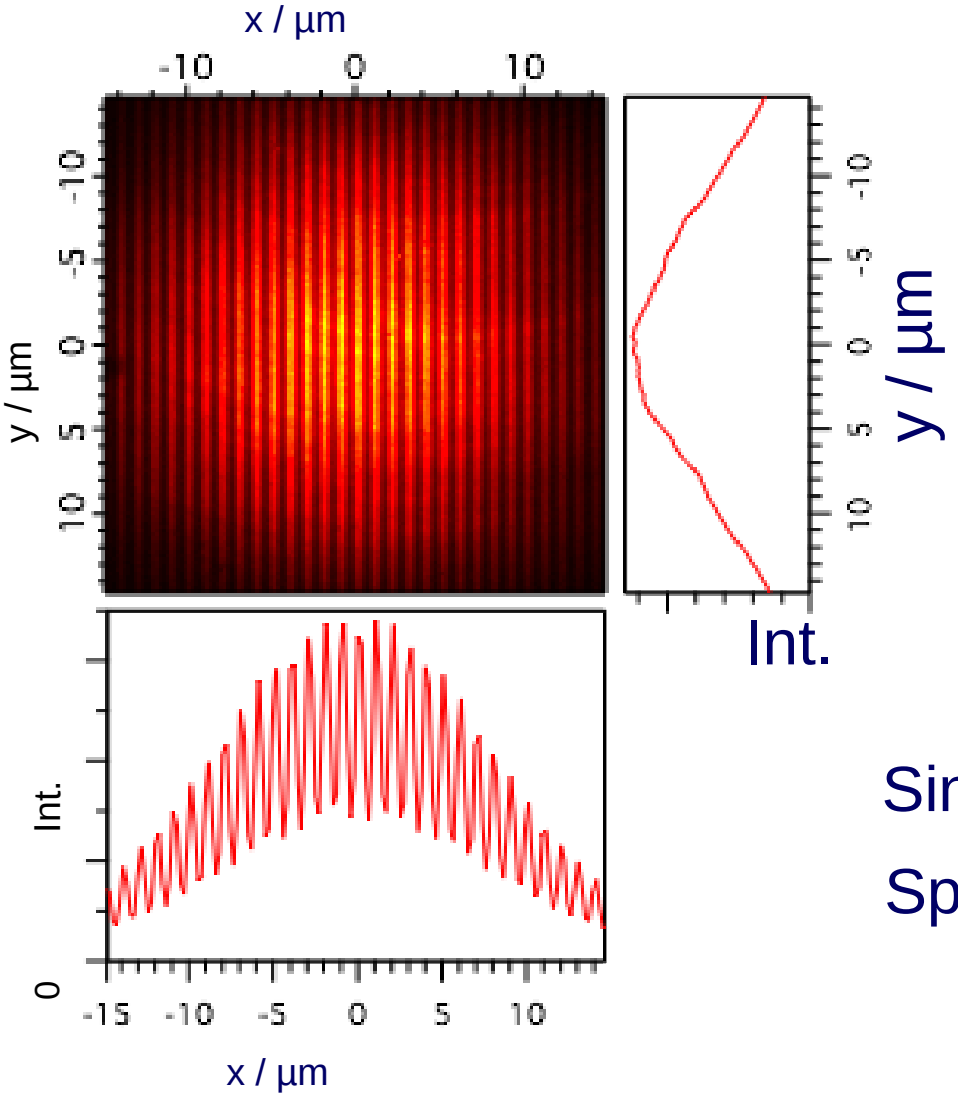

Envelope of the laser intensity follows gaussian beam profile

Sinusoidal pattern

Spacing: 1 µm

SIRM image

3 μm polystyrene beads

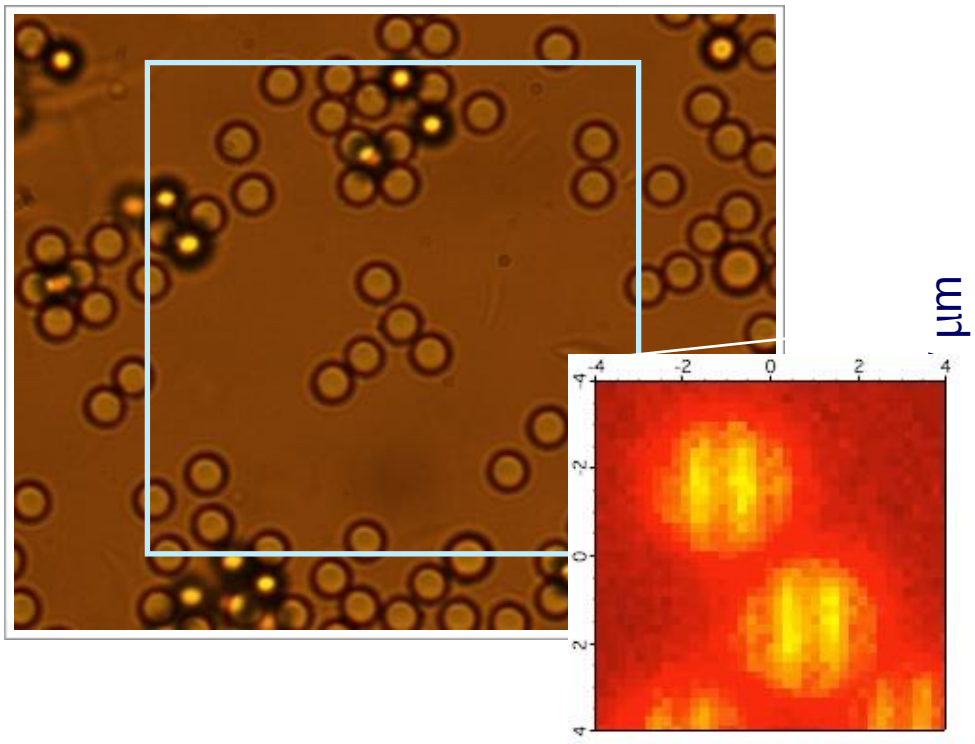

Raman image
(10s exposure/frame)

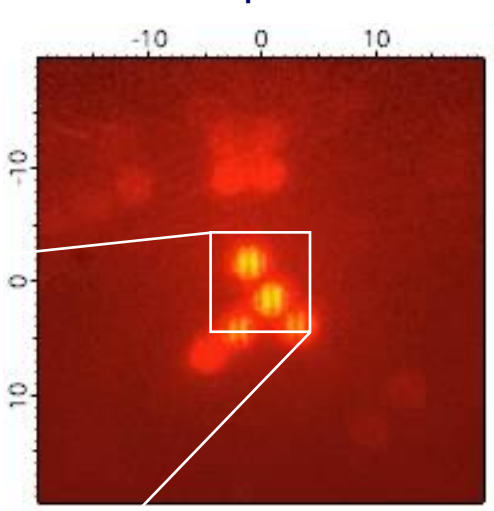

186 x 186 pixels
210 nm pitch

10 sec / 1 grid position
190 sec (total) / image
Raman shift @ 1000 cm^{-1}

Sectioned image

Oscillating component

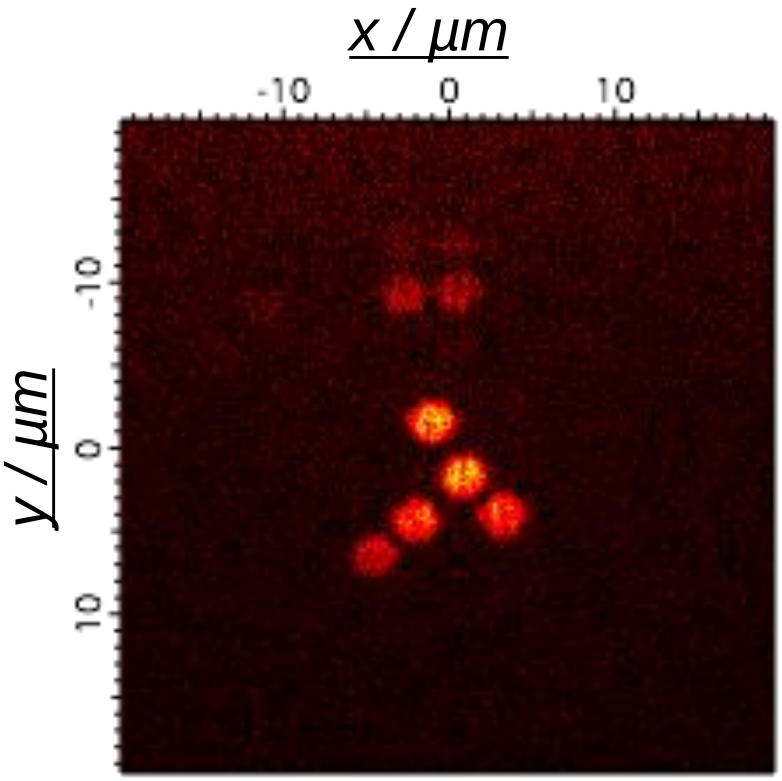

Sectioned image

Constant component

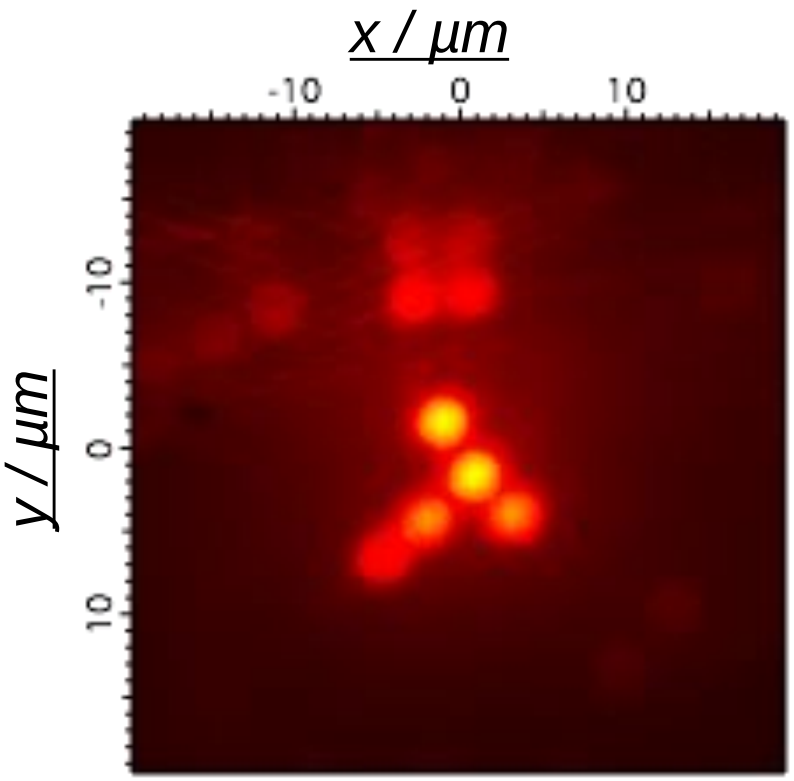

Conventional wide-field image

Lateral Spatial Resolutions

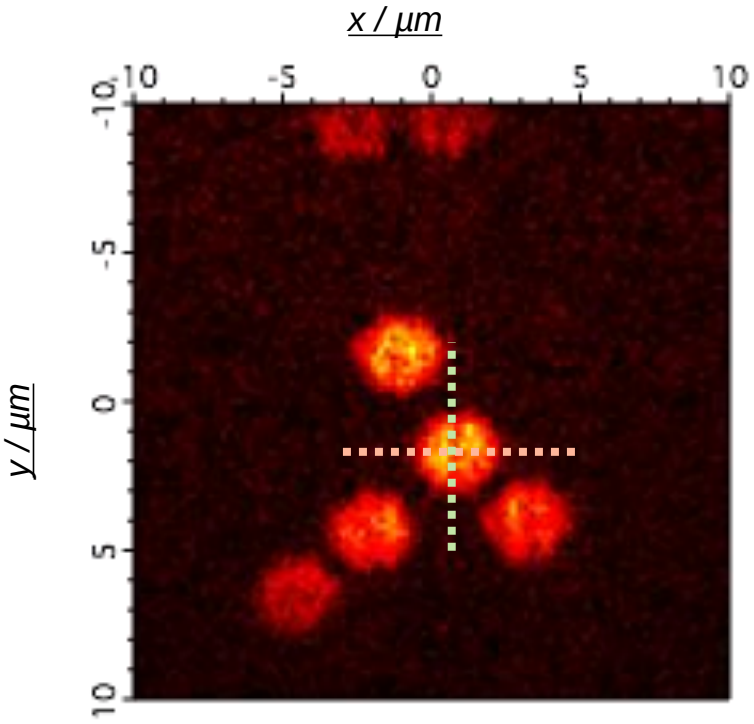

Perpendicular to the grid

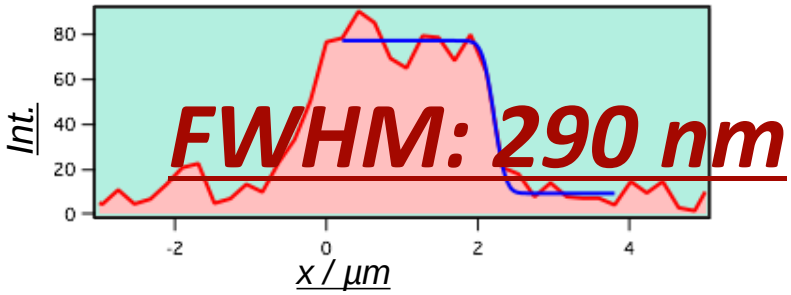

Parallel to the grid

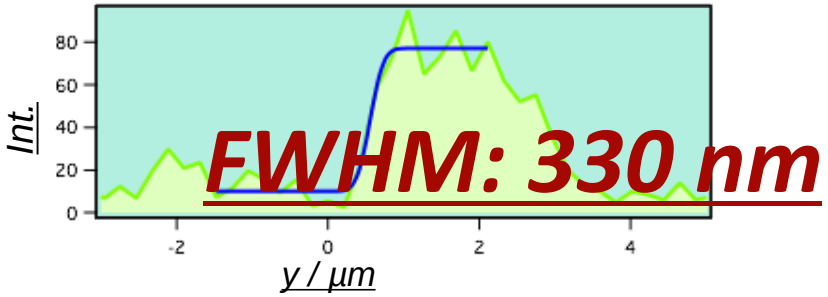

In plane spatial resolution close to the diffraction limit (~250 nm)!

Depth resolution

Z (µm)

+1.0 +.5 0.0 -.5 -1.0 -1.5 -2.0

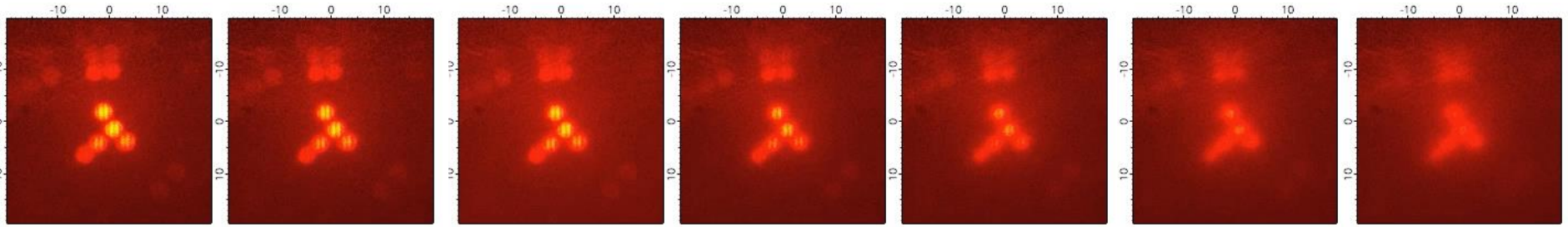

Reconstructed sectioned wide-field image

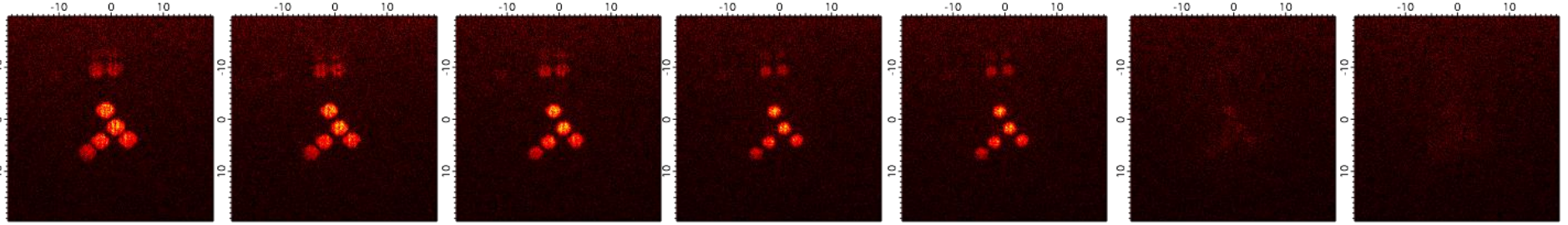

Reconstructed conventional wide-field image

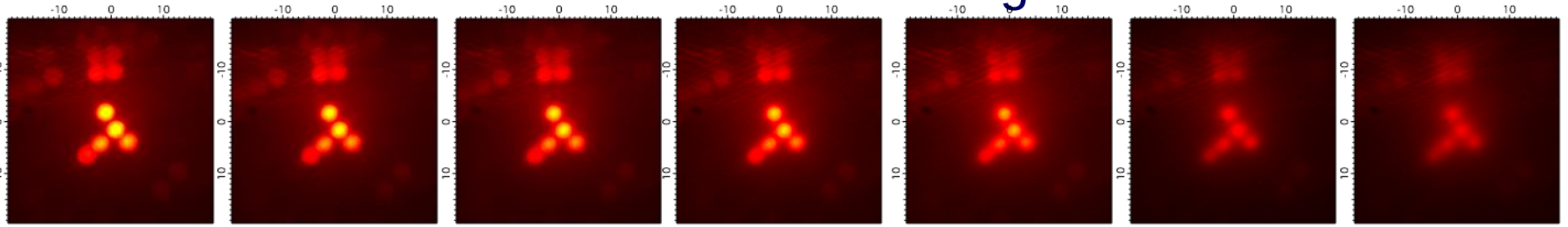

Axial Resolution

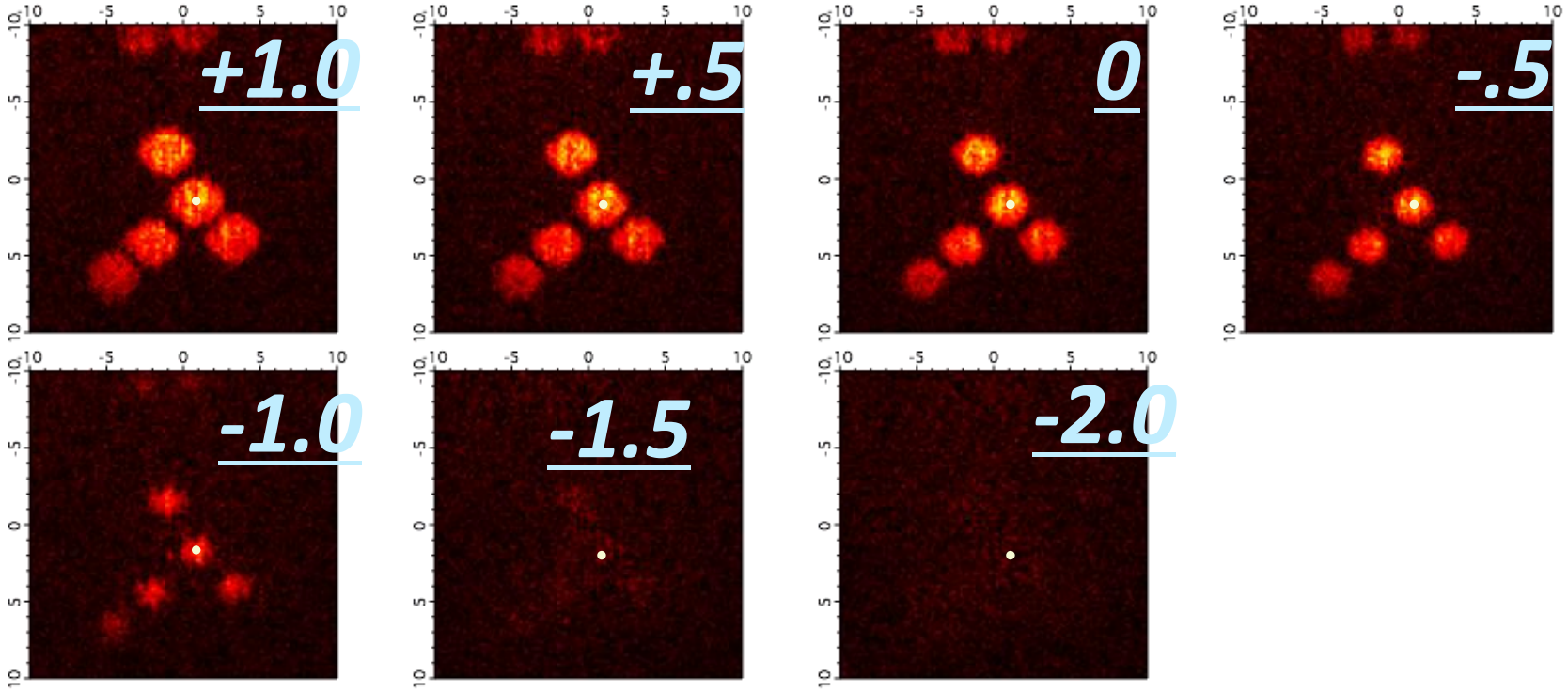

Depth profile

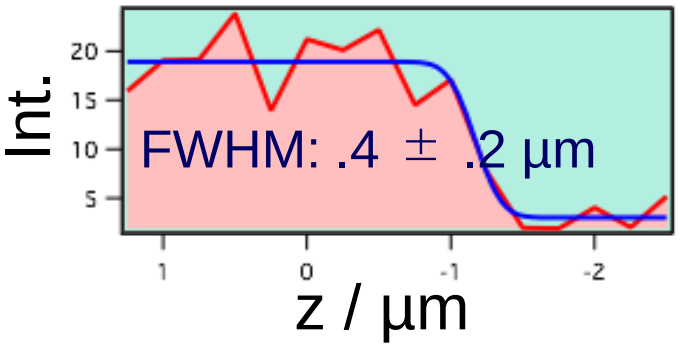

Axial resolution better than that of confocal Raman microscopes!

Sectioning capability

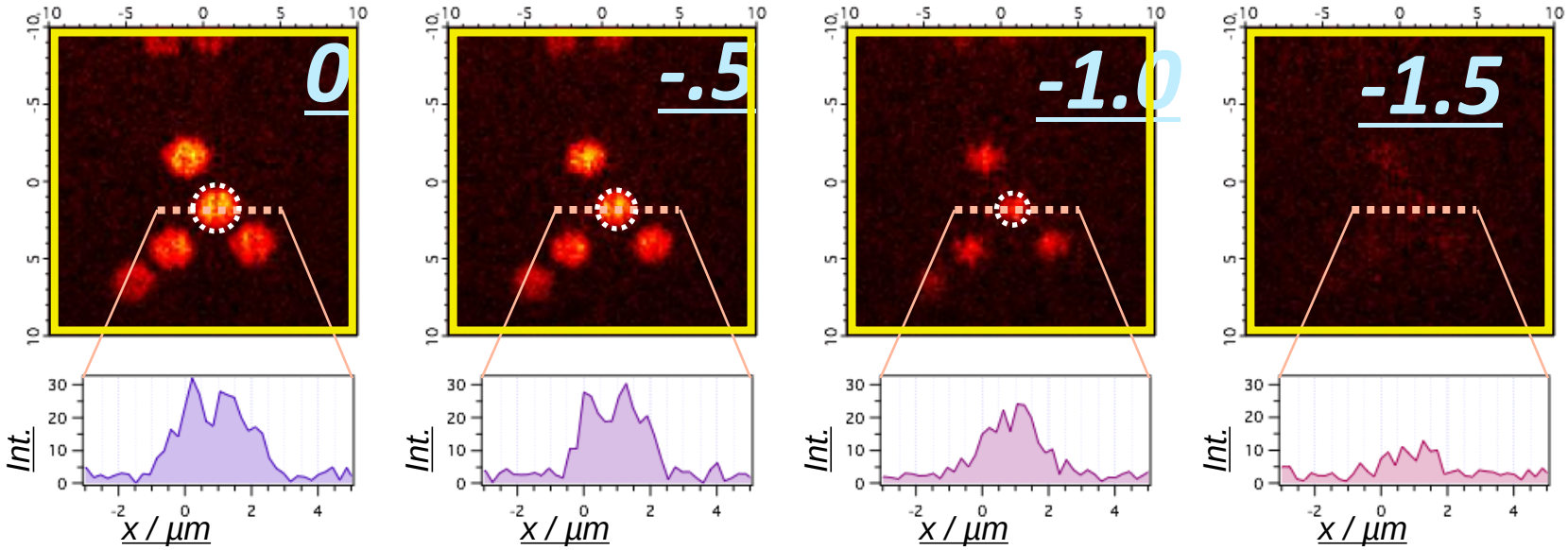

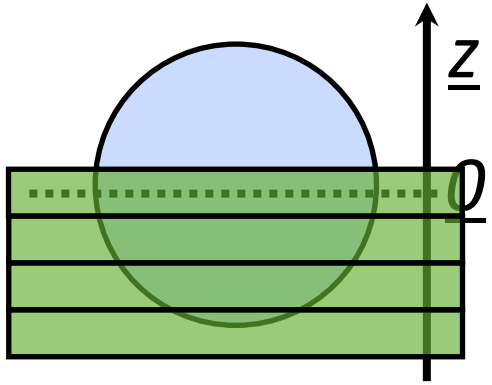

3D Sectioning!!

Quantitative imaging

Beetles in Taiwan

Diversity of Life

More Reliable and Useful Bio-imaging:

From Univariate to Multivariate

One particular physical quantity is not sufficient

From Imaging to Spectral Imaging

Imaging with well defined molecular signature

From Qualitative to Quantitative

Linear optical phenomenon must be used

From a Single Cell to a Large Number Single Cells

Molecular Component Distribution Imaging (MCDI) of Living Cells with Multivariate Curve Resolution Analysis

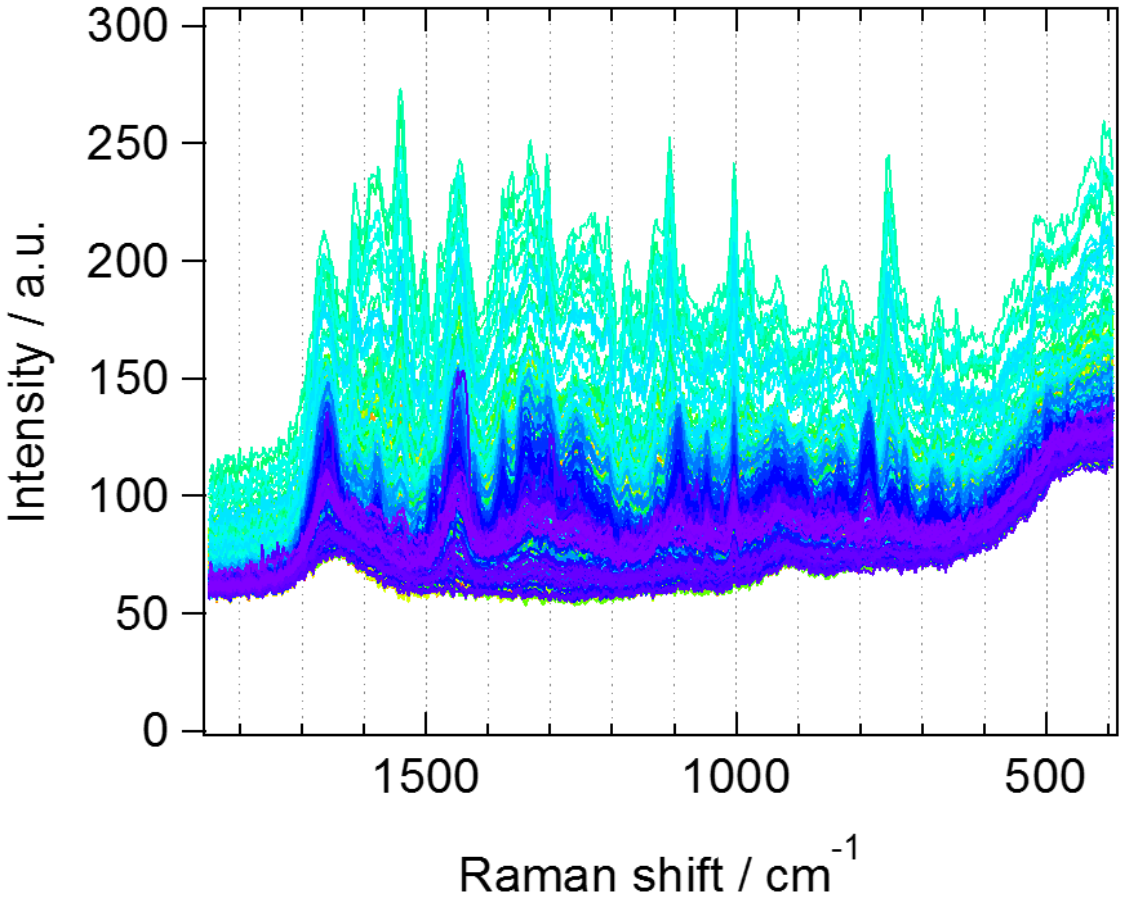

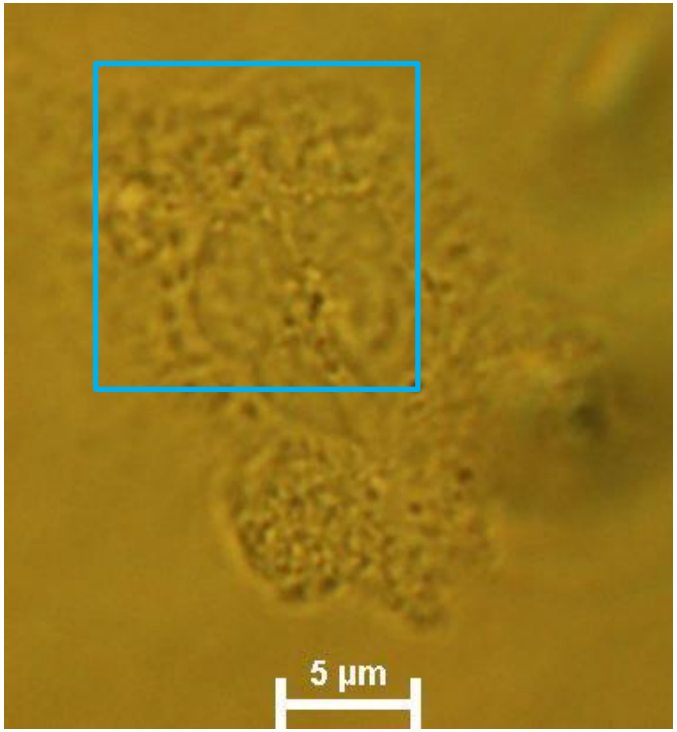

white blood cell

Thorough interpretation of complicated spectra is very difficult.

Multivariate Analysis

Experimental data is approximated by a linear combination of several “pure” spectral components.

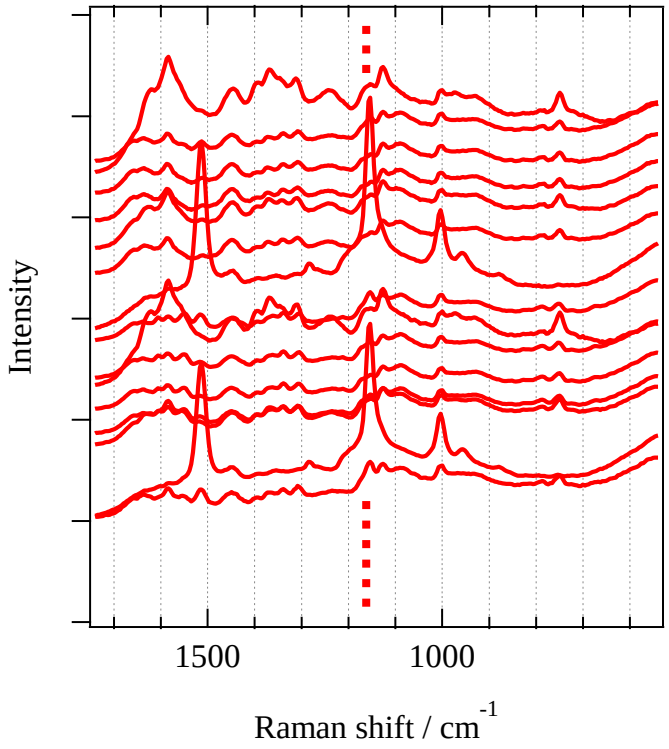

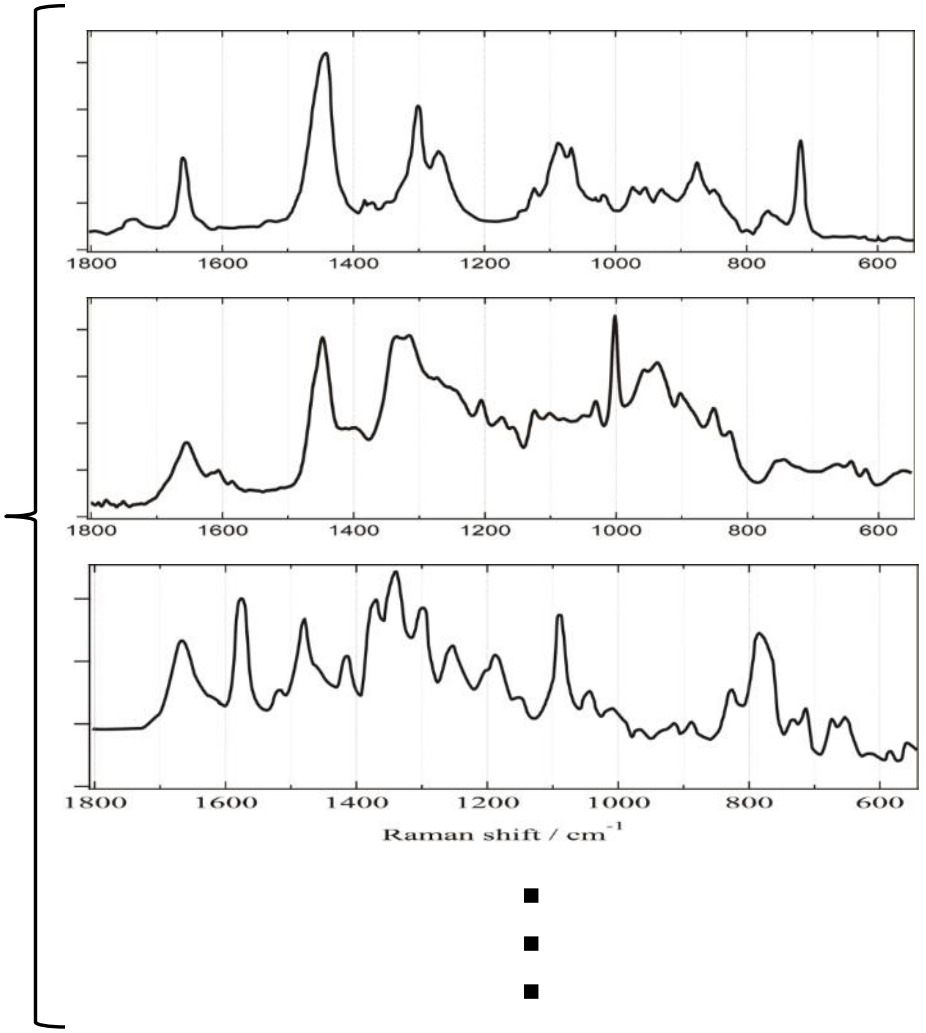

lipids

proteins

nucleic acid

Multivariate Analysis (1)

Matrix factorization by Singular Value Decomposition (SVD)

A ≈ WSH

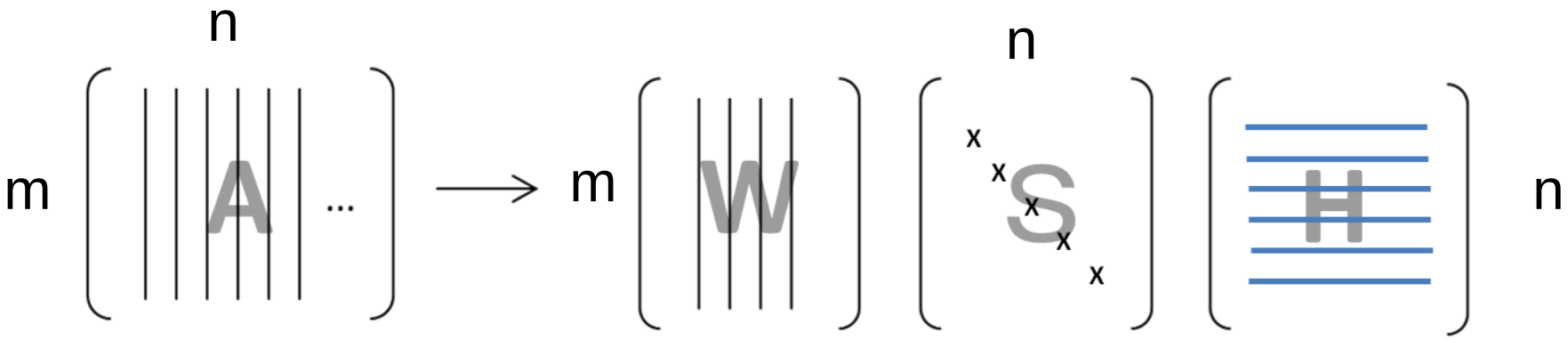

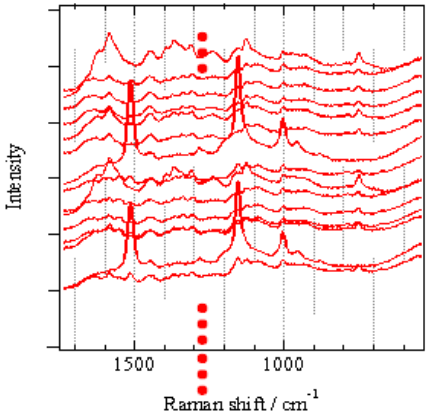

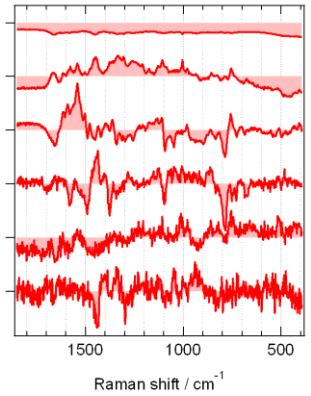

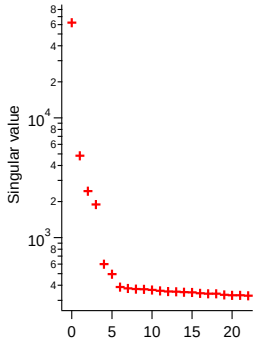

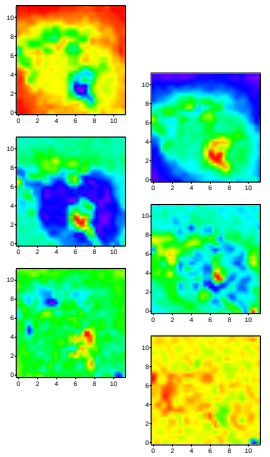

Singular Value Decomposition

A = WSH

W S H

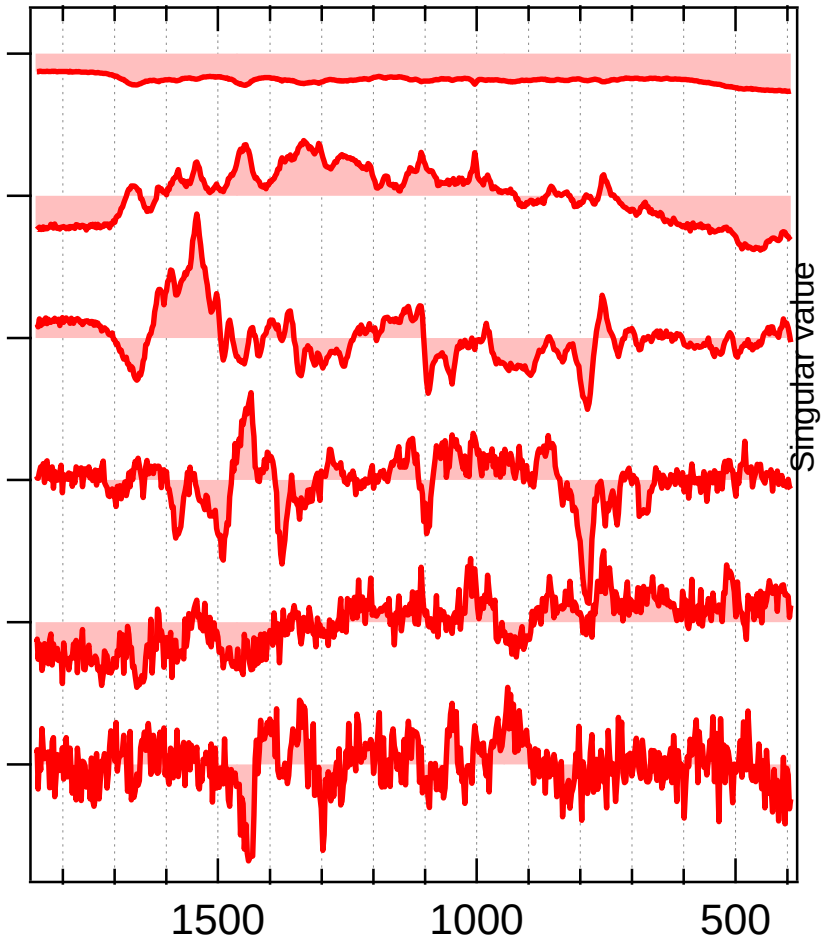

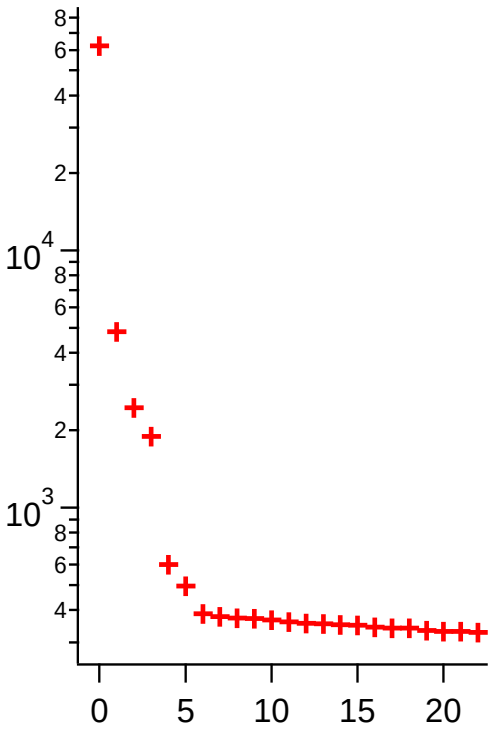

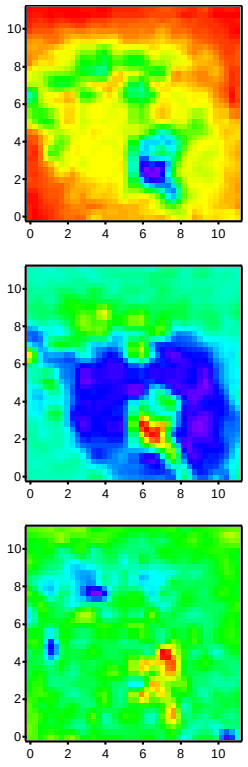

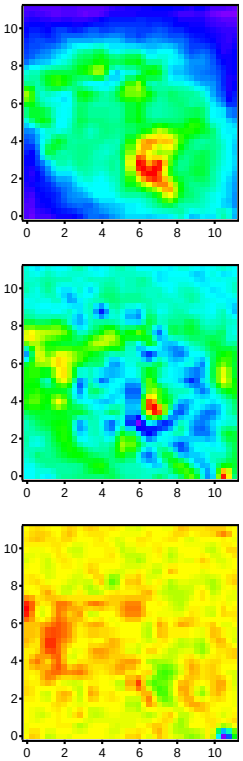

Multivariate Analysis (2)

Multivariate Curve Resolution (MCR)
(Non-negative matrix factorization (NMF)[1])

Approximate a non-negative matrix with two non-negative matrix:

$$\mathbf{A} \approx \mathbf{WH}, \quad \mathbf{W}, \mathbf{H} \geq \mathbf{0}$$

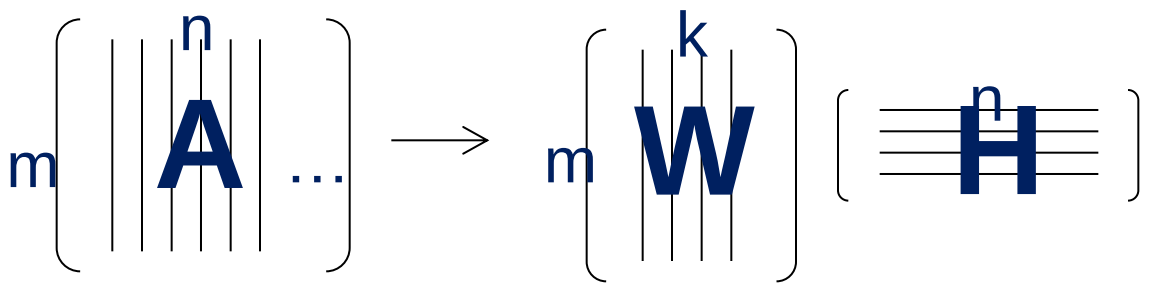

Alternating Least Squares — Frobenius norm $||\mathbf{A} - \mathbf{WH}||^2$ is minimized

$$\left.\begin{aligned} \mathbf{W}^T\mathbf{WH} &= \mathbf{W}^T\mathbf{A} \\ \mathbf{HH}^T\mathbf{W}^T &= \mathbf{HA}^T \end{aligned}\right\}$$ iteratively solved with non-negative constraints

Compared to other multivariate analysis, such as SVD or PCA, MCR provides more physically interpretable spectral components.

1. D. D. Lee and H. S. Seung, “Nature **401**(6755), 788–791 (1999)。

Multivariate Curve Resolution(MCR)

k is determined

m n A …

→

m k W n H

SVD

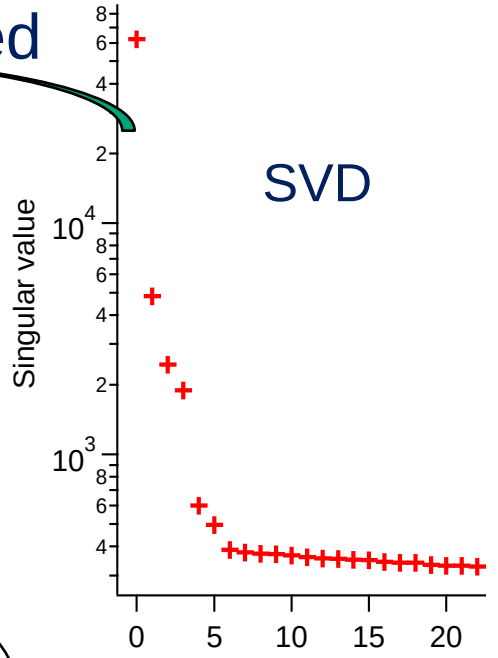

Initial guess

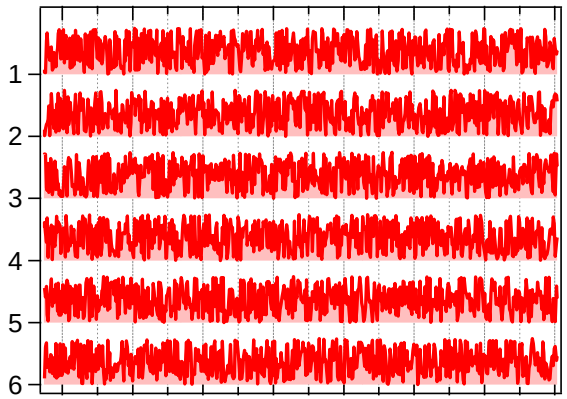

Random

or

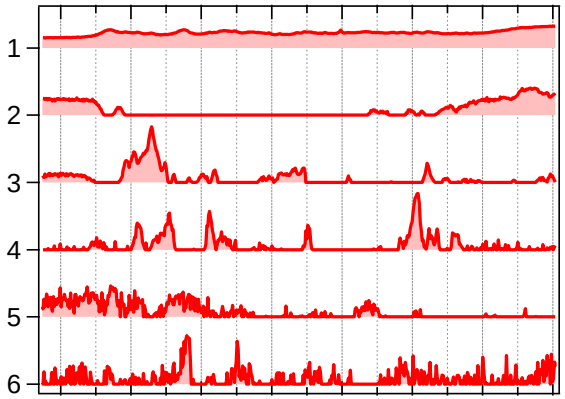

SVD based

Alternating Least-Squares

$||\mathbf{A} - \mathbf{WH}||^2$ is minimized

MCR Spectra and Spatial Distribution

$$A \approx WH, \quad W, H \geq 0$$

W

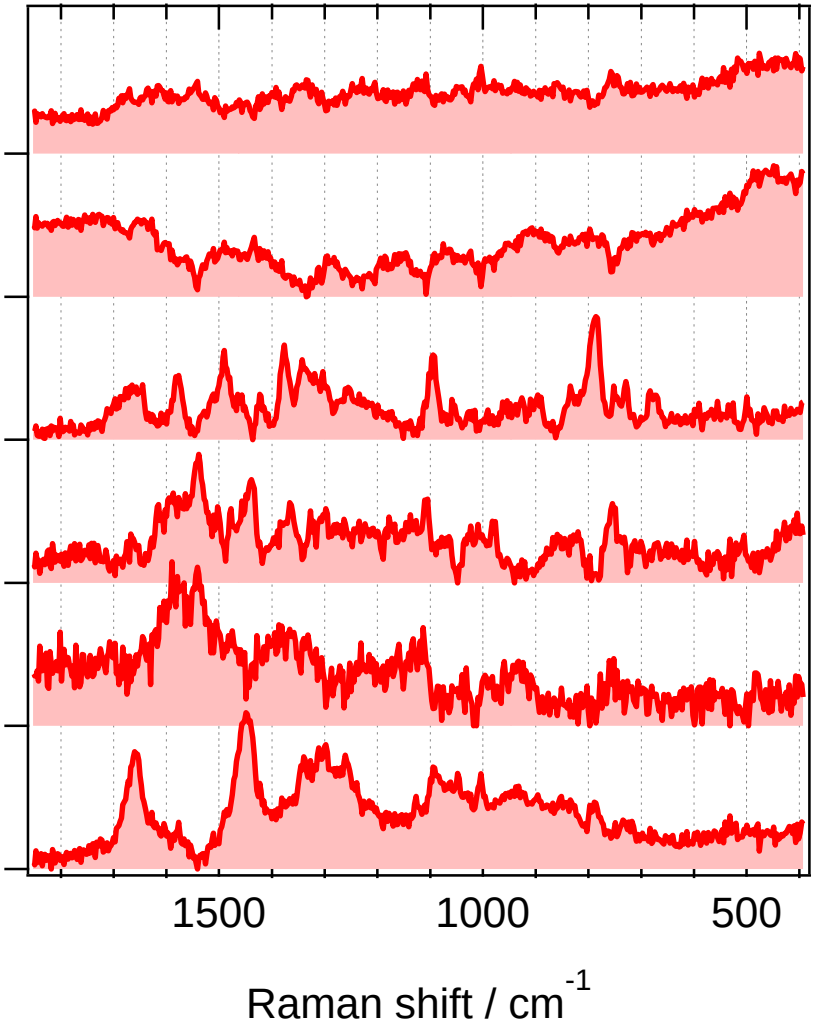

H

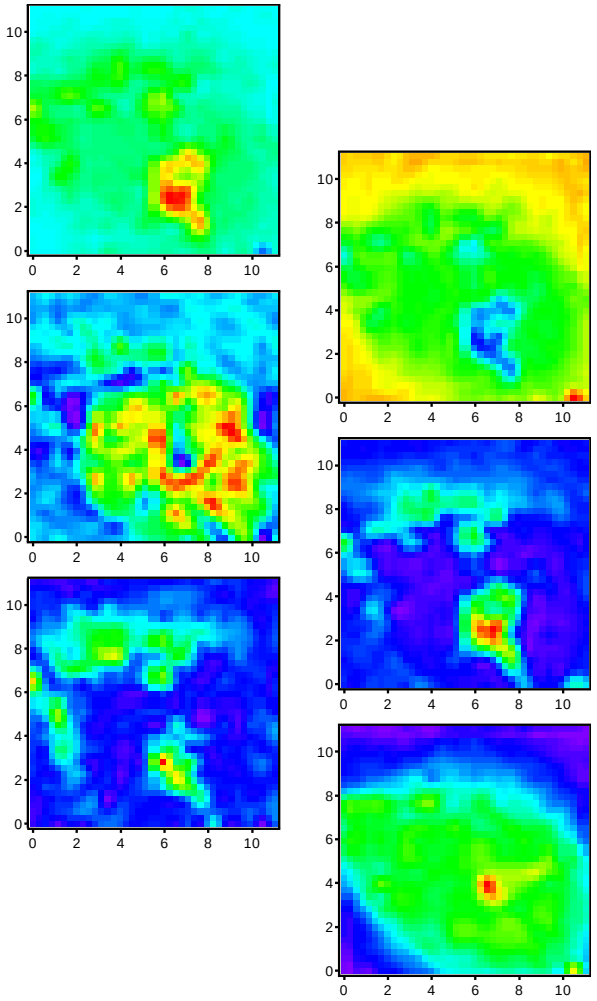

Multivariate Analysis (3)

MCR with additional constraint

Approximate a non-negative matrix with two non-negative matrix:

$A \approx WH, \quad W, H \geq 0$

Additional constraint terms are used for ALS optimization:

$(||A - WH||^2 + f(H))$ is minimized instead of $||A - WH||^2$

L1 norm regularization:

$(W^TW + [L_{1H}]E)H = W^TA$
$HH^T W^T = HA^T$

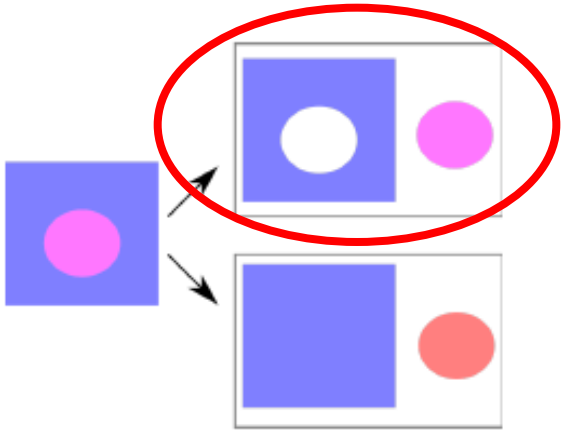

Sparser solutions are obtained.

L1-norm Regularization

$$(\mathbf{W}^T\mathbf{W} + [L_{1H}]\mathbf{E})\mathbf{H} = \mathbf{W}^T\mathbf{A}$$

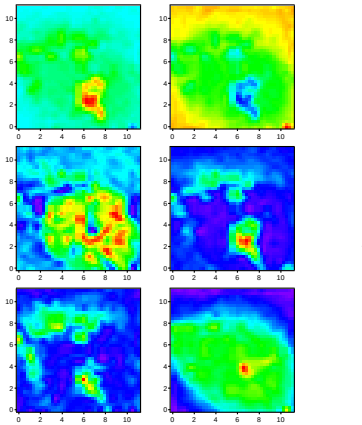

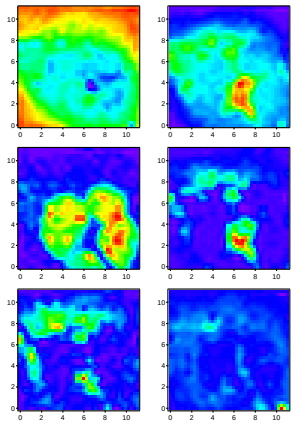

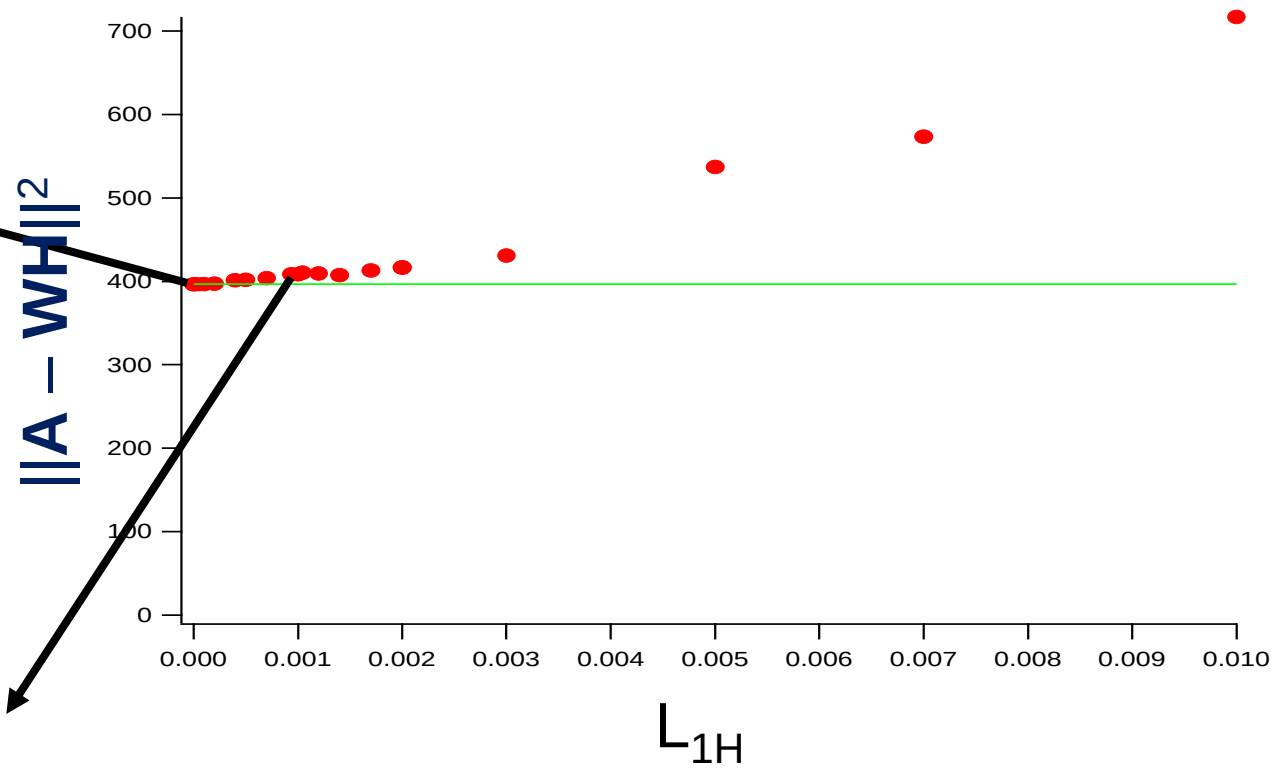

MCR with L1 Norm Regularization

W **A ≈ WH**, **W**, **H ≥ 0**, L_1=0.001 **H**

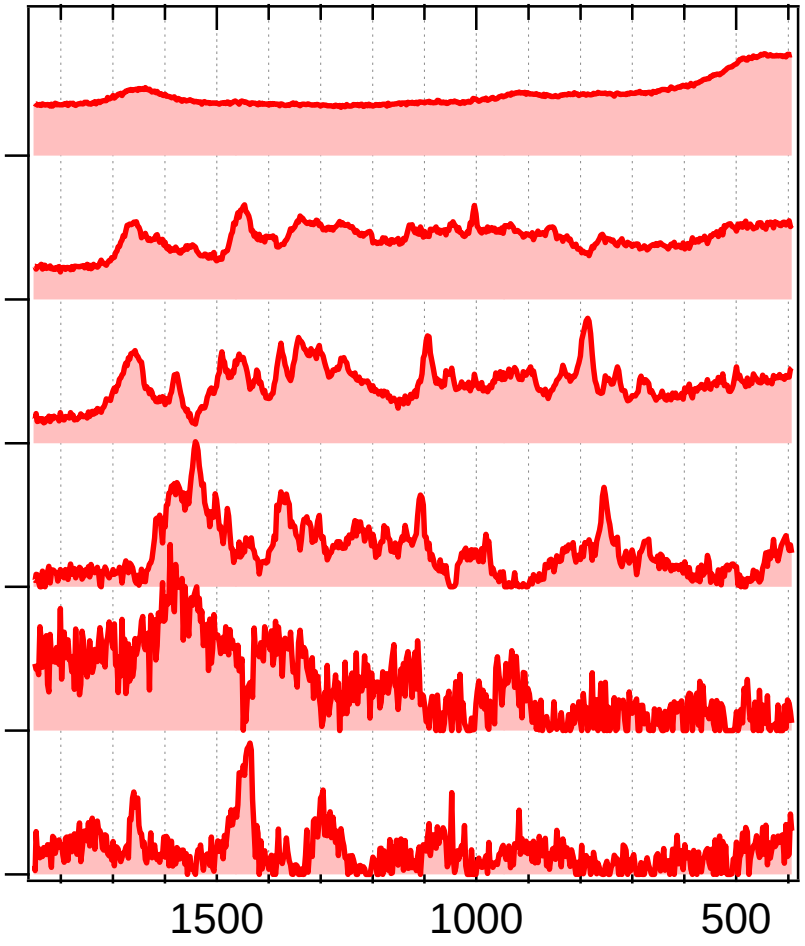

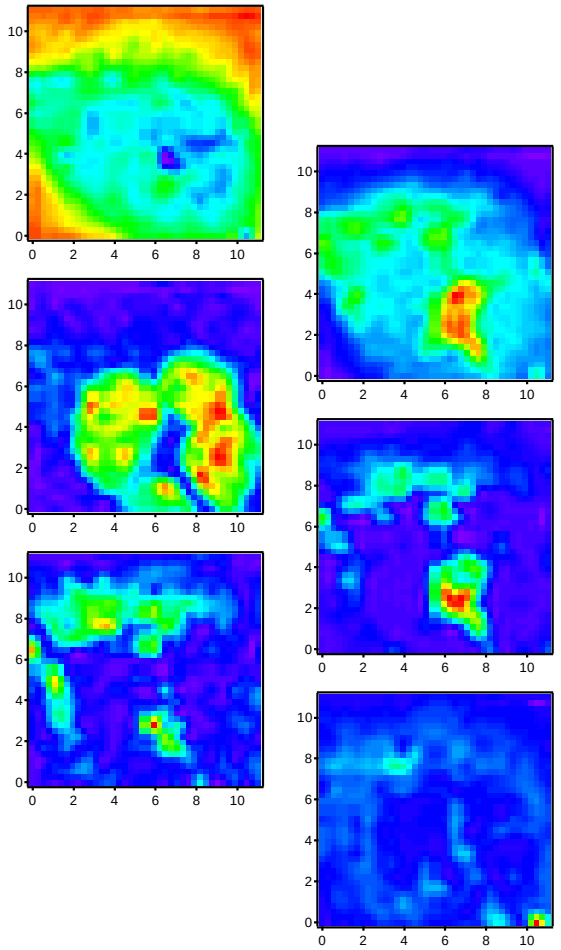

Multivariate Analyses: Comparison

SVD

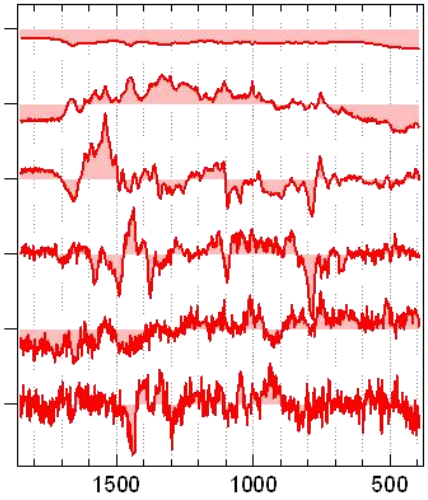

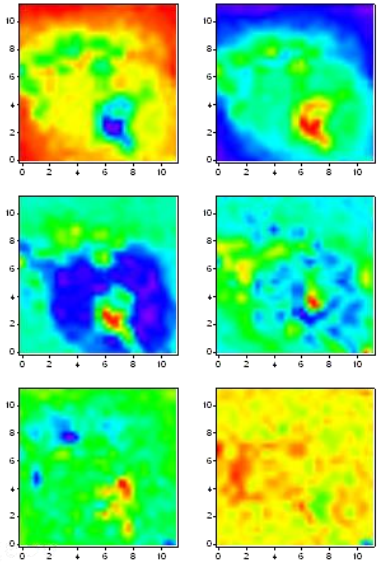

MCR

W, **H** ≥ 0 , $L_1 = 0$

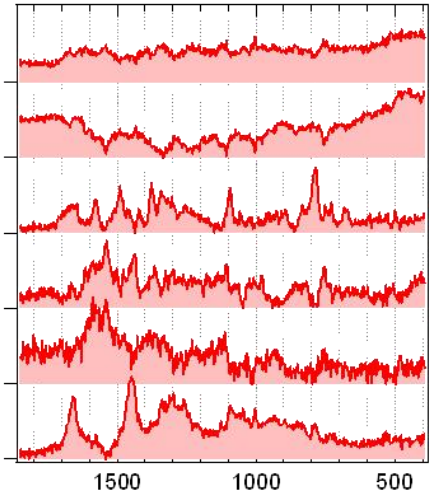

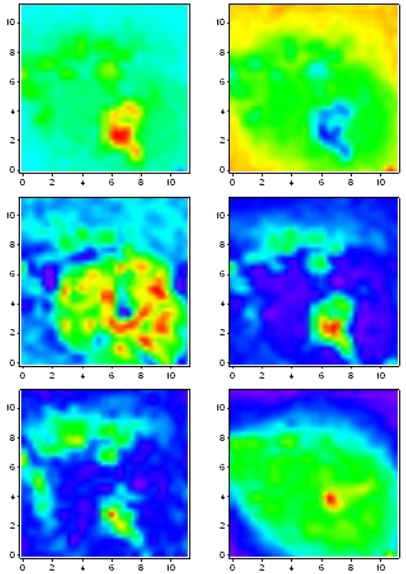

MCR

W, **H** ≥ 0 , $L_1 = 0.001$

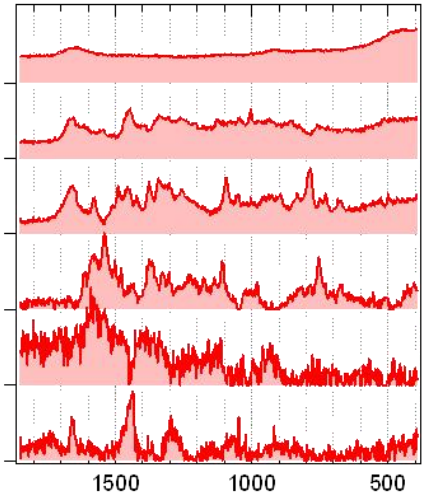

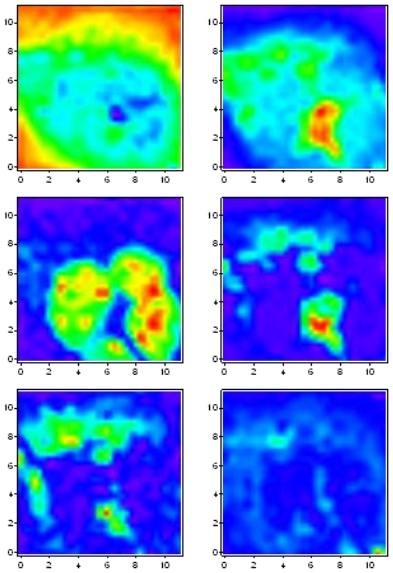

White Blood Cells

Neutrophil 	50-70 %	10-12 μm	Phagocytosis - bacteria, fungi
Eosinophil 	2-5 %	10-12 μm	Combating parasites Modulate allergic inflammatory responses
Basophil 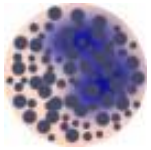	< 1 %	12-15 μm	release histamine for inflammatory responses
Lymphocyte 	20-40 %	7-8 μm	B cells T cells NK cells
Monocyte 	3-6 %	14-17 μm	Differentiate into tissue resident macrophages

Neutrophil

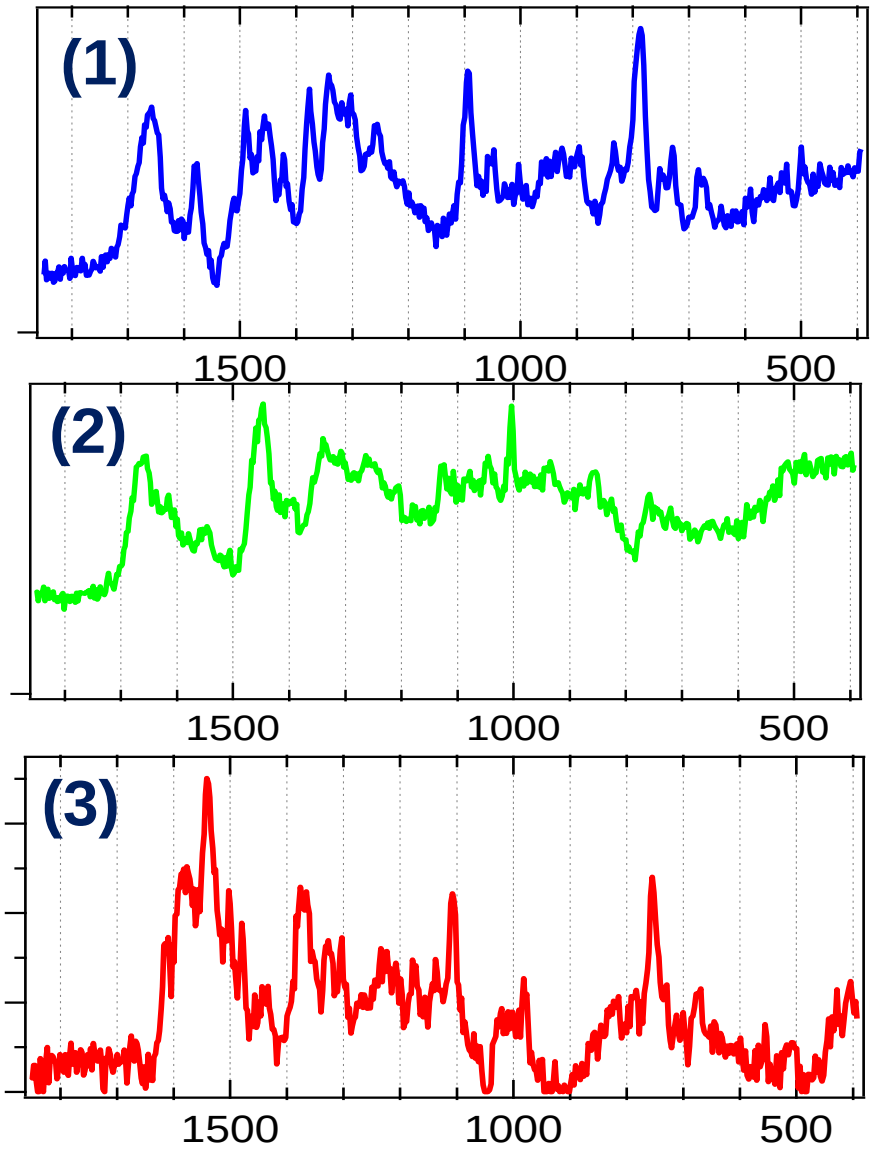

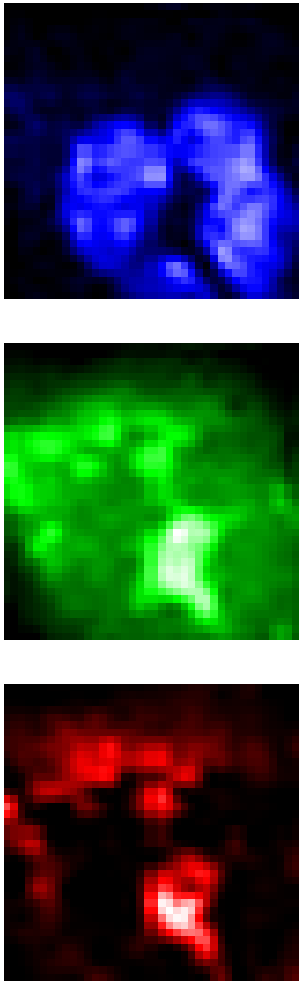

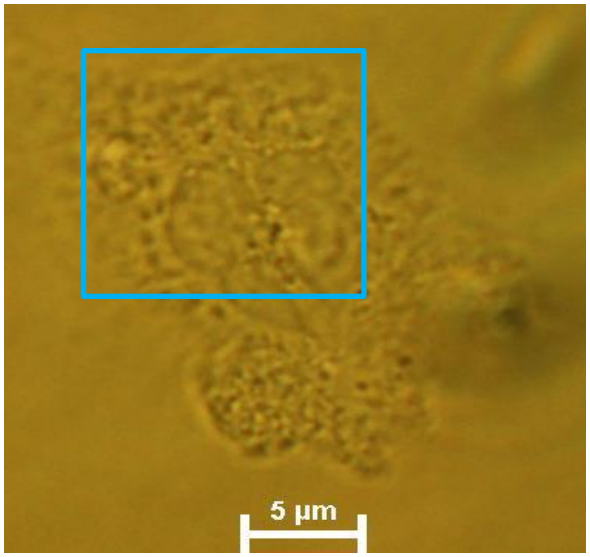

Neutrophil

excitation: 632.8 nm

Neutrophil Component (1)

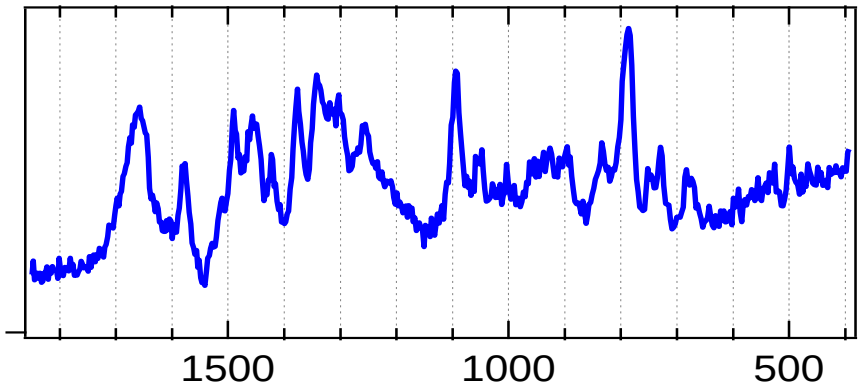

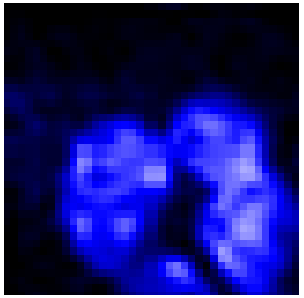

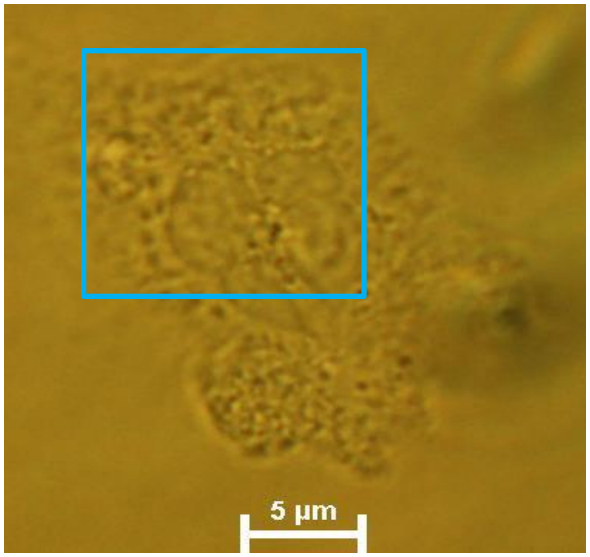

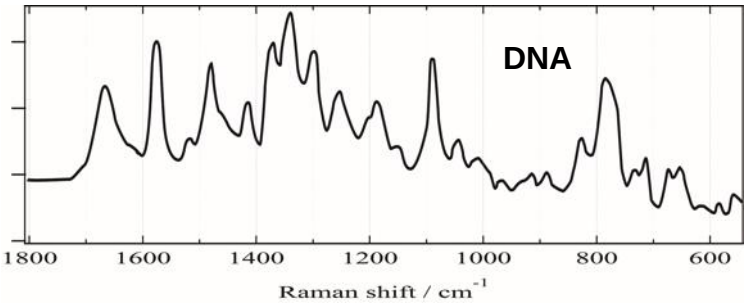

nucleic acid

Neutrophil

excitation: 632.8 nm

Neutrophil Component (2)

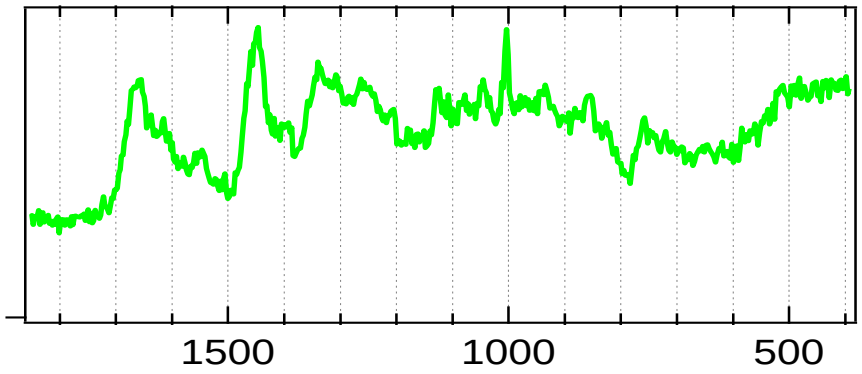

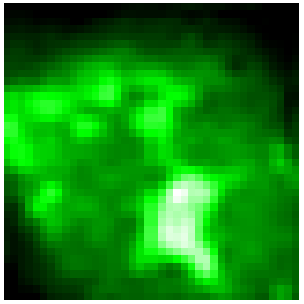

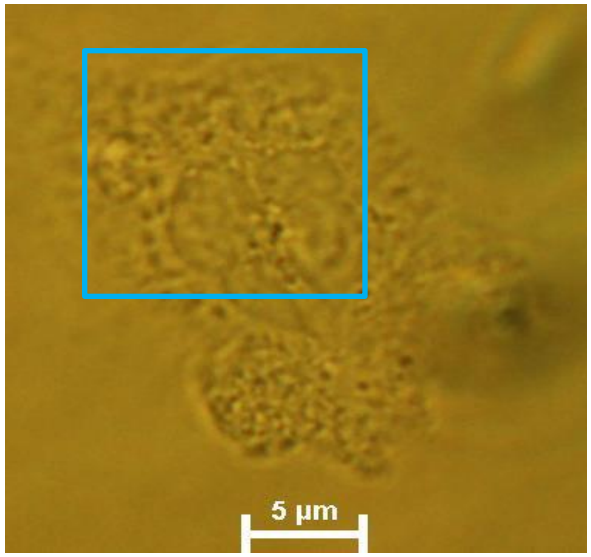

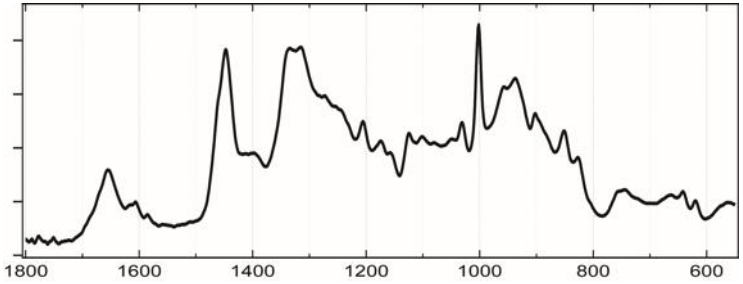

protein

Neutrophil

excitation: 632.8 nm

Neutrophil Component (3)

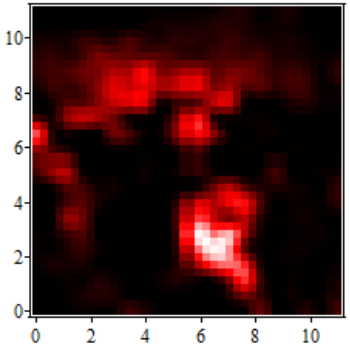

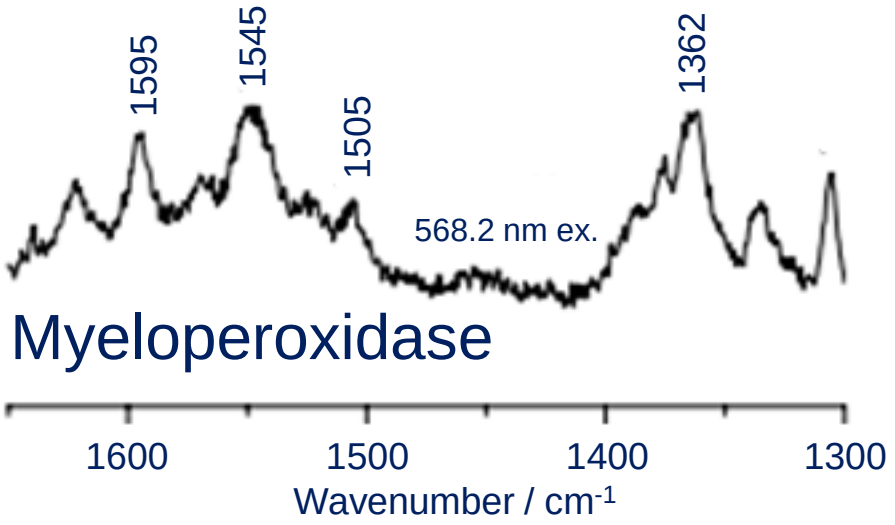

Brogioni, S., et al. **J. Raman Spectrosc.** (2006).

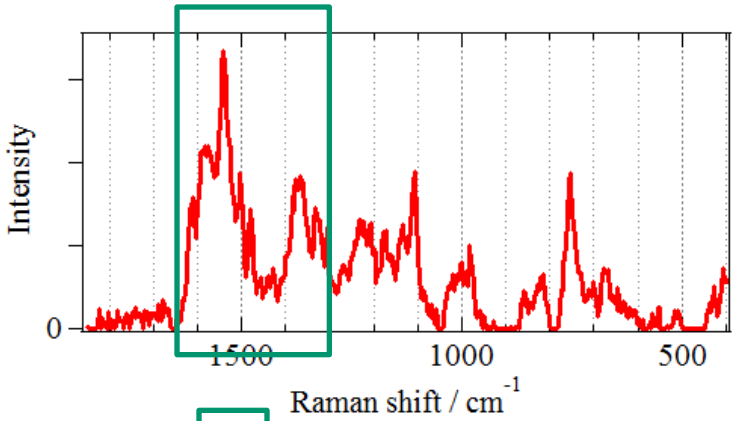

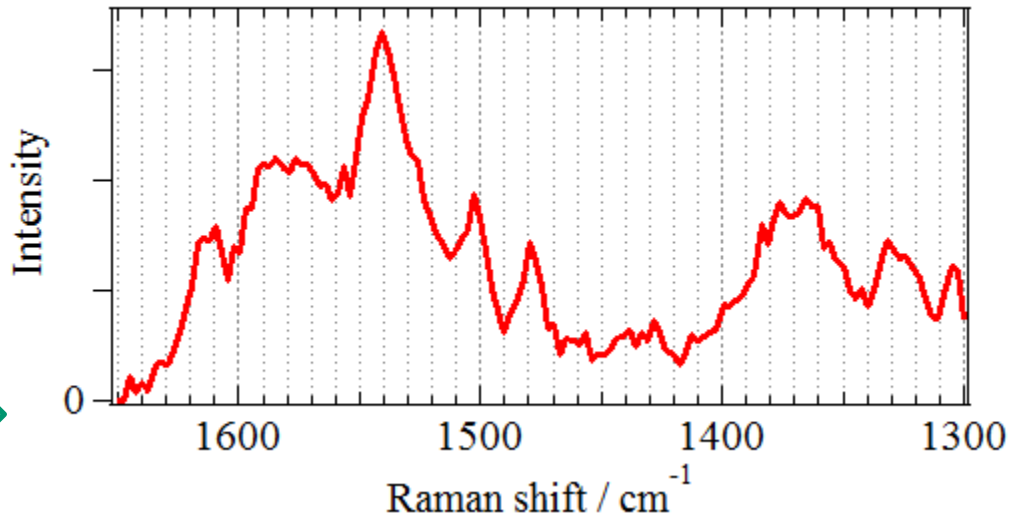

Neutrophil

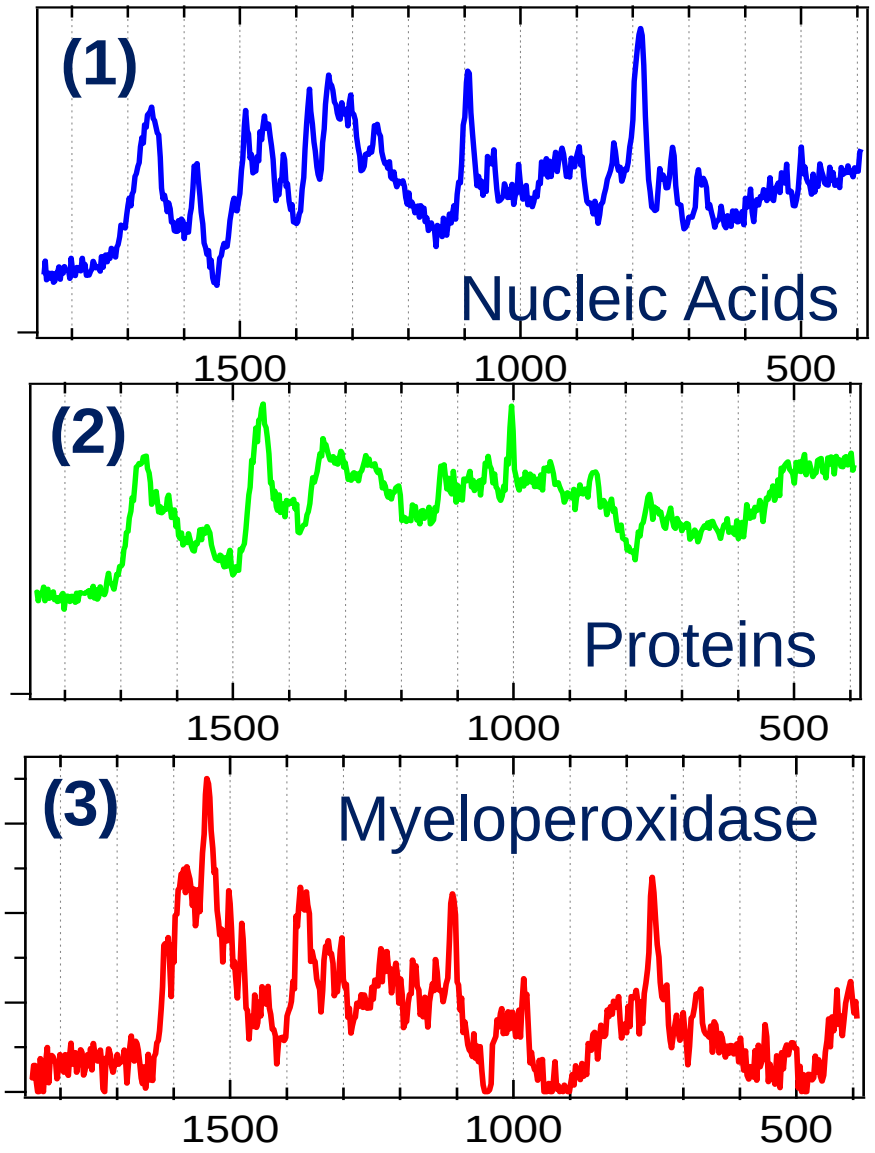

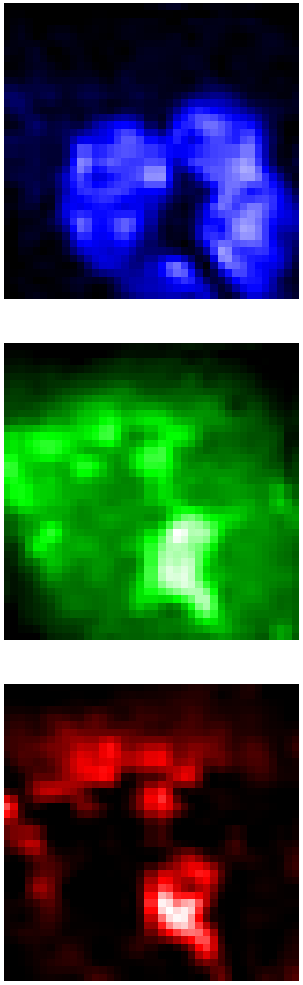

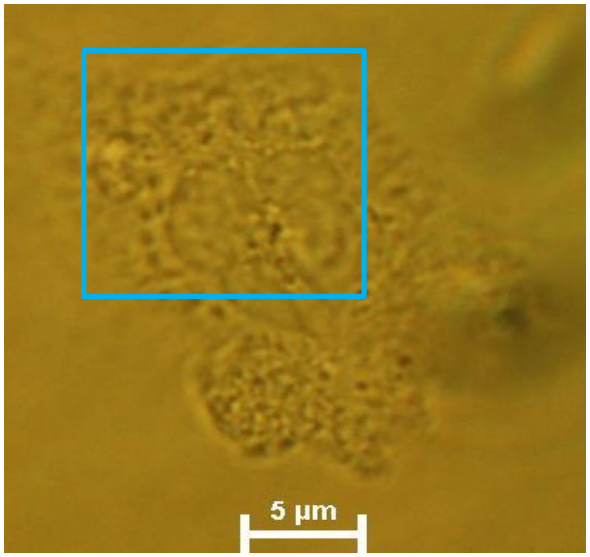

Neutrophil

excitation: 632.8 nm

Lymphocyte

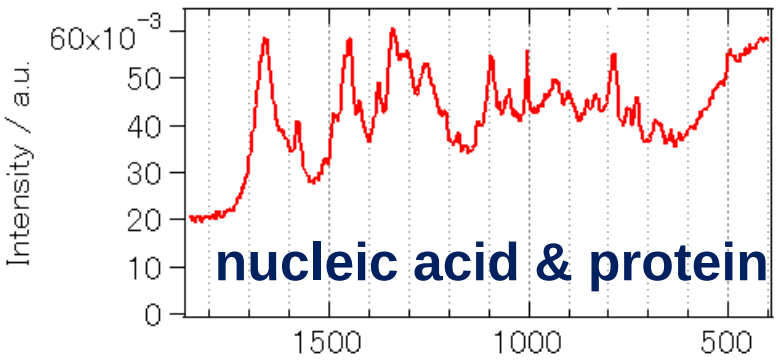

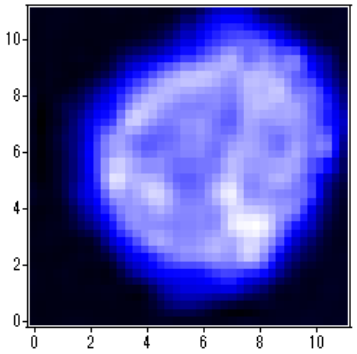

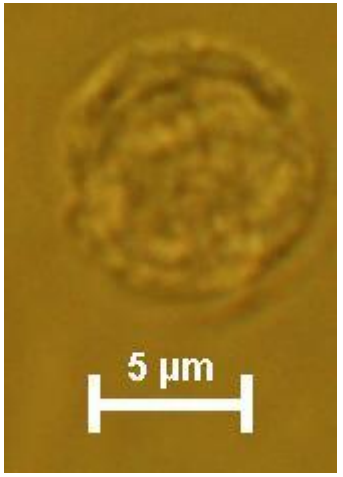

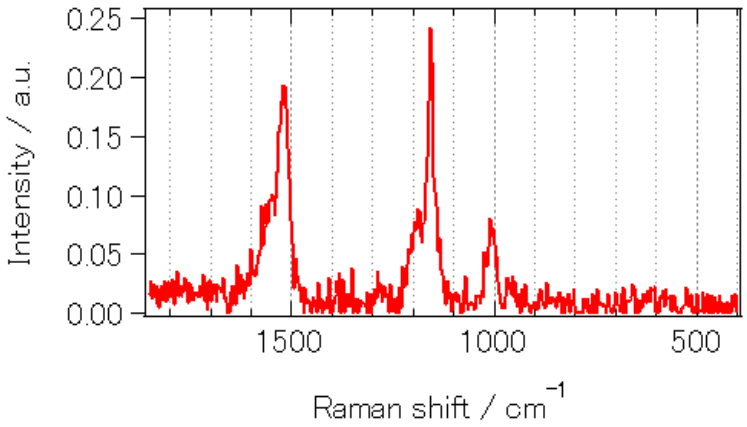

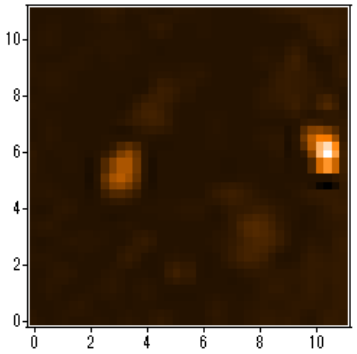

Carotenoid

- antioxidant
- biomarker of health condition (Int. J. of Cancer **74**, 20 (1997))

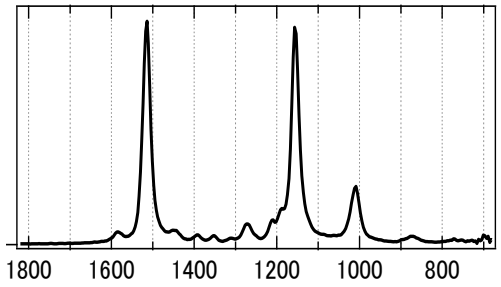

β-carotene

Activated Eosinophil

(Lipopolysaccharide (LPS) / phorbol 12-myristate 13-acetate (PMA))

nucleic acid & protein

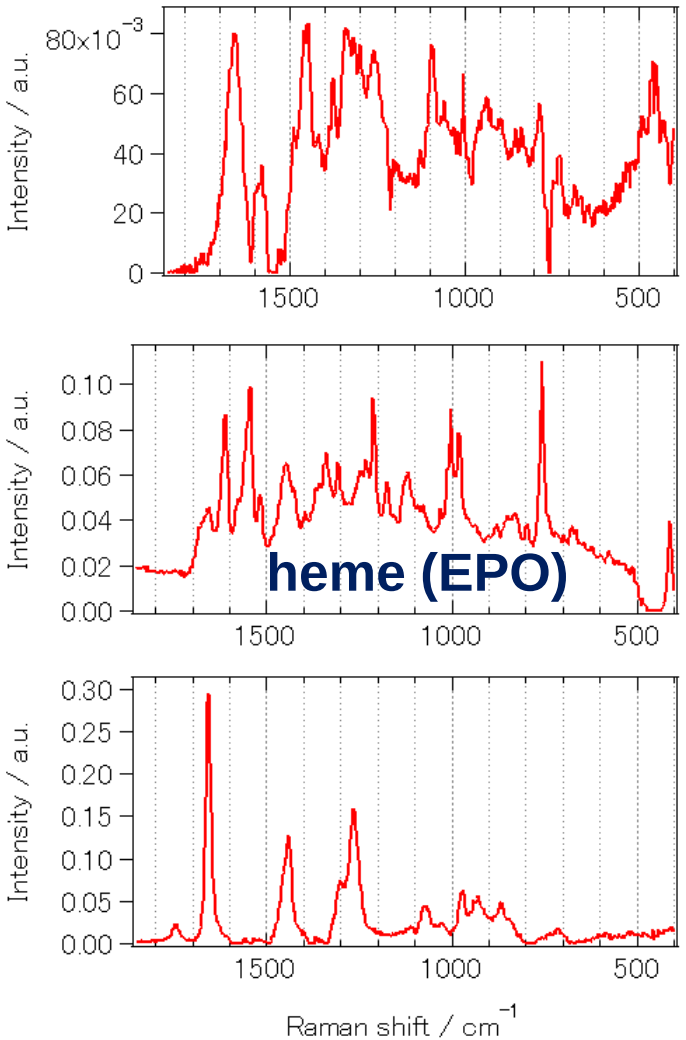

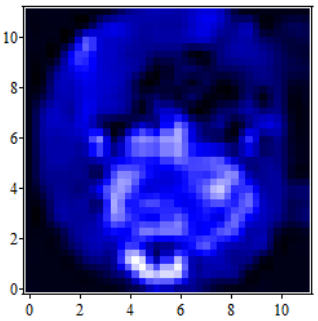

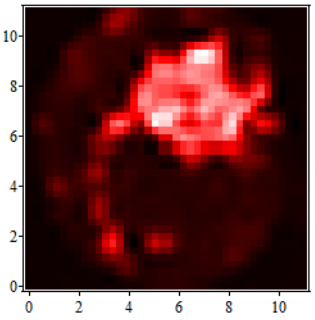

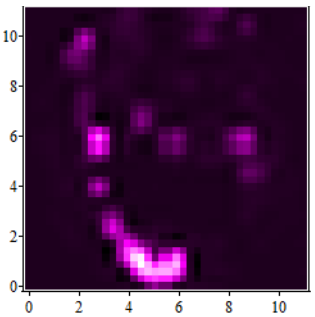

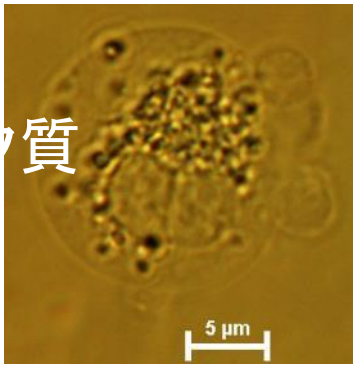

Lipid particle

Lipid Particle in Eosinophil

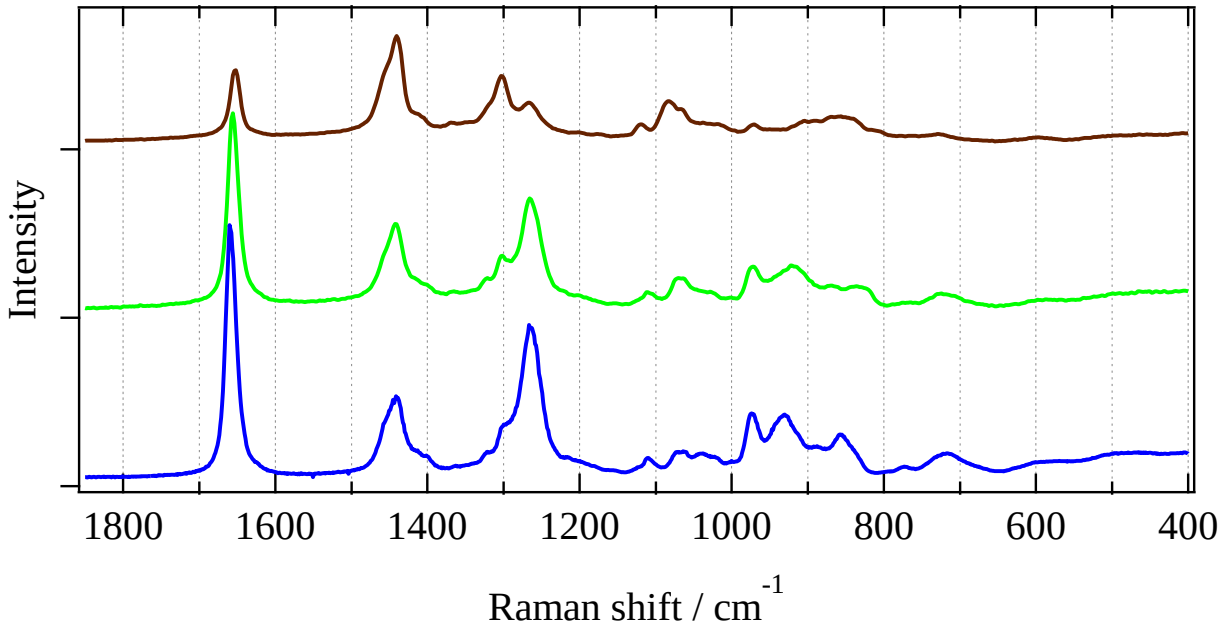

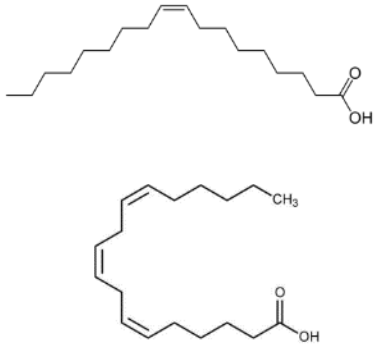

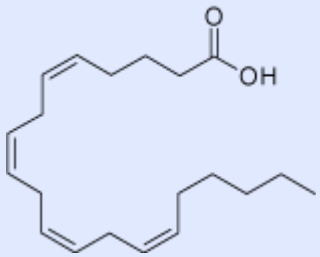

Arachidonic acid

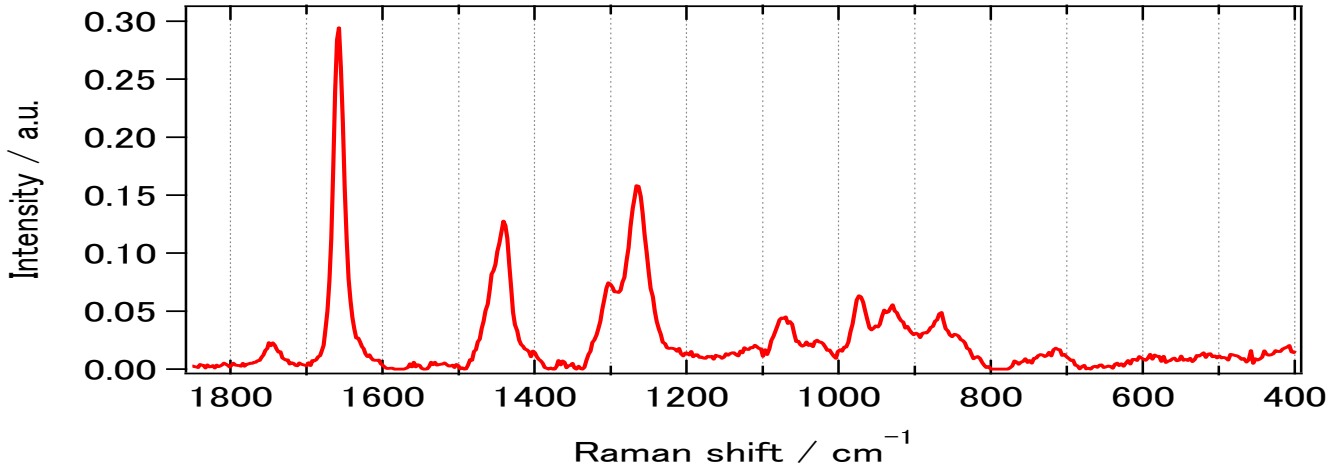

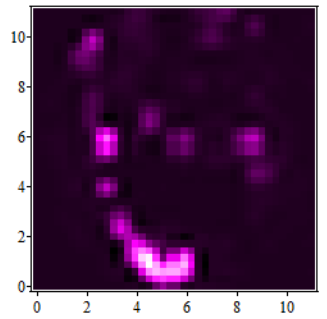

Lipid Particle in Eosinophil

Arachidonic acid cascade

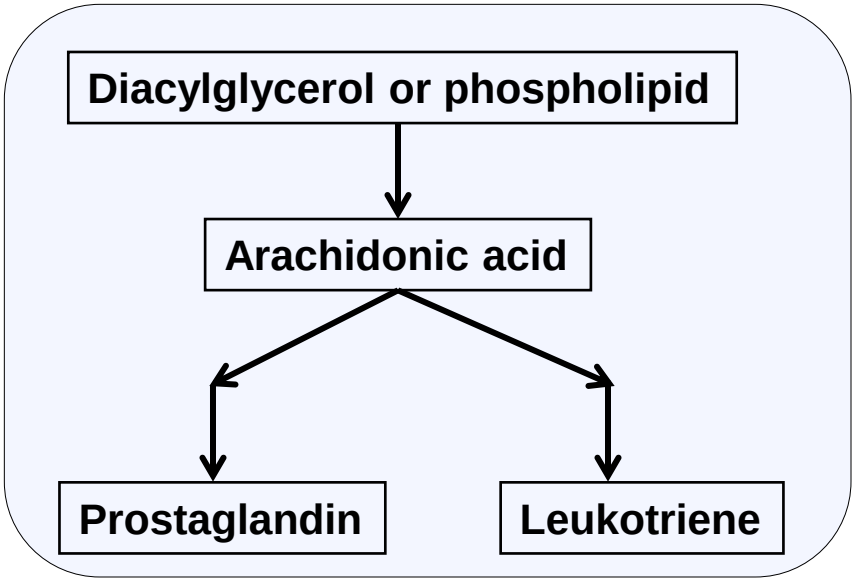

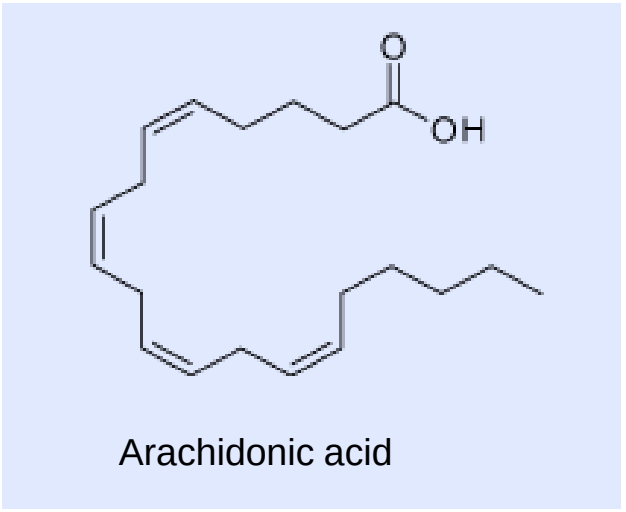

Arachidonic acid

mediator of inflammation

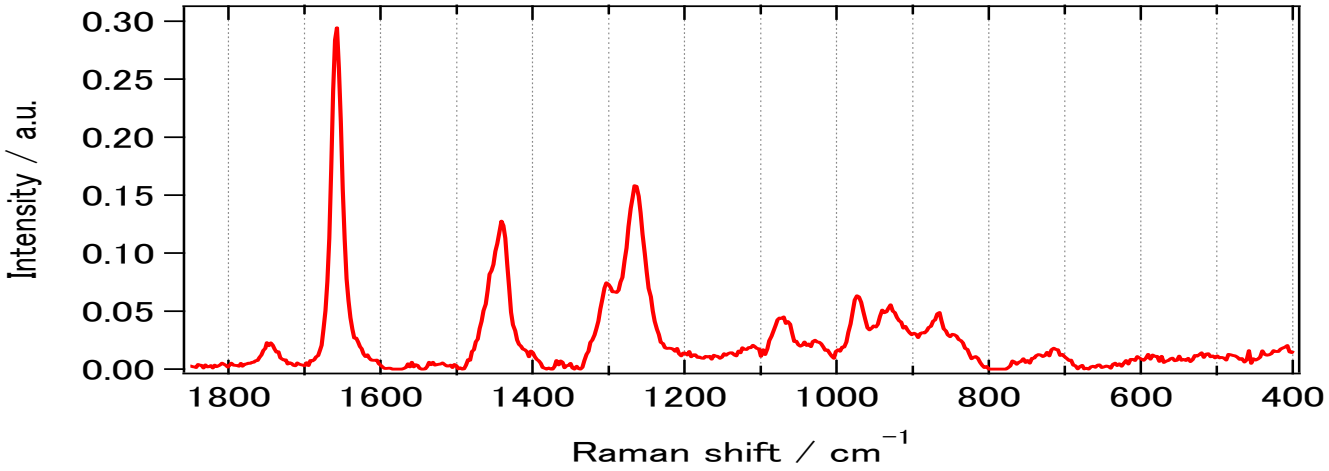

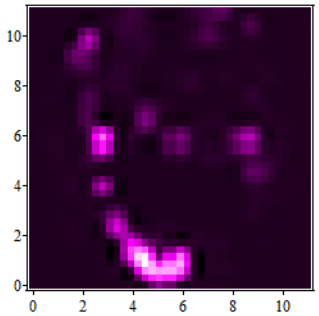

MCR Analysis of White Blood Cells

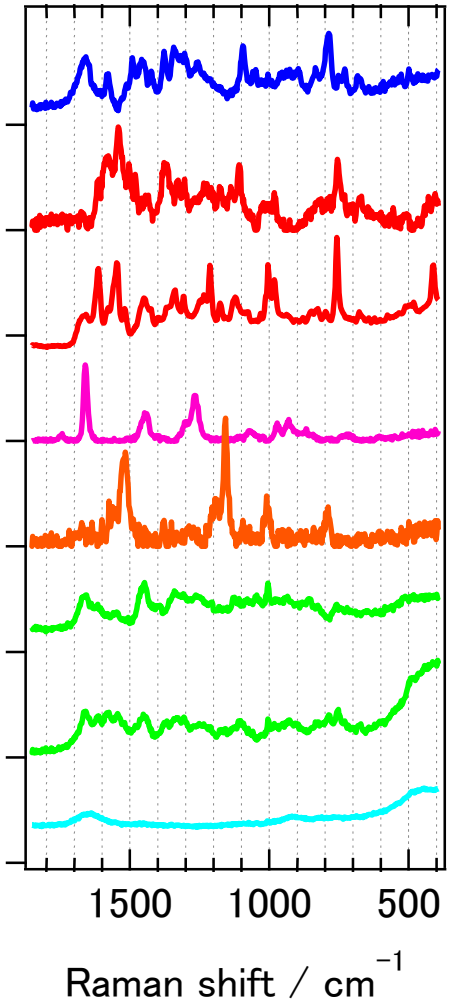

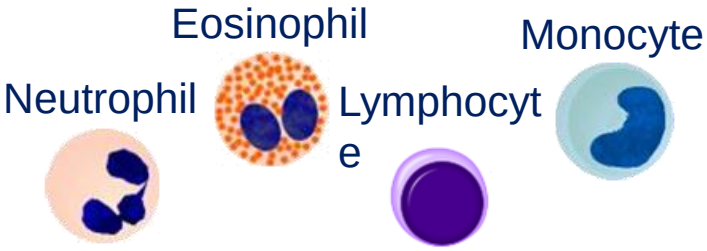

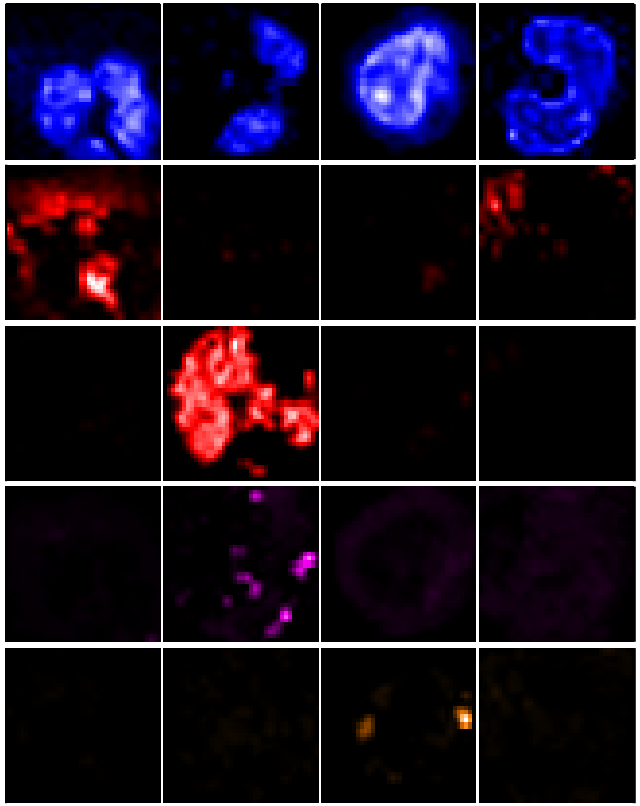

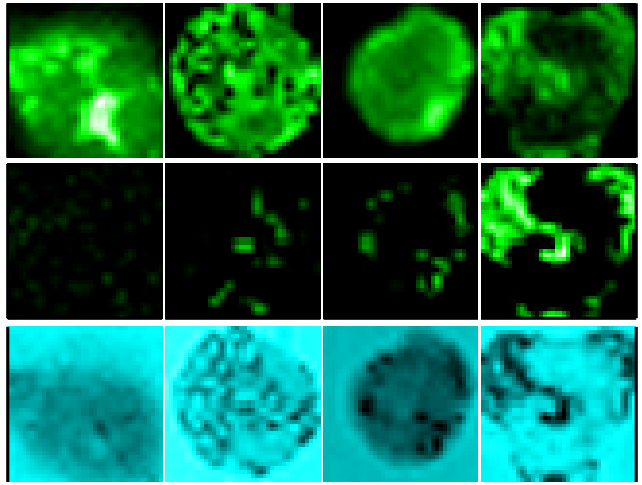

MCDI of White Blood Cells

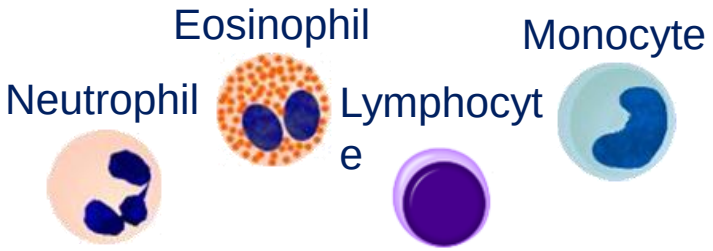

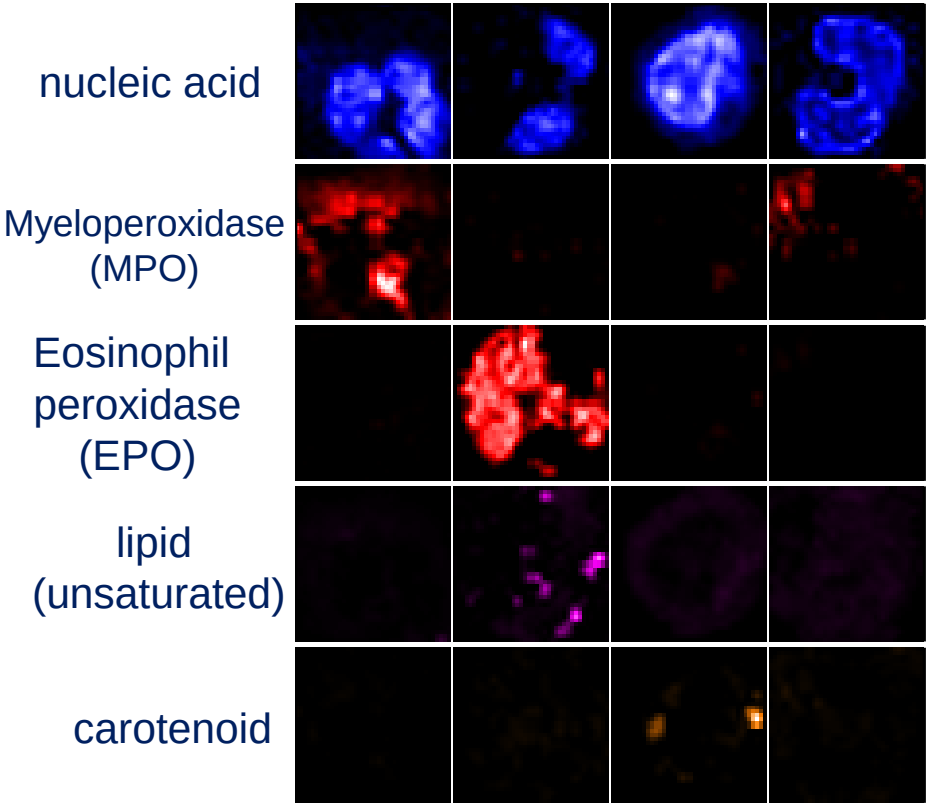

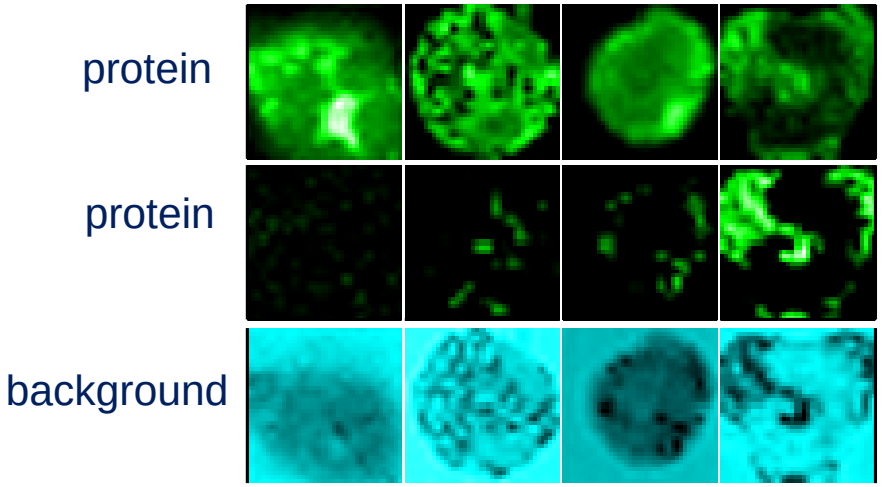

BACTERIAL GROWTH

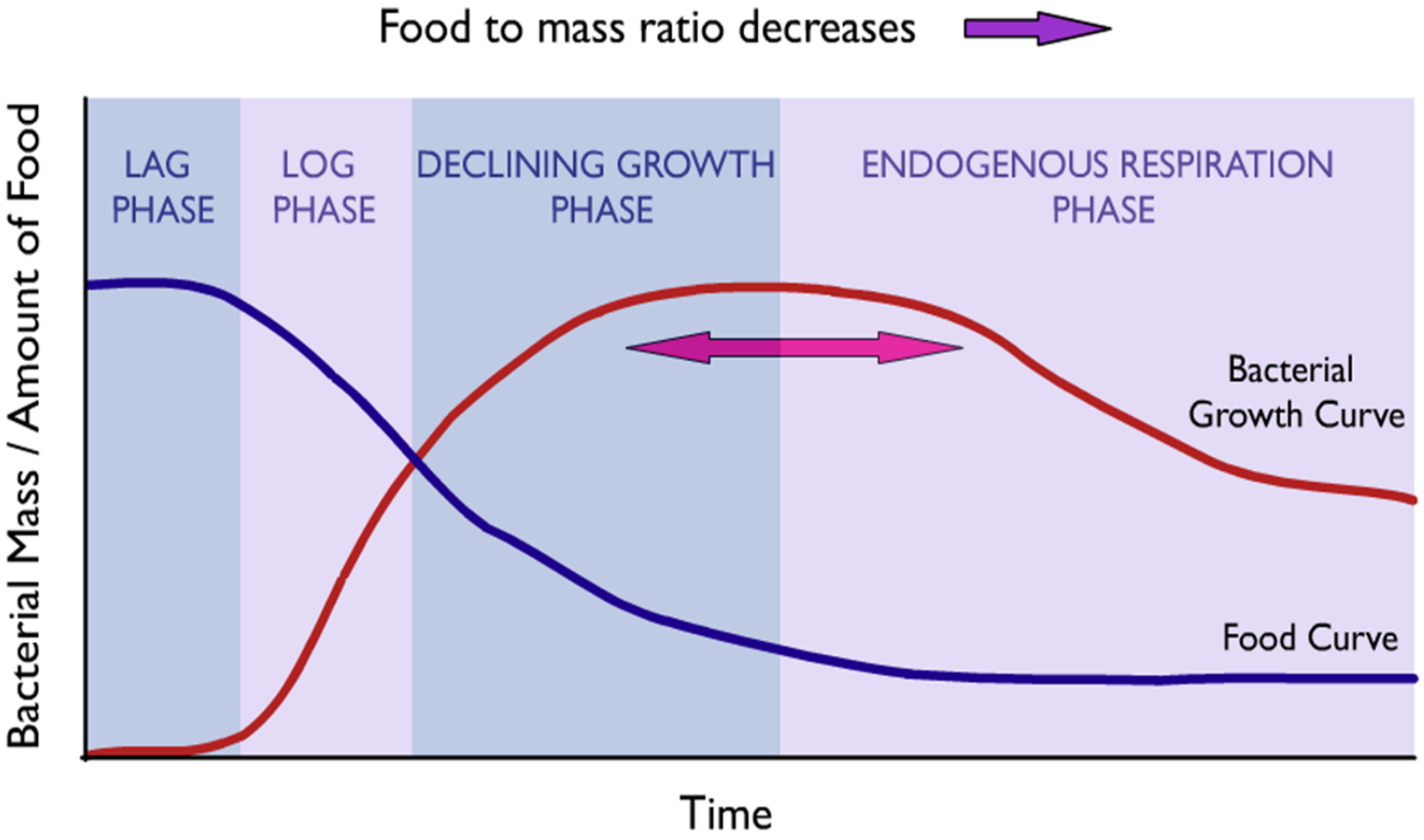

Raman Spectra (276-646 averages) of Laser-trapped E-coli at Different Time of Growth Curve

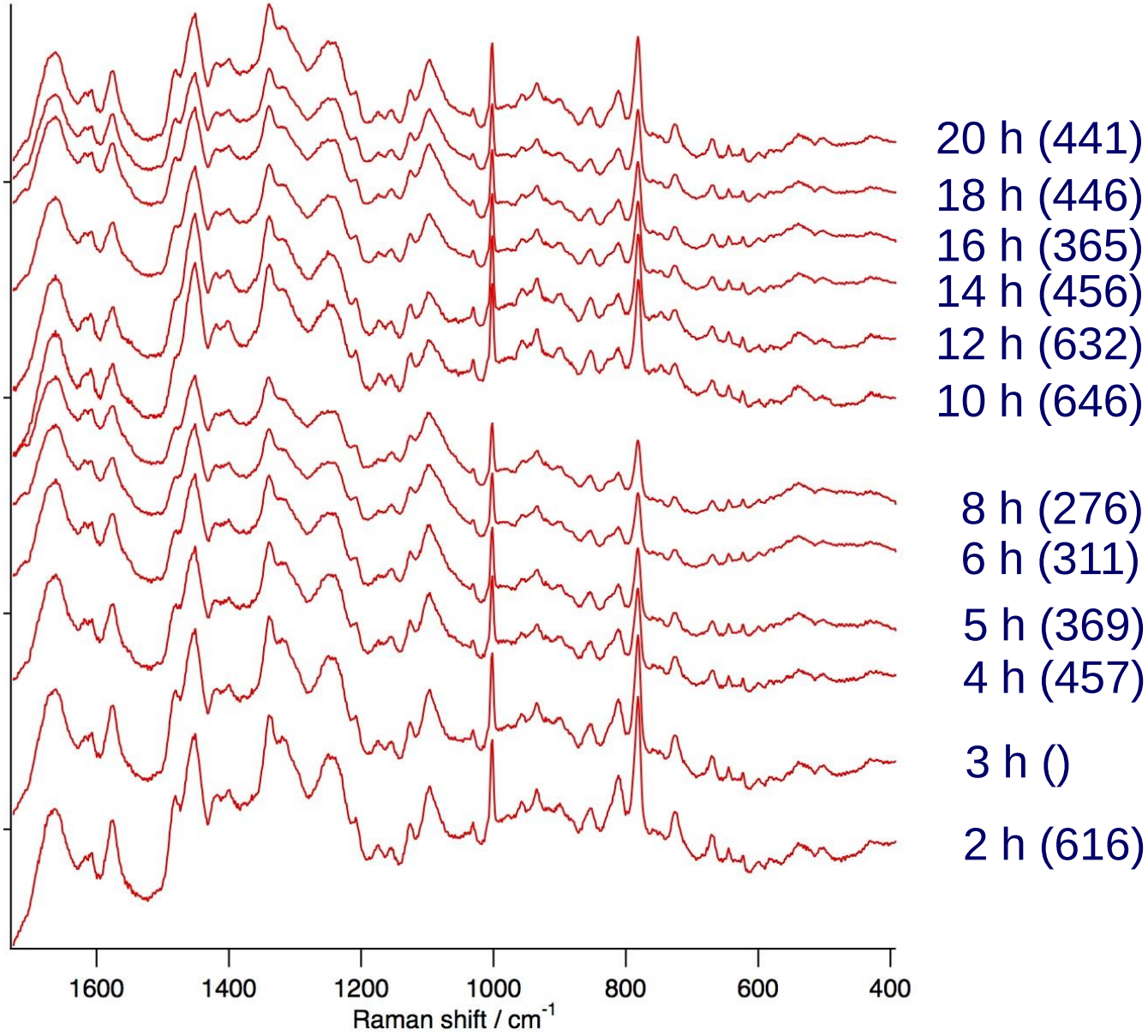

Variation in the Nucleic Acid/Protein Ratios of Single E-coli at Different Time of Growth Curve

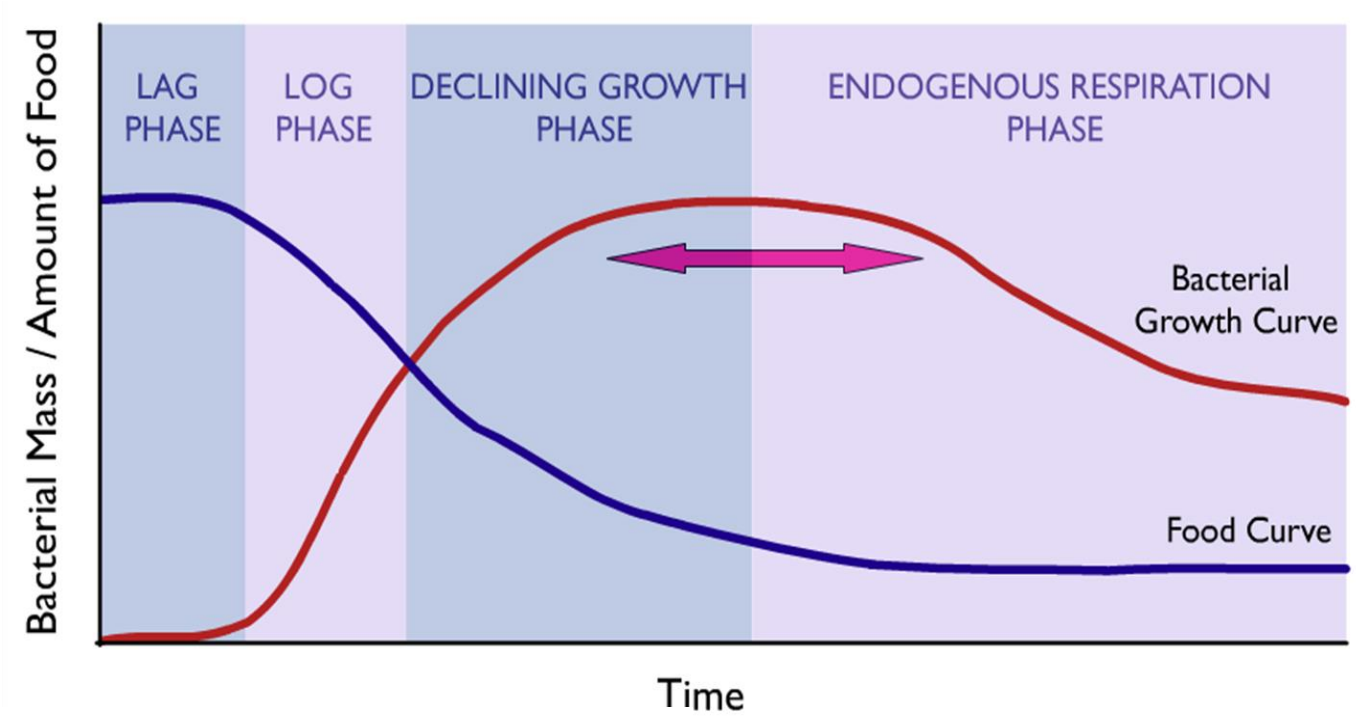

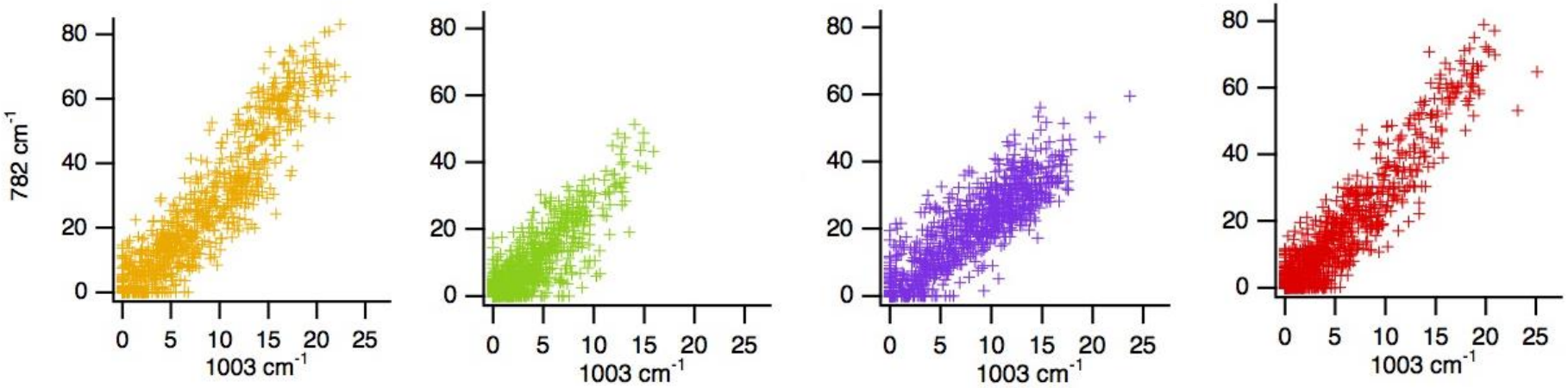

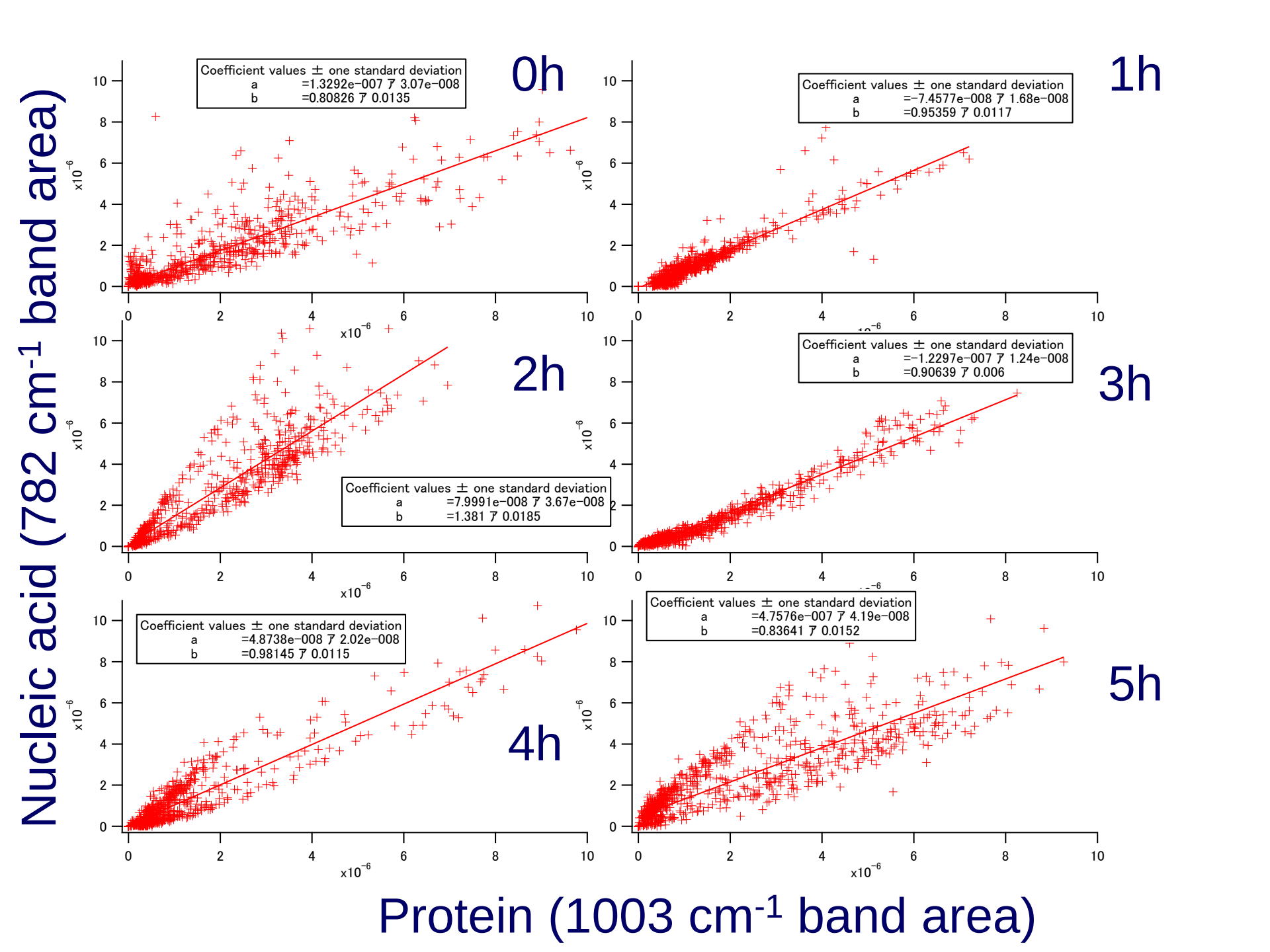
Nucleic acid (782 cm-1 band area)
Protein (1003 cm-1 band area)
0h
Coefficient values ± one standard deviation
a =1.3292e-007 ± 3.07e-008
b =0.80826 ± 0.0135
1h
Coefficient values ± one standard deviation
a =-7.4577e-008 ± 1.68e-008
b =0.95359 ± 0.0117
2h
Coefficient values ± one standard deviation
a =7.9991e-008 ± 3.67e-008
b =1.381 ± 0.0185
3h
Coefficient values ± one standard deviation
a =-1.2297e-007 ± 1.24e-008
b =0.90639 ± 0.006
4h
Coefficient values ± one standard deviation
a =4.8738e-008 ± 2.02e-008
b =0.98145 ± 0.0115
5h
Coefficient values ± one standard deviation
a =4.7576e-007 ± 4.19e-008
b =0.83641 ± 0.0152
x10-6